

**Spectroscopic Determination of Major
Nutrients (N, P, K)
of Soil**

By

İlknur ŞEN

**A Dissertation submitted to the
Graduate School in Partial Fulfillment of the
Requirements for the Degree of**

MASTER OF SCIENCE

**Program: Food Engineering Department
Major: Food Engineering**

**İzmir Institute of Technology
İzmir, Turkey**

September, 2003

ACKNOWLEDGEMENTS

I would like to thank to my advisor Assist. Prof. Handan Ertürk and to my co-advisors Assist. Prof. Durmuş Özdemir and Assoc. Prof. Ahmet Erođlu for their guidance, support and supervision throughout this study. I am so grateful to Assist. Prof. Salih Dinleyici for his support, guidance and valuable commends. I also would like to thank to Prof. Şebnem Harsa for her valuable suggestions and recommendations.

Special thanks to the Agricultural Engineering Department of Ege University for the laboratory analyses.

I am so grateful to my family for their support, encouragement and understanding during this thesis as in all stages of my life. Finally, I would like to thank to my roommates and Selda Göktaş for their support and help.

ABSTRACT

The aim of this study was to determine the major soil nutrients (nitrogen, phosphorus and potassium) which mainly affect the raw material quality of food, using near infrared reflectance spectroscopy (1000-2500 nm). Genetic inverse least squares and partial least squares were used to predict the concentrations of major soil nutrients.

The soil samples, collected from Menemen Application and Research Farms, were prepared for the near infrared analysis by using two different methods. According to the first method, two experiments were performed. The soil samples of which were oven dried and screened through a 2 mm sieve, were mixed with NPK fertilizer in the concentration range of 1-15% (wt/wt) (first experiment), and with NH_4NO_3 and TSP fertilizers in the concentration range of 0.075-0.3% (wt/wt) (second experiment). Using genetic inverse least squares method, regression coefficients of 0.9820, 0.9779 and 0.9906 were obtained for the prediction of nitrogen, phosphorus and potassium concentrations in samples containing NPK fertilizer, respectively. In the second experiment, prediction of nitrogen concentration in samples containing NH_4NO_3 fertilizer was done reliable with a regression coefficient of 0.8409 using genetic inverse least squares method. On the other hand, regression coefficient of 0.6005 was obtained for the prediction of phosphorus concentration in samples containing TSP fertilizer with the same statistical method.

The second method differed from the first one by eliminating the drying of soil samples and moisturizing step following the addition of fertilizers into soil samples. The aim was to prevent baseline shifts in the spectra arising from the moisture changes in the samples. Five types of fertilizer [KNO_3 , CaNO_3 , TSP, $(\text{NH}_4)_2\text{SO}_4$, NPK] were used in the preparation of samples in the concentration range of 0.02-0.5% (wt/wt). Using genetic inverse least squares method, calibration models produced between the reflectance spectra and the nutrient concentrations had regression coefficients greater than 0.80, however the prediction ability of the models was poor ($R^2 < 0.50$) except for the samples containing $(\text{NH}_4)_2\text{SO}_4$ and NPK fertilizers. The regression coefficients for the prediction of nitrogen and sulfur concentrations in $(\text{NH}_4)_2\text{SO}_4$ containing samples were found as 0.8620 and 0.8555, respectively. For the prediction of nitrogen, phosphorus and potassium concentrations in NPK containing samples, the regression coefficients were found as 0.6737, 0.7633 and 0.8724, respectively. The partial least

squares method was also used for the prediction of nutrient concentrations in the samples prepared according to the second method. Except samples containing $(\text{NH}_4)_2\text{SO}_4$ fertilizer, nitrogen, phosphorus and potassium amounts could not be predicted in the other samples using partial least squares method ($R^2 < 0.20$). The regression coefficients obtained for the prediction of nitrogen and sulfur amounts in $(\text{NH}_4)_2\text{SO}_4$ containing samples were 0.9301.

An additional work was carried out with laboratory analyzed soil samples collected from several points of two agricultural fields in Menemen Application and Research Farms. Total nitrogen, extractable phosphorus and exchangeable potassium amounts were determined by Agricultural Engineering Department of Ege University according to the Kjeldahl method, Bingham method and ammonium acetate method, respectively. Predictions of these nutrient concentrations by genetic inverse least squares method were poor ($R^2 < 0.20$). Using partial least squares method, the nutrient concentrations could not be predicted (factor number = 0).

The results of this study indicate that, near infrared reflectance technique provided rapid, non-destructive and simultaneous determination of nitrogen, phosphorus and potassium concentrations in soil- fertilizer mixtures depending on the sample preparation steps, fertilizer types and concentrations and multivariate calibration methods (genetic inverse least squares and partial least squares methods).

ÖZ

Bu çalışmanın amacı gıdanın hammadde kalitesini başlıca etkileyen ana toprak besin elementlerini (azot, fosfor ve potasyum) yakın kızılötesi reflektans spektroskopisi kullanarak tayin etmektir. Ana toprak besin elementlerinin konsantrasyonlarını tahmin etmek için genetik ters en küçük kareler ve kısmi en küçük kareler metotları kullanılmıştır.

Menemen Uygulama ve Araştırma Çiftliği'nden toplanan toprak örnekleri yakın kızılötesi analizlerine iki farklı metot kullanılarak hazırlanmıştır. Birince metoda göre iki deney yapılmıştır. Etüvde kurutulmuş ve 2 mm'lik elekten elenmiş toprak örnekleri, kütlece %1-15 konsantrasyon aralığında NPK gübresi ile (birinci deney) ve kütlece %0.075-0.3 konsantrasyon aralığında NH_4NO_3 ve TSP gübrelere ile karıştırılmıştır (ikinci deney). Genetik ters en küçük kareler metodu kullanılarak, NPK gübresi içeren örneklerdeki azot, fosfor ve potasyum konsantrasyonlarının tahmini için sırası ile 0.9820, 0.9779 ve 0.9906 regresyon katsayıları elde edilmiştir. İkinci deneyde, NH_4NO_3 gübresi içeren örneklerdeki azot konsantrasyonunun tahmini 0.8409 regresyon katsayısı ile genetik ters en küçük kareler metodu kullanılarak güvenilir bir şekilde yapılmıştır. Diğer taraftan, TSP gübresi içeren örneklerdeki fosfor konsantrasyonunun tahmini için ise aynı istatistiksel metot ile 0.6005 regresyon katsayısı elde edilmiştir.

İkinci metot, birincisinden toprak örneklerinin kurutulması ve toprak örneklerine gübre ilavesini takiben uygulanan nemlendirme basamağının çıkarılması ile farklılık göstermektedir. Amaç, örneklerdeki nem farklılıklarından kaynaklanan spektrumlardaki zemin çizgisinin kaymasını engellemektir. Kütlece %0.02-0.5 konsantrasyon aralığındaki örneklerin hazırlanmasında beş gübre çeşidi kullanılmıştır [KNO_3 , CaNO_3 , TSP, $(\text{NH}_4)_2\text{SO}_4$, NPK]. Genetik ters en küçük kareler metodu kullanarak, reflektans spektralleri ile besin elementi konsantrasyonları arasında oluşturulan kalibrasyon modelleri 0.80'nin üzerinde regresyon katsayısına sahiptirler fakat $(\text{NH}_4)_2\text{SO}_4$ ve NPK gübrelere içeren örnekler dışında, modellerin tahmin etme yetenekleri zayıftır ($R^2 < 0.50$). $(\text{NH}_4)_2\text{SO}_4$ içeren örneklerdeki azot ve sülfür konsantrasyonlarının tahmini için regresyon katsayıları sırası ile 0.8620 ve 0.8555 olarak bulunmuştur. NPK içeren örneklerdeki azot, fosfor ve potasyum konsantrasyonlarının tahmini için regresyon katsayıları sırası ile 0.6737, 0.7633 ve 0.8724 olarak bulunmuştur. İkinci metoda göre hazırlanmış olan örneklerdeki besin elementi konsantrasyonlarının tahmini için kısmi en

küçük kareler metodu da kullanılmıştır. $(\text{NH}_4)_2\text{SO}_4$ gübresi içeren örnekler dışında, diğer örneklerdeki azot, fosfor ve potasyum miktarları kısmi en küçük kareler metodu kullanılarak tahmin edilememiştir ($R^2 < 0.20$). $(\text{NH}_4)_2\text{SO}_4$ içeren örneklerdeki azot ve sülfür miktarlarının tahmini için bulunan regresyon katsayısı 0.9301'dir.

Menemen Uygulama ve Araştırma Çiftliği'nde bulunan iki zirai tarlanın farklı noktalarından toplanan, laboratuarda analizlenmiş toprak örnekleri ile ilave bir çalışma gerçekleştirilmiştir. Toplam azot, yarayışlı fosfor ve yarayışlı potasyum miktarları Ege Üniversitesi'nin Ziraat Mühendisliği Bölümü tarafından sırası ile Kjeldahl metodu, Bingham metodu ve amonyum asetat metoduna göre belirlenmiştir. Bu besin elementlerinin genetik ters en küçük kareler metoduna göre tahmini zayıftır ($R^2 < 0.20$). Kısmi en küçük kareler metodunu kullanarak, besin elementi konsantrasyonları tahmin edilememiştir (faktör sayısı = 0).

Bu çalışmanın sonuçları göstermektedir ki, yakın kızılötesi reflektans tekniği toprak-gübre karışımlarındaki azot, fosfor ve potasyum konsantrasyonlarını, örnek hazırlama basamaklarına, gübre çeşidine ve konsantrasyonlarına ve çoklu değişkenli kalibrasyon metotlarına (genetik ters en küçük kareler ve kısmi en küçük kareler metotları) bağlı olarak hızlı, tahrip etmeksizin, ve eşzamanlı belirlenmesini sağlamaktadır.

TABLE OF CONTENTS

LIST OF FIGURES	x
LIST OF TABLES	xii
NOMENCLATURE	xiv
Chapter 1. INTRODUCTION	1
Chapter 2. SOIL	4
2.1. Soil Profile	5
2.2. Soil Composition	5
2.2.1. Types of soil	5
2.2.2. Soil water	6
2.2.3. Soil air	6
2.2.4. Mineral content of soil	7
2.2.5. Organic matter	7
Chapter 3. SOIL NUTRIENTS	10
3.1. Factors Affecting Plant Growth	10
3.2. Soil Nutrients	10
3.2.1. Soil Nitrogen	11
3.2.1.1. Effect on Plant Growth and Food	12
3.2.1.2. Forms of Nitrogen in Soil	13
3.2.1.3. Nitrogen Cycle	15
3.2.1.4. Factors Affecting the Availability of Nitrogen	16
3.2.2. Soil Phosphorus	19
3.2.2.1. Effect on Plant Growth and Food	19
3.2.2.2. Forms of Soil Phosphorus	20
3.2.2.3. Phosphorus Cycle	23
3.2.2.4. Factors Affecting the Availability of Phosphorus	24
3.2.3. Soil Potassium	26
3.2.3.1. Effect on Plant Growth and Food	26
3.2.3.2. Forms of Potassium in Soil	27
3.2.3.3. Factors Affecting Availability of Potassium	29
Chapter 4. SPECTROSCOPIC TECHNIQUES COUPLED WITH MULTIVARIATE CALIBRATION METHODS	30
4.1. Near Infrared Spectroscopy	30
4.1.1. Theory of near infrared spectroscopy	30
4.1.2. Applications of Near Infrared Spectroscopy	36
4.2. Laser Induced Fluorescence Spectroscopy	41
4.2.1. Applications of Laser Induced Fluorescence Spectroscopy	44
4.3. Multivariate Calibration Methods	47
4.3.1. Univariate calibration methods	47

4.3.2. Multivariate Calibration Methods	51
Chapter 5. MATERIALS AND METHODS	58
5.1. Materials	58
5.2. Methods	58
5.2.1. First Method	58
5.2.2. Second Method	63
5.2.3. Near infrared analyses of soil samples collected from clover and melon fields	64
Chapter 6. RESULTS AND DISCUSSION	68
6.1. Results of near infrared reflectance analyses of soil-fertilizer mixtures prepared according to the first method	68
6.2. Results of near infrared reflectance analyses of soil-fertilizer mixtures prepared according to the second method	74
6.3. Results of near infrared reflectance analyses of soil samples collected from different fields	78
Chapter 7. CONCLUSIONS AND RECOMMENDATIONS	81
7.1. Conclusions	81
7.2. Recommendations	82
REFERENCES	84
APPENDICES	89
APPENDIX A. Calculation of nutrient concentrations	90
APPENDIX B. Nutrient concentrations	91
APPENDIX C. Calibration and validation sets	93
APPENDIX D.1 Kjeldahl Method	98
APPENDIX D.2 Bingham Method	99
APPENDIX D.3 Ammonium acetate Method	100

LIST OF FIGURES

Figure 2.1. The portions of regolith, soil and bedrock	4
Figure 2.2. Soil profile	5
Figure 2.3. Composition of a mineral soil	6
Figure 2.4. Composition of a green plant tissue	8
Figure 3.1. Principle of limiting factors	10
Figure 3.2. Fixed and exchangeable nitrogen	15
Figure 3.3. Nitrogen cycle	16
Figure 3.4. The major gains and losses of available soil nitrogen	17
Figure 3.5. Phosphate ions in soil solution at different pH levels	20
Figure 3.6. Classification of phosphate compounds in three groups	23
Figure 3.7. Phosphorus cycle	24
Figure 3.8. Gains and losses of available phosphorus in soil solution	24
Figure 3.9. Forms of soil potassium	28
Figure 4.1. Types of molecular vibrations	30
Figure 4.2. Potential diagram of harmonic oscillation	31
Figure 4.3. Potential energy of anharmonic oscillation	33
Figure 4.4. Near infrared absorption bands and their locations	34
Figure 4.5. Near infrared reflectance spectrometer	35
Figure 4.6. Diffuse reflectance analysis	35
Figure 4.7. Transition between electronic energy levels	42
Figure 4.8. A typical fluorimeter schematic	43
Figure 5.1. Sample preparation steps for the near infrared reflectance analyses according to the first method	59
Figure 5.2. Sample cup of near infrared reflectance spectrometer	61
Figure 5.3. Sample preparation steps for the near infrared reflectance analyses according to the second method	63
Figure 5.4. Sample preparation steps for laboratory analyses and near infrared reflectance analyses	64
Figure 6.1. Diffuse reflectance spectra of NPK fertilizer and samples containing the minimum (1%) and maximum (15%) concentrations of NPK fertilizer	69

Figure 6.2. Calibration curves of nitrogen, phosphorus and potassium nutrients in the samples containing NPK fertilizer	70
Figure 6.3. Diffuse reflectance spectra of NH_4NO_3 fertilizer and samples containing the minimum (0.075%) and maximum (0.3%) concentrations of NH_4NO_3 fertilizer	71
Figure 6.4. Diffuse reflectance spectra of TSP fertilizer and samples containing the minimum (0.075%) and maximum (0.3%) concentrations of TSP fertilizer	71
Figure 6.5. Calibration curves of nitrogen and phosphorus nutrients in the samples containing NH_4NO_3 and TSP fertilizers	72
Figure 6.6. Diffuse reflectance spectra of pure fertilizers	73
Figure 6.7. Calibration curves of nitrogen and phosphorus, potassium and sulfur nutrients in the samples containing $(\text{NH}_4)_2\text{SO}_4$ and NPK fertilizers	76
Figure 6.8. Calibration curves of nitrogen and sulfur nutrients in the samples containing $(\text{NH}_4)_2\text{SO}_4$ fertilizers	77
Figure 6.9. Validation curves of nitrogen and sulfur nutrients in the samples containing $(\text{NH}_4)_2\text{SO}_4$ fertilizers	78
Figure 7.1 Experimental set up of laser spectroscopy established in the optics laboratory of Electronic Engineering Department, İzmir Institute of Technology	83
Figure D.1. Kjeldahl method, which is applied by soil laboratory of Agricultural Engineering Department of Ege University	98
Figure D.2. Bingham method, which is applied by soil laboratory of Agricultural Engineering Department of Ege University	99
Figure D.3. Ammonium acetate method, which is applied by soil laboratory of Agricultural Engineering Department of Ege University	100

LIST OF TABLES

Table 3.1. Essential Nutrient Elements in Soil	10
Table 3.2. Nitrogen Fertilizers	19
Table 3.3. Calcium Containing Inorganic Phosphorus Compounds	21
Table 3.4. Phosphorus Fertilizers	26
Table 3.5. Potash Fertilizers	29
Table 4.1. Near infrared applications of cereal products	36
Table 5.1. Fertilizers and their properties	58
Table 5.2. Nutrient and fertilizer concentrations (g/100 g) in the samples containing NPK fertilizer in the first experiment	60
Table 5.3. Nutrient and fertilizer concentrations (g/100 g) in the samples containing NH_4NO_3 and TSP fertilizers in the second experiment	60
Table 5.4. Calibration and validation sets of nutrients in the samples containing NPK fertilizer (g/100 g) in the first experiment	62
Table 5.5. Calibration and validation sets of nutrients in the samples containing NH_4NO_3 and TSP fertilizer (g/100g) in the second experiment	62
Table 5.6. Calibration and validation sets of total nitrogen (N) (g/100 g)	65
Table 5.7. Calibration and validation sets of extractable phosphorus (P) (ppm)	66
Table 5.8. Calibration and validation sets of exchangeable potassium (K) (ppm)	67
Table 6.1. Concentration profiles of nutrients (g/100 g) for the first and second experiments	68
Table 6.2. SEC, SEP and R^2 (calibration) values of the nutrients in the samples containing NPK fertilizer	69
Table 6.3. SEC, SEP and R^2 (calibration) values of the nutrients in the samples containing NH_4NO_3 and TSP fertilizers	72
Table 6.4. SEC, SEP and R^2 (calibration) values of the nutrients in the samples prepared according to the second method	75
Table 6.5. Partial least squares analyses of samples containing fertilizers NPK, KNO_3 and $\text{Ca}(\text{NO}_3)_2$	78
Table 6.6. SEC, SEP, R^2 (calibration) values of nitrogen, phosphorus and potassium in soil samples	79

Table 6.7. Results of laboratory analyses done by the soil laboratory of Agricultural Engineering Department of Ege University	80
Table B.1. Nutrient and fertilizer concentrations (g/100 g) in the samples prepared with KNO_3 , $\text{Ca}(\text{NO}_3)_2$ and $(\text{NH}_4)_2\text{SO}_4$ fertilizers according to the second method	91
Table B.2. Nutrient and fertilizer concentrations (g/100 g) in the samples prepared with NPK and TSP fertilizers according to the second method	92
Table C.1. Calibration and validation sets of nutrients in the samples prepared with KNO_3 fertilizer according to the second method (g/100 g)	93
Table C.2. Calibration and validation sets of nutrients in the samples prepared with $\text{Ca}(\text{NO}_3)_2$ fertilizer according to the second method (g/100 g)	94
Table C.3. Calibration and validation sets of nutrients in the samples prepared with NPK fertilizer according to the second method (g/100 g)	95
Table C.4. Calibration and validation sets of nutrients in the samples prepared with $(\text{NH}_4)_2\text{SO}_4$ fertilizer according to the second method (g/100 g)	96
Table C.5. Calibration and validation sets of nutrients in the samples prepared with TSP fertilizer according to the second method (g/100 g)	97

NOMENCLATURE

a	$m \times l$ vector of absorbance spectra
A	$m \times n$ matrix of absorbance spectra
a_i	Absorbance of i th sample
a_u	Abosorbance of unknown analyte concentration
B	$h \times n$ matrix of loading spectra or basis vector in partial least squares model
b_0	Unknown parameter in classical univariate calibration model
b_1	Unknown parameter in classical univariate calibration model
b_f	Final calibration coefficient in partial least squares method
c	$m \times l$ vector of analyte concentration
c	Analyte concentration
C	$m \times l$ matrix of analyte concentrations in inverse least squares model
C	$m \times 2$ matrix of analyte concentrations in classical univariate calibration model
c_i	Analyte concentration of i th sample
c_o	Average concentration of calibration samples in partial least squares model
c_u	Unknown analyte concentration
df	Degrees of freedom
E	Potential Energy
e_a	$m \times l$ vector of errors associated with absorbance in classical univariate calibration model
E_A	$m \times n$ matrix of errors related to absorbance in partial least squares model
e_c	$m \times l$ vector of errors related to analyte concentrations
E_c	$m \times l$ matrix of errors related to concentration in inverse least squares model
e_i	Measurement error related to absorbance of i th sample in univariate calibration model
h	Planck's constant

k	Number of parameters extracted from the sample set in genetic inverse least squares method
k	Force constant
l	Thickness of the sample
m	Number of samples in the calibration set
m_1	Mass of atom 1
m_2	Mass of atom 2
\mathbf{p}	$n \times 1$ vector of calibration coefficients in inverse least squares model
\mathbf{P}	$n \times l$ matrix of unknown calibration coefficients in inverse least squares model
p_1	Unknown parameter in inverse univariate calibration model
p_0	Unknown parameter in inverse univariate calibration model
r	Instrument response
R	Reflectance
R^2	Regression coefficient
\mathbf{T}	$m \times h$ matrix of scores in the coordinate system in partial least squares model
\mathbf{v}	$h \times 1$ vector of unknown calibration coefficients in partial least squares model
x	Displacement of internuclear distance
\hat{c}	Predicted analyte concentration
\hat{c}_i	Predicted analyte concentration of i th sample
\hat{p}_0	Least squared estimate of p_0 in inverse univariate calibration model
$\hat{\mathbf{b}}_h$	Estimate of partial least squares loading vector
$\hat{\mathbf{v}}_h$	Least squares estimate of \mathbf{v} in partial least squares model
ν	Frequency of vibration
\hat{b}_0	Least squares estimate of b_0
\hat{b}_1	Least squares estimate of b_1
$\hat{\mathbf{p}}$	Least squares estimate of \mathbf{p} in inverse least squares method
\bar{a}	Mean values of absorbance

\bar{c}	Mean values of analyte concentrations
$\hat{\mathbf{w}}_h$	$n \times 1$ vector of first order approximation of the analyte spectra.
ν	Vibrational quantum number
$\hat{\boldsymbol{\beta}}$	2×1 vector of least square estimate of b_0 and b_1 in classical univariate calibration model
$\boldsymbol{\beta}$	2×1 vector of unknown coefficients b_0 and b_1 in classical univariate calibration model
\hat{p}_1	Least squares estimate of p_1 in inverse univariate calibration model
ε	Extinction coefficient
μ	Reduced mass of two atoms

Chapter 1

INTRODUCTION

Methods for determining the chemical composition of samples of matter are topics of analytical chemistry. These analytical methods are often classified as classical or instrumental methods. In the early years of chemistry, most analyses were carried out by classical methods whereas from the beginning of twentieth century, researchers have started to use the measurement of physical properties of analytes such as light absorption or emission, fluorescence, mass to charge ratio, conductivity etc. Among these newer methods called instrumental methods, spectroscopy deals with the interactions of electromagnetic radiation with matter (1).

The spectroscopic techniques have been increasingly used in agricultural and food industries in the recent decades. The classical analysis methods, namely laboratory analyses for food, soil or plant samples are expensive, time-consuming and require much work first in the collection of samples from fields or foods, and second in the laboratory work itself. They also require highly skilled operators and are not easily adapted to on-line monitoring. Related to these disadvantages, sampling and laboratory analysis methods are not effective enough to meet the growing demand of industry.

To comply with this problem, several instrumental techniques such as reflectance spectroscopy, fluorescence spectroscopy etc. are used for the determination of product composition. These analytical techniques are relatively advantageous, as they are low-cost, rapid and non-destructive. Together with fiber optic sensors, they allow on-line monitoring of products in factory or in field as remote or in-situ sensors.

For instance, in food industry soft cheeses with different textural properties were discriminated with fluorescence spectroscopy by detecting the fluorescence emission of constituents, protein tryptophan and vitamin A. On the other hand, infrared reflectance spectroscopy was also used to measure cheese composition, based on the observation of absorption peaks of cheese-fat, protein and water in the near and mid infrared portions of the spectrum. In addition, it was also shown that the joint analysis of fluorescence and infrared data contributes to a better discrimination of cheeses (2).

Another study of near infrared reflectance spectroscopy involves the simultaneous prediction of total polyphenols and alkaloids in green tea leaves. Using partial least square algorithm, good calibrations of these compounds such as gallic acid, (-) epicatechin and caffeine were obtained between the reference laboratory analysis and near infrared spectra ($R^2 > 0.85$). The study demonstrates as well, that the near infrared spectroscopy can be useful in controlling process steps of tea such as decaffienation and estimating the quality and taste of green tea (3).

In addition to the analysis of food and plant samples, infrared and fluorescence spectrosopes are also considered as advantageous techniques for soil analysis in precision agriculture. Site Specific Crop Management (SSCM, also known as precision agriculture) is a management technique that seeks to address the variability within a field, and optimize the application of inputs. In this concept, soil fertility is considered as one of the important soil variable to be sensed and may show variance within a field due to the spatial differences in soil, soil type, previous management practices and agronomic changes (4). As soil is an important source of food and fertilizers are necessary for plant growth to maintain their fertility, proper type and amount of fertilizer application improves both the quality and yield of food raw material. On the other hand, in case of both deficiency and excessive utilization, such problems as low quality and yield, unhealthy crops, increased input costs or environmental pollution of groundwater are encountered. The most important and deficient nutrients are known as nitrogen, phosphorus and potassium. With the aid of laboratory analyses and soil sampling procedures, it is possible to acquire data about fertility status of soil and to apply the necessary amounts of fertilizers. Such laboratory analyses are Kjeldahl method or Dumas method for total nitrogen determination, Olsen, Bray or Mehlich methods for plant available phosphorus and ammonium acetate (NH_4OAc) method for plant available potassium (5).

However, there is a tremendous need for the effective collection of data for precision agriculture, since the soil sampling and laboratory techniques are costly prohibitive. At this point, development of sensors and utilization of spectroscopic techniques enhance the efficiency of precision agriculture techniques by giving the chance of making rapid soil analyses. Hence, with the use of instrumental techniques, site specific crop management becomes a promising strategy that may be able to increase food production as well as reducing the input costs and providing environmental sustainability.

In this thesis study, the source of food, that is soil, was the sample used in the experiments and was collected from agricultural farms in Menemen, Turkey. The objective was to determine the major soil nutrients (nitrogen, phosphorus and potassium) which mainly affect the raw material quality of food using near infrared reflectance spectroscopy (NIRS). This instrumental technique is a rapid and non-destructive analytical technique that eliminates the time consuming sample preparation steps in laboratory. Moreover, it is adaptable to on-line monitoring of samples with the aid of fiber optic sensors. With this characteristic, making soil fertility analysis on the field may be possible by developing a portable instrument based on the working principle of near infrared reflectance spectroscopy. Two multivariate calibration methods, genetic inverse least squares and partial least squares methods were used to determine the soil nutrient amounts by developing a calibration model that relates the soil reflectance data obtained from the NIRS measurements to the known nutrient concentrations in soil. The study also demonstrates the applications of laser induced fluorescence spectroscopy (LIFS) and near infrared spectroscopy as well as the combination of these two techniques in food and agriculture industries through a literature review.

Chapter 2

SOIL

Soil is a natural body covering earth's surface with biological, chemical and physical properties that gives the ability to support plant growth. Moreover, they are the natural beds for houses, factories, roads; a natural and limited resource for plant production and a food source for animal and human being. They are the receivers of industrial, municipal or animal wastes. Each soil type, in its complex structure, has a profile, which consists of some layers in the *regolith* part, extending down to bedrock as shown in Figure 2.1.

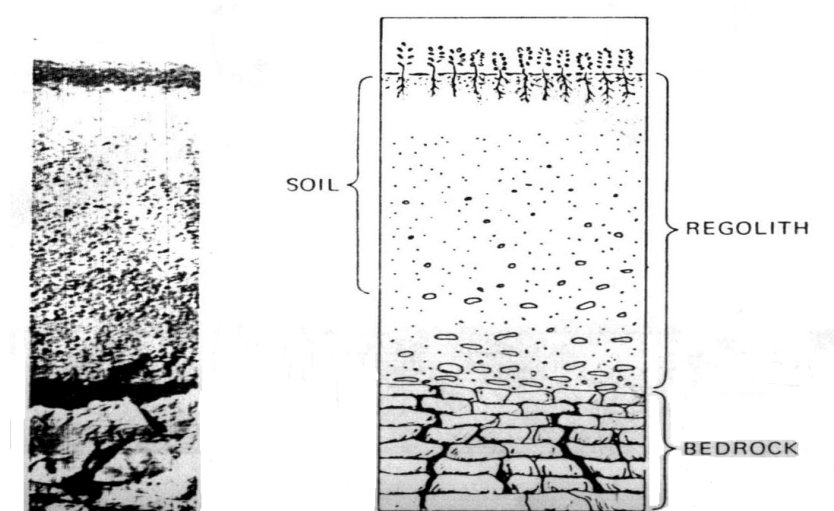


Figure 2.1. The portions of regolith, soil and bedrock (6).

Bedrock is the underlying rock on which the regolith portion is deposited. Regolith is all the loose material, formed by weathering of bedrock or by transportation action of wind, water or ice and thus displays great variations in composition from place to place. The upper part of the regolith is distinguished from the lower layers by the presence of roots of plants, soil organisms, high organic matter content, and minerals and by the presence of characteristic horizontal layers, which promote the growth of higher plants (6).

2.1. Soil Profile

Soil *profile* is the vertical section of soil exposing the layers as shown in Figure 2.2. The upper layer is called the *A-horizon* or topsoil, which is higher in organic matter content and darker in color than the layers below. *B-horizon* or subsoil is the middle part having relatively a brighter color and containing more clay. The A and B horizons together, are referred to as the true soil. The *C-horizon*, in other words parent material, can be thick, thin or even absent (7).

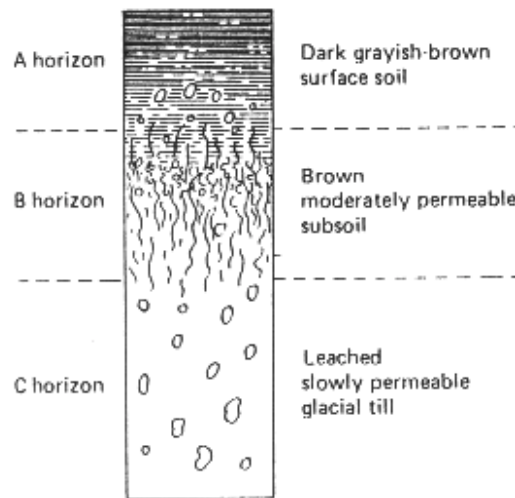


Figure 2.2. Soil profile (7).

2.2. Soil Composition

The solid portion of soil contains the mineral matter and organic matter. The mineral matter is formed from the parent rock, in other words the C-horizon. In addition, the organic matter is formed from the living organisms in soil. Besides the solid portion, water and air make up the pore space.

2.2.1. Types of soil

Soil, according to its composition, is divided into two categories: mineral soils, and organic soils. Soils, formed in bogs and such wet areas, and containing more than 12-18 % organic carbon (approximately 20 to 30% organic matter) are called as organic soils. They consist of living microbes such as bacteria, fungi and living macroorganisms such as plant roots, earthworms, insects and remains of dead macroorganisms as well as the finally divided non-living organic materials. Organic soils are useful for high value crop

production like fresh market vegetables when drained and cleared. They can also be prepared as organic supplements for home gardens and potted plants. Therefore, these soils submit an economical significance in localized regions. Mineral soils occupy the highest portion of total land area and hence are considered as more important soils than organic soils. They are formed from rocks and sediments, in other words they are the upper and biologically weathered portion of the regolith. A typical mineral soil contains approximately 45% mineral matter, 5% organic matter and 25% soil air and 25% soil water as shown in Figure 2.3 (6).

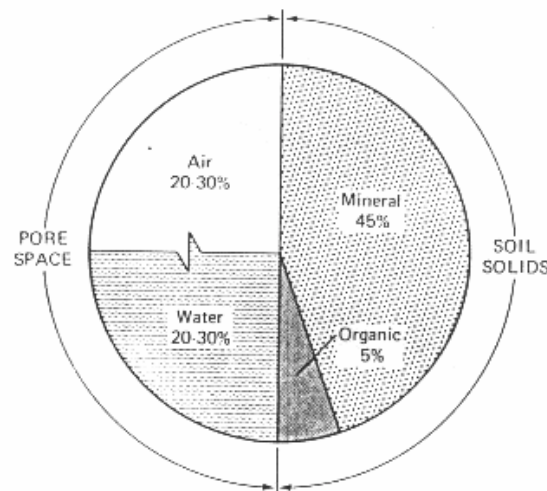


Figure 2.3. Composition of a mineral soil (6).

2.2.2. Soil water

Soil water forms the soil solution together with its dissolved salts, which is essential not only because plants need water for their physiological process but also because water is a supply of nutrients to growing plants. It is an effective soil temperature regulator and held within the soil pores. As plants consume some amount of water in soil, the soil solids hold some either (6).

2.2.3. Soil air

Soil air is essential to the life cycles of soil animal and plants and held between the solid and liquid particles in soil. The discriminating points of soil air from the atmosphere are listed as follows. First, soil air is located in the soil pores between the solid parts. Second, the moisture content of soil air exceeds that of atmosphere and

third, the content of CO₂ is higher and that of O₂ is lower than the amounts in atmosphere. Finally, it is not continuous. The most commonly found gases in soil air are N₂, O₂, and CO₂ (6).

2.2.4. Mineral content of soil

The mineral constituents in soil are formed from rock by physical and chemical weathering processes and are generally variable in size and composition. The sizes range from submicroscopic clay to stones. The particles greater than 76 mm in diameter are referred to as *stones* and those smaller than stone size but greater than 2 mm in diameter are called as gravel. Mineral particles that are smaller than 2 mm. in diameter can be sand, silt or clay. Sand particles are between 0.05 and 2 mm in size whereas silt is between 0.002 to 0.05 mm. The clay particles are smaller than 0.002 mm in diameter (7). The primary minerals are formed with little change in composition from the country rock and they are present in the coarser fractions of soil. Sand, stone, gravel are some examples. The weathering process of primary minerals in the presence of air, water and organic matter in time forms the secondary minerals and soluble salts (Na⁺, K⁺, Ca⁺, etc.). They are mostly in clay size. Some examples are silicate minerals, montmorillonite, kaolinite, illite, vermiculite or the insoluble oxides of aluminum, iron and silicium (6).

2.2.5. Organic matter

The accumulation of partially decayed and partially synthesized plant and animal residues represents the organic matter content of soil. Tops and roots of trees, shrubs, grasses and other native plants are examples of plant tissue considered as the original source of soil organic matter. The secondary source is the animals and microorganisms, which attack plant tissues, leave their waste products or either their bodies by death and play a role in the translocation of plant residues, especially the earthworms, ants, insects. The organic matter in soil is permanently being broken down by the work of decomposing microorganisms in soils but again is renewed by the formation of new plant tissues. Hence, the composition of plant residue is important as it is modified to organic matter in soil. The green plant tissue is composed of carbon, oxygen, hydrogen and nitrogen, which exist in the ash as shown in Figure 2.4.

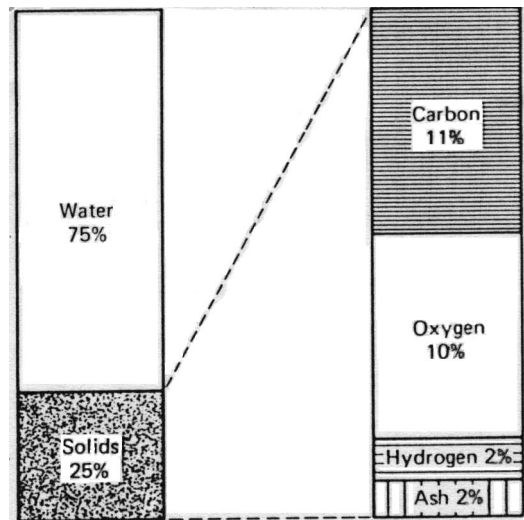


Figure 2.4. Composition of a green plant tissue (6).

The organic compounds present in the plant tissue are:

- | | | |
|---|---|------------------------|
| 1-sugars, starches, and simple proteins | → | rapidly decomposed |
| 2-crude proteins | | |
| 3-hemicelluloses | | |
| 4-cellulose | | |
| | | ↓ |
| 5-lignins, fats, waxes.etc. | → | very slowly decomposed |

From the above list, it can be understood that the sugars and water-soluble proteins are the readily available material for decomposition and on the contrary, lignins are the most resistant compounds. As these compounds exist in soil, under favorable conditions, the decay bacteria, fungi and actinomycetes become active and commence decomposing the rapidly decomposed organic material and produce energy with CO_2 , water and various simple products. Because of breakdown of proteins, the nitrates (NH_4^+ , NO_2^- , and NO_3^{2-}) are formed and with other specific reactions sulfates (S , H_2S , SO_3^- , SO_4^{2-} , and CS_2) and phosphorus (H_2PO_4^- , HPO_4^{2-}) are released. As soon as the rapidly decomposing food source is diminished, the microorganisms attack both the resistant organic compounds (e.g.: lignins) and the synthesized material with a decline in their number. In time, the decayed plant tissue and the synthesized compounds form the soil humus, which is resistant against microbial action. Furthermore, the decomposition of organic matter produces acids and other substances, which cause to decompose soil minerals and release plant nutrients. All this process is an enzymatic digestion of soil organic matter in soil.

Although the organic matter content in a usual mineral soil is small about 3-5% by weight, its functions are important. Soil organic matter maintains a granular and a loose structure, which ensures breathing of organisms, and enough space for plants to grow as well as an easily managed soil condition. It affects the water capacity of soil by increasing the water amount detained in soil and the available portion to plant as well. The main source of energy for microorganisms in soil is organic matter. In addition to this, organic matter affects the soil fertility in which the nitrogen, phosphorus and sulfur are present in organic forms. Another effect is on soil color, converting it from brown to black. Moreover, organic matter has high cation adsorption capacity and includes the easily replaceable cations. The soil organic matter can be considered in two general groups: a) original tissue and, b) humus. The undecomposed roots tops of higher plants and their partially decomposed equivalents are the original tissue, which are available to the attack of soil organisms to utilize them as an energy source or tissue building material. Humus is the complex, rather resistant mixture of brown or dark brown, amorphous and colloidal substance produced from the original tissues or synthesized by the soil microorganisms. It has a high capacity to hold water and nutrient ions, exceeding that of clay, its inorganic counterpart. Thus, it has a promoting effect on plant production in soil (6).

Chapter 3

SOIL NUTRIENTS

3.1. Factors Affecting Plant Growth

Soil is an agent, which supplies most of the factors affecting plant growth. The factors affecting plant growth can be counted as a) sunlight, b) mechanical support, c) heat, d) air, e) water and f) nutrients. Thus, the essential elements are not the only factor affecting the plant growth. Moreover, the plant growth is described by a principle named as “the principle of limiting factors” which means that the plant growth can be no greater than that allowed by the most limiting factor affecting plant growth (Figure 3.1). Namely, the plant growth is dependent on the combination of the factors explained above, and any of them, in lesser amounts than the others can limit the growth of plants. Consequently, when considering the supply of nutrient elements to soil, the relationship of all these factors should also be examined (6).

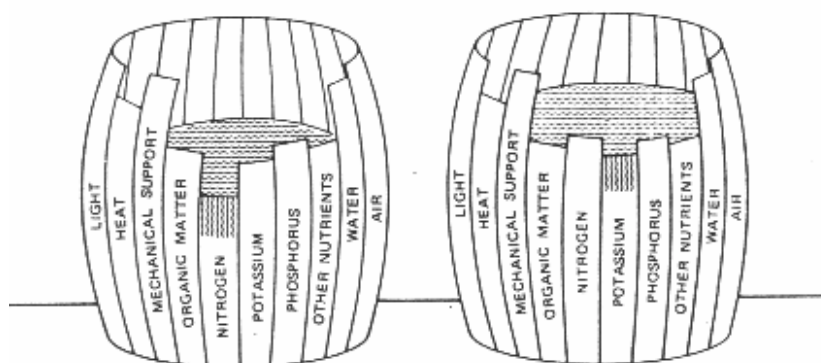


Figure 3.1. Principle of limiting factors (6).

3.2. Soil Nutrients

Table 3.1. Essential Nutrient Elements in Soil (6).

Essential Elements Used in Large Amounts		Essential Elements Used in Small Amounts	
Mostly from Air and Water	From Soil Solids	From Soil Solids	
Carbon	Nitrogen	Iron	Copper
Hydrogen	Phosphorus	Manganese	Zinc
Oxygen	Potassium	Boron	Chlorine
	Calcium	Molybdenum	Cobalt
	Magnesium		
	Sulfur		

As seen in the Table 3.1, there are 17 essential elements in which three of them, carbon, hydrogen and oxygen are mostly supplied from air and water, whereas the rest are supplied from soil. Most of the carbon and oxygen requirements are met from air by photosynthesis, the process by which sugar is synthesized in plant leaves from water and CO₂. And the hydrogen is derived from the water of the soil. As mentioned before, about 94-99.5% of fresh plant tissue is comprised of carbon, hydrogen and oxygen, and about 0.5-6% is of soil constituents, however, it is the nutrient elements gained from soil that the plants mostly face the deficiency. Of the 14 nutrients obtained from soil, six are utilized in large amounts and hence are called as macronutrients. From these, nitrogen, phosphorus and potassium are the primary elements, which are supplied to soil by the addition of commercial fertilizers or manure. They are the critical macronutrients, which are known as the most commonly deficient fertilizer elements retarding plant growth because of their low or slow availability, lack or because of their imbalance with the other nutrients. On account of this, they will be examined thoroughly in the further sections. In the same way, calcium, magnesium, and sulfur are the secondary elements. Calcium and magnesium are added to acid soils in limestone, hence are called as lime elements, not fertilizer elements. And sulfur is applied to soil as an ingredient of fertilizers (e.g.: superphosphate, ammonium sulfate, or farm manure). The other nutrient elements (iron, manganese, copper, zinc, boron, molybdenum, chlorine, cobalt) obtained from soil are utilized in very small amounts by higher plants, hence are called as micronutrients. They are mostly present in most soils with low availability; however, the deficiency problems concerning micronutrients are not widespread as that of macronutrients (6).

3.2.1. Soil Nitrogen

Soil nitrogen is a vital nutrient compound for plant growth. The primary source of soil nitrogen is gaseous N₂ in atmosphere; however a few bacteria can use this directly. The other plants and organisms can use nitrogen unless it is chemically bound to oxygen, hydrogen or carbon. About 99% of combined nitrogen is present in the organic matter fraction of soil, and can be converted to plant available nitrogen due to various biochemical reactions, that naturally take place in soil. The amount of nitrogen utilized by crops is large; however, the available amount to crops is small. Consequently, the crop uptake of nitrogen exceeds the rate at which organic nitrogen becomes available.

Thus, soil nitrogen gains much attention and importance due to its deficiencies in soil, costly supply to soil and difficult retention in soil (7, 8).

3.2.1.1. Effect on Plant Growth and Food

Of the macronutrients applied in fertilizers, nitrogen has the most rapid and the most pronounced effect on plant growth. Plants utilize nitrogen to form new cells and organic compounds in their structure. Amino acids, nucleic acids, many enzymes, energy transferring compounds ADP and ATP are some examples to the nitrogen containing compounds synthesized in the plant tissue. For instance, with cereals, the uptake of nitrogen increases the plumpness of the grain and their percentage of protein. Succulence, which is a desired quality in such crops as lettuce and radishes, is again observed by the application of nitrogen. In addition to this, nitrogen regulates to a considerable degree, the utilization of potassium, phosphorus and other constituents and gives deep green colour to leaves of vegetables. The deficiency symptoms of nitrogen in plants are stunted growth and restricted root systems as well as reduced ability of absorbing sunshine radiation. Consequently, the leaves lose their green colour and turn to yellowish green. For instance, the cabbage leaves lose their color and turn to yellow or red color. The head part of the vegetable grows up smaller than usual. Another example is cauliflower, in which the nitrogen deficiency causes inadequate leaf and small crown formation (9). The nitrogen insufficiency also possesses premature leaf death and the leaves tend to drop off. However, as soon as the deficiency is satisfied by the addition of nitrogen containing fertilizers, a remarkable change can be observed rapidly. In the case of oversupply of nitrogen, the crop maturation is delayed by encouraging excessive vegetative growth. Related to this, the stems and lodging of grains are weakened. The growth of crops is generally dark-green and succulent. For instance, the oversupply of nitrogen causes potatoes to be watery. The leaves of cauliflower become darker and curly, and leafy and loose crown is formed. Moreover, resistance to disease is diminished and the quality of grain is adversely affected as in the case of apples, peaches and barley. The excessive amount of nitrogen in soil is usually accumulated in the form of nitrate. Excess nitrate in soil, reduces bacterial populations, and because of solubility, leaching can carry them to groundwater, which causes environmental pollution in streams, lakes or rivers (6, 7).

3.2.1.2. Forms of Nitrogen in Soil

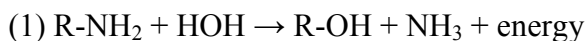
Soil nitrogen is present in three major forms in soils: a) organic nitrogen, b) mineral nitrogen in soil solution, and c) ammonium nitrogen fixed in clay minerals.

Organic nitrogen

Nitrogen in organic material is present in the form of amine groups (-NH₂) as constituents of aminoacids and aminosugars. This nitrogen in the amine group is covalently bound to a carbon and two hydrogen atoms in ring and chain structures and thus becomes unionizable. The remaining two electrons of nitrogen atom can bond to the negatively charged clay surfaces. In this way, both the soil structure and the organic compounds are stabilized and the organic matter becomes resistant to decomposition. About 2-3% of organic nitrogen is being mineralized in a year and becomes available to plant (6, 7).

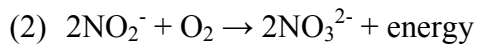
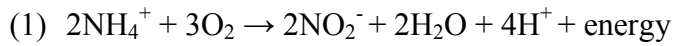
Mineral nitrogen in soil solution:

Types of mineral nitrogen in soil solution include the exchangeable ammonium (NH₄⁺), nitrate (NO₃²⁻), and under certain conditions very small amounts of nitrite (NO₂⁻). The total amount of mineral nitrogen in soil solution accounts to less than 0.1% of total combined nitrogen in soil (8). When the organic matter of soil is decomposed by microbial activity, the covalent bond between the carbon and nitrogen in the amine group is broken. In this way, the amine group absorbs a hydrogen ion and a molecule of ammonia (NH₃) is released. The ammonia molecule soon absorbs another hydrogen ion and becomes an ammonium ion (NH₄⁺). This process, namely release of ammonium ions from decomposing organic matter due to microbial activity, is called as ammonification.



The ammonium ions present in the soil solution can be utilized by crops and microorganisms; however, a vast amount is attracted by the minerals having negative internal charges. In other words, the cation-exchange sites in soil adsorb these ions. These adsorbed ammonium ions can move freely into and out of these sites, hence are called as exchangeable ammonium. They remain in this form unless they are utilized by plants or microorganisms or are oxidized to nitrate. They can either be converted to the organic forms. The next step following ammonification is the two-stage oxidation of

ammonium ion to nitrite and nitrate, respectively. This process, called as nitrification, is carried out by specific microorganisms (*Nitrosomonas* sp. and *Nitrobacter* sp.) unlike ammonification.



The important factor affecting these two processes is the condition of soil. For any microorganism, a moist and warm soil containing adequate amounts of nutrients and organic matter is ideal to complete ammonification step rapidly. In the case of nitrification, the specific microorganisms require a well-aerated moist and warm soil. Because the ammonification step proceeds more slowly than nitrification, the amount of ammonium ions in soil is smaller than the nitrate amount. In addition to this, soils hardly contain significant amounts of nitrite because it is soon oxidized to nitrate to prevent the accumulation of this toxic compound. Consequently, the ammonium and nitrate forms exist as plant available mineral nitrogen in soil; however the principal form is nitrate (7, 8, 10).

Fixed ammonium

Fixation of ammonium occurs in two ways; however, both result in the same way that ammonium ions become unavailable to plants or microorganisms. This form of ammonium is called as the non-exchangeable ammonium and is released to soil solution very slowly.

Fixation by clay minerals:

Several clay minerals such as vermiculite, illite, montmorillonite, and kaolinite attract the ammonium ions in soil solution. The ammonium ions, which are held on the surfaces, are the exchangeable ones; however, sometimes the interlayer areas of these minerals trap these ions. In other words, they are fixed to the mineral like a rigid part of it and can not move (Figure 3.2).

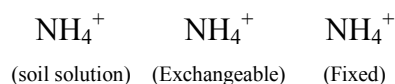




Figure 3.2. Fixed and exchangeable nitrogen (8).

Fixation by organic matter:

This kind of fixation occurs when the ammonium containing fertilizers are added to soil. The free ammonium ion reacts with the organic matter and becomes resistant to decomposition (6, 10).

3.2.1.3. Nitrogen Cycle

In all kinds of soil, there is an intake and loss of nitrogen through various complex transformations. Figure 3.3 explains all these transformations, in which nitrogen goes around and around. This is why; it is called as the nitrogen cycle.

The major portions of the cycle are mineralization and immobilization processes. Mineralization is the release of inorganic nitrogen ions (NH_4^+ and NO_3^-) from decomposing organic matter. This process involves the ammonification and nitrification steps. Immobilization is the reverse process, namely the conversion of inorganic ions to organic forms. Microorganisms use the inorganic ions in soil, to build up protein for their bodies, as well as if there is insufficient nitrogen in the plant and animal residues they are decomposing. In the same way, plants utilize the inorganic ions to produce building blocks of their organic bodies' (7).

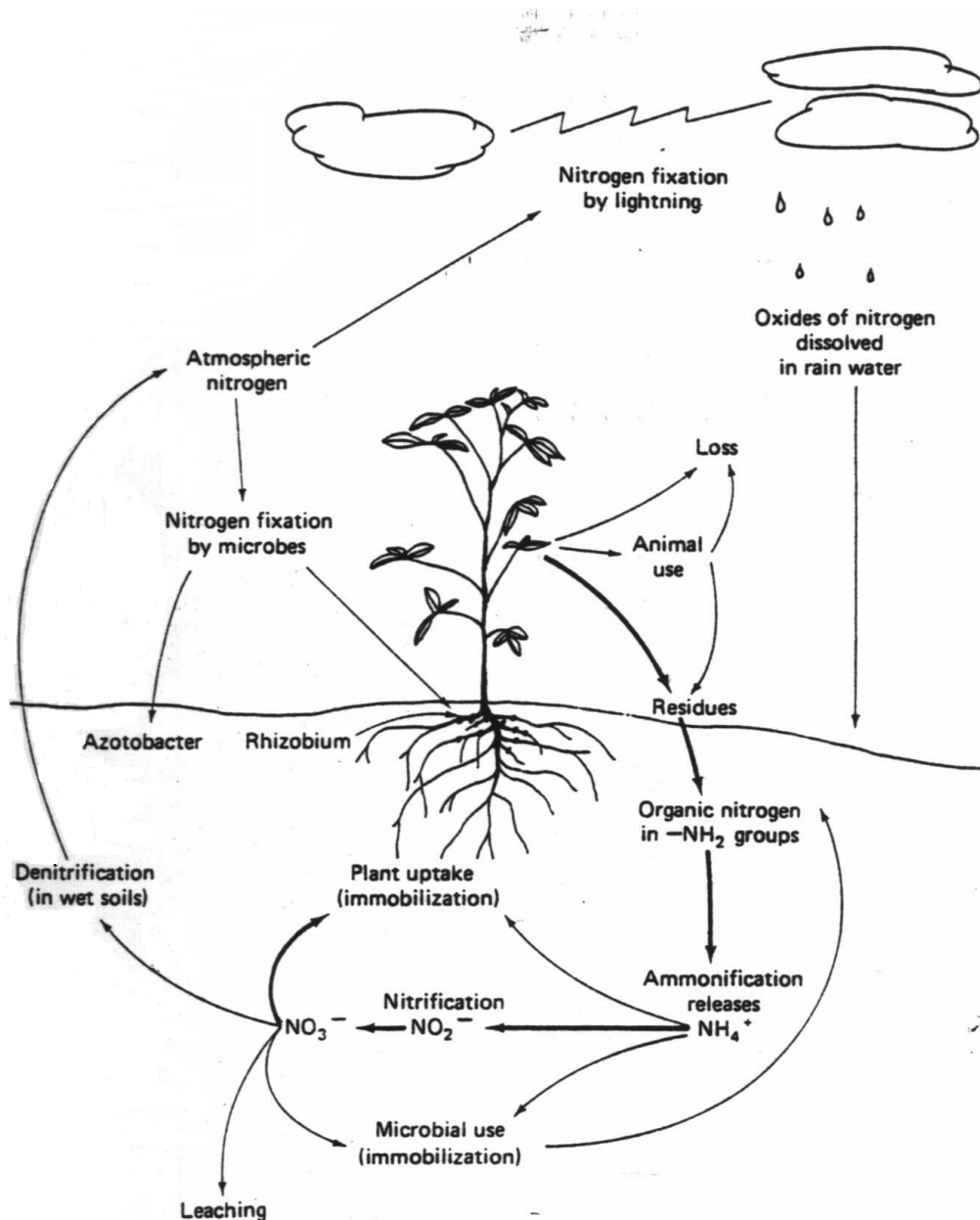


Figure 3.3. Nitrogen cycle (7).

3.2.1.4. Factors Affecting the Availability of Nitrogen

The maintenance of nitrogen in soil at adequate levels and regulation of its continuous availability to satisfy crop requirements are the problems encountered in the control of soil nitrogen. These problems arise from several factors: fixation of ammonia, immobilization and loss of nitrogen due to leaching, volatilization, denitrification, erosion and crop uptake. On the other hand, supply of nitrogen occurs by mineralization, fertilizer addition or by atmospheric fixation (Figure 3.4).

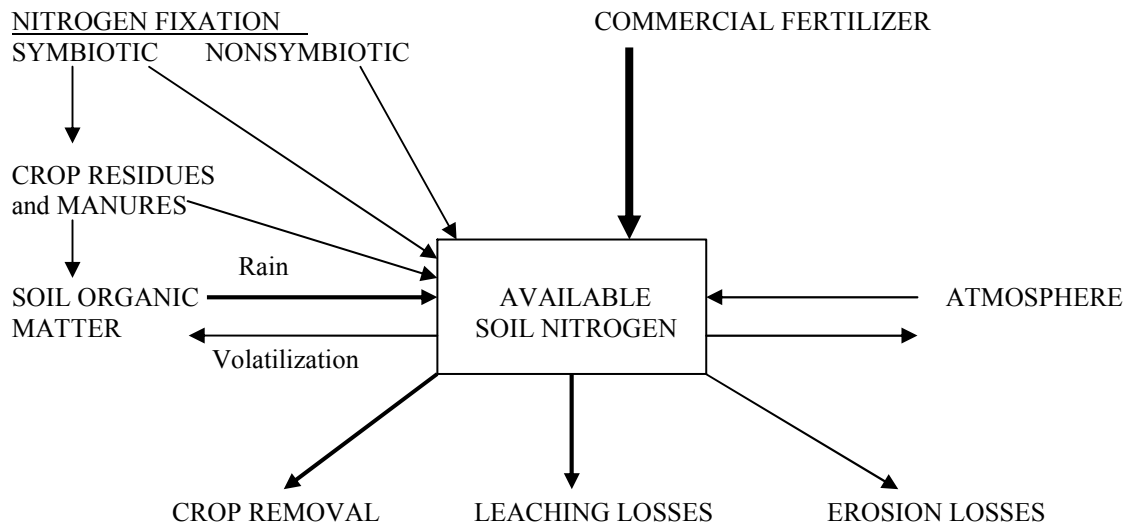


Figure 3.4. The major gains and losses of available soil nitrogen. The width of arrows shows the magnitude of gains and losses (6).

Losses of nitrogen

1) Leaching

The entire nitrate exists in the soil solution. Hence, it can readily be leached from soil. It is very soluble and mobile like ammonium. However, ammonium ions can be present as exchangeable ammonium in soil solution or as fixed ammonium. Therefore, some amount of ammonium ions can be prevented from leaching. The leached nitrates can be carried to groundwater levels, thereafter to lakes, rivers or streams. Since supply and regulation of this nutrient at adequate levels in soil is difficult and expensive, it will be a burden economically to lose significant amounts by leaching. Moreover, the accumulation of nitrate in the drinking water sources causes an environmental pollution problem. These hazards caused by leaching can be reduced by controlled application of nitrate fertilizers (7, 8).

2) Volatilization

Nitrogen can be lost to the atmosphere in the form of ammonia. At high pH and temperature, volatilization occurs whenever ammonium is at the surface of soil. However, the volatilization rate from ammonium fertilizers reduces when the soil cation-exchange capacity is high and when there is plant growth in soil (7, 8).

3) Denitrification

Denitrification is the most widespread volatilization type, which is the biochemical reduction of nitrate to gaseous form (N_2O), by the activity of anaerobic bacteria when

the soil is saturated with water. Under inadequate aerated soil conditions, the microorganisms, although they prefer elemental oxygen, utilize the oxygen of nitrate and transform it to gaseous nitrogen (6, 7).

4) Erosion

Nitrogen losses due to erosion can be estimated by multiplying the amount of soil, lost with the organic matter content percent. The erosion losses can be reduced by cultivation. The cultivated soils will have the nutrients homogeneously distributed throughout a certain depth of soil. However, in undisturbed lands, the nutrients are concentrated near the surface. Therefore, the erosion losses in these soils occur more seriously than that of in cultivated soil (10).

5) Plant uptake

The amount of nitrogen removed by crops for their growth, depends upon the land use, and varies widely from crop to crop.

Sources of nitrogen

1) Atmospheric fixation

The primary source of nitrogen is atmosphere. The original soil nitrogen is fixed by lightening and carried to the soil through rainfalls. The fixation of atmospheric nitrogen also takes place as a result of microbial activity either in a symbiotic or non-symbiotic way.

The best known microorganism is *Rhizobia*, which is capable of using molecular nitrogen (N_2) from atmosphere through symbiotic (mutually beneficial) relations. The other free-living microorganisms such as *Azotobacter*, *Clostridium*, or blue-green algae are responsible from non-symbiotic fixation of atmospheric nitrogen.

2) Nitrogen fertilizers

Either organic or inorganic, fertilizers are applied to soil to satisfy the demand of crop to nitrogen. Their presence is an advantage to maintain nitrogen at adequate levels in soil. Commonly, their application rate ranges from 20 or 30 lb/ac or kg/ha to a high of few hundred pounds per acre (6).

The examples to organic forms are manure, sewage sludge and effluent or compost piles. The inorganic, in other words mineral fertilizer are easier to use, more rapidly available to plants, more concentrated and are cheaper than the organic forms (Table3.2). Especially, the fertilizers containing nitrate. The nitrate ions will easily and soon be solubilized in the soil solution and become available to crop (7).

Table 3.2. Nitrogen Fertilizers (6).

Fertilizer	Chemical form	Percent Nitrogen
Ammonium Sulfate	$(\text{NH}_4)_2\text{SO}_4$	20.5
Ammonium Nitrate	NH_4NO_3	33.5
Sodium Nitrate	NaNO_3	16
Calcium Nitrate	$\text{Ca}(\text{NO}_3)_2$	15.5
Potassium Nitrate	KNO_3	14
Calcium Cyanamid	$\text{Ca}(\text{CN})_2$	18-21
Ammonium nitrate sulfate	$\text{NH}_4\text{NO}_3\text{-(NH}_4)_2\text{SO}_4$	26
Urea	$\text{CO}(\text{NH}_2)_2$	46
Ammonium chloride	NH_4Cl	25

3.2.2. Soil Phosphorus

Soil phosphorus is a widely used fertilizer element and is of great importance as nitrogen in the growth of plants. It is a key element in plant metabolism. However, at times, the supply of phosphorus can even be more critical than that of nitrogen. If the proper legume bacteria exist in soil, considerable amount of nitrogen can be supplied to soil temporarily, through atmospheric fixation of these bacteria. However, in the case of phosphorus supply, there is no such event of microbial aid. Consequently, the source of phosphorus is more limited than that of nitrogen. On the other hand, the lack of this element seriously affects the availability of other nutrients. For instance, the growth of legume bacteria is strongly influenced by phosphorus, which means that soil nitrogen is indirectly dependent on the supply of phosphorus. With various other factors that will be explained further, soil phosphorus becomes a critical nutrient element.

3.2.2.1. Effect on Plant Growth and Food

Phosphorus is distributed to every living cell in plant as a part of nucleoproteins that carry the genetic code of living things. It becomes united with carbon, hydrogen, oxygen, nitrogen and other elements to form complex organic molecules in the cell and is an essential constituent of the genetic material of cell nucleus.

Phosphorus has effects on cell division process, fat and albumin formation, therefore the deficiencies cause stunting and delayed maturity. Phosphorus in plants is concentrated mostly in the growing parts of plants and seeds. Thereof, shrivelled seeds are observed in the lack of this nutrient. It is also responsible for the storage, transfer and release of energy within plant through such compounds as adenosine diphosphate and adenosine triphosphate (ATP and ADP). For instance, some metabolic processes

such as starch and cellulose can be synthesized from sugar by expanding energy. Lack of phosphorus prevents this synthesis and causes conversion of sugar to anthocyanins, which shows its physical effect on plant as purple spots or streaks in leaves and stems. Moreover, in phosphorus deficiency, chlorophyll amount increases together with the presence of abundant nitrogen. This results in dark green colour of leaves as in the case of cabbage (6, 7, 9).

3.2.2.2. Forms of Soil Phosphorus

Phosphorus in soil can be present in two forms as organic phosphorus and inorganic phosphorus.

Inorganic phosphorus

Practically all the inorganic phosphorus in soils is present in the form of orthophosphates in the amounts ranging between 0.01 to 0.30% (10). Plants acquire all or most of their phosphorus requirement from soil solution in the form of phosphorus ions (mostly H_2PO_4^- and HPO_4^{2-}) although their amount at any one time is extremely small. This available form to plant is referred to as the dissolved phosphorus. The orthophosphate ions are formed by the ionization of one, two or all hydrogen of phosphoric acid (H_3PO_4) to form H_2PO_4^- , HPO_4^{2-} and PO_4^{3-} ions due to soil pH (Figure 3.5). It is considered that, plants demand mostly for the dihydrogen phosphate ion (H_2PO_4^-) in the rest of all and relatively smaller amount of HPO_4^- ions are utilized by plants when the soil has higher pH values. However, the PO_4^{3-} and H_3PO_4 molecule do not possess much importance in plant nutrition as the other two ions. Their predominance between each other strongly depends on soil pH (7).

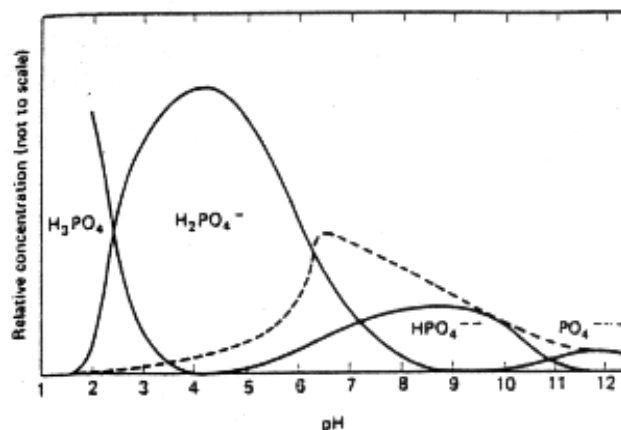



Figure 3.5. Phosphate ions in soil solution at different pH levels (7).

Most of the inorganic phosphorus in soil is combined with calcium, iron or aluminum (10). Some important calcium containing minerals are shown in the Table 3.3.

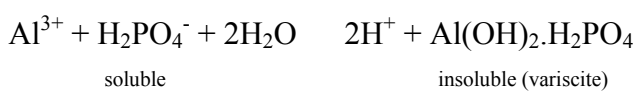
Table 3.3. Calcium Containing Inorganic Phosphorus Compounds (6).

Compound	Formula	
Fluor apatite	$3\text{Ca}_3(\text{PO}_4)_2 \cdot \text{CaF}_2$	
Carbonate apatite	$3\text{Ca}_3(\text{PO}_4)_2 \cdot \text{CaCO}_3$	
Hydroxy apatite	$3\text{Ca}_3(\text{PO}_4)_2 \cdot \text{Ca}(\text{OH})_2$	
Oxy apatite	$3\text{Ca}_3(\text{PO}_4)_2 \cdot \text{CaO}$	
Tricalcium phosphate	$\text{Ca}_3(\text{PO}_4)_2$	
Dicalcium phosphate	CaHPO_4	
Monocalcium phosphate	$\text{Ca}(\text{H}_2\text{PO}_4)_2$	

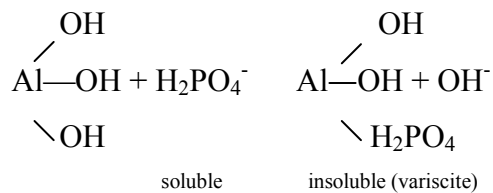
From these minerals, fluor apatite is the most insoluble thereby the most unavailable mineral, which is an original mineral, inherited from rocks. It occurs as tiny crystals well dispersed in rocks. As the rocks or minerals decompose by weathering or leaching, the phosphate ions dissolve into the soil solution. The simpler compounds of calcium such as mono or di calcium phosphate are more available for plant than the phosphorus in apatite crystals. The calcium phosphate compounds are stable in alkaline soils. Examples to the iron containing minerals are vivianite $[\text{Fe}(\text{PO}_4)_2 \cdot 8\text{H}_2\text{O}]$ and strengite $[\text{FePO}_4 \cdot 2\text{H}_2\text{O}]$ and the aluminum containing minerals are wavellite and variscite $(\text{AlPO}_4 \cdot 2\text{H}_2\text{O})$. These two types of minerals are extremely insoluble and stable in acid soils.

Sorption of phosphate:

As is well known, the major problem of phosphorus is solubility. The dissolved phosphorus in soil can be rapidly converted to insoluble inorganic forms by precipitation and adsorption (fixation) processes (10). In acid soil conditions such as pH 4, the concentration of iron and aluminum exceeds the H_2PO_4^- ion concentration. Consequently, the iron or aluminum ions rapidly react with H_2PO_4^- ions and precipitate as insoluble aluminum or iron phosphate compounds. This type of sorption is called as chemical precipitation by soluble aluminum or iron.

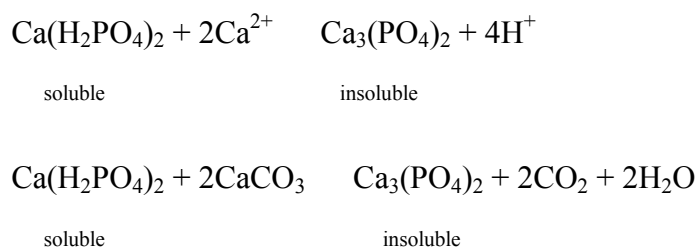


Besides chemical precipitation, under same acid conditions, the soluble phosphate ions can also react with the hydrous oxides of aluminum and iron. This reaction is the fixation by hydrous oxides of aluminum and iron. Both reactions end with the formation of hydroxyphosphates. However, fixation occurs relatively at a wider pH compared to precipitation.



The adsorption of phosphate ions by the positively charged sites on silicate minerals such as kaolinite, montmorillonite and illite takes place also under acid conditions. The adsorption occurs by the exchange of hydroxyl ions (OH^-) exposed on the surfaces of silicate minerals with the phosphate ion. In time, these adsorbed ions can migrate into the interior parts of the mineral, hence become less available than the adsorbed ones.

On the other hand, under mildly alkaline conditions, there is an abundance of exchangeable calcium (Ca^{2+}) and calcium carbonate (CaCO_3). The dissolved phosphate ions readily react with calcium and revert to insoluble calcium phosphate compounds.



In the same way, these inorganic calcium phosphate compounds can be converted to more insoluble compounds if sufficient time and favourable conditions are allowed (6, 7).

Organic phosphorus

Organic phosphorus is covalently bound to carbon and oxygen. Thus, it can not be ionised unless the organic matter is decomposed. Decomposition breaks the carbon oxygen bond and the organic phosphorus is mineralised to plant available form. The decomposition is a non-specific process that almost every microorganism can perform. However, the decomposition rate is slow. Examples to the organic phosphorus compounds in soil are inositol phosphates, which are sugar molecules containing phosphate groups replacing hydrogen; nucleic acids, phytin, phytin derivatives and phospholipids. The availability of organic phosphorus is more than the one in apatite crystals (6, 7). Below is a figure, classifying the phosphate compounds in soil.

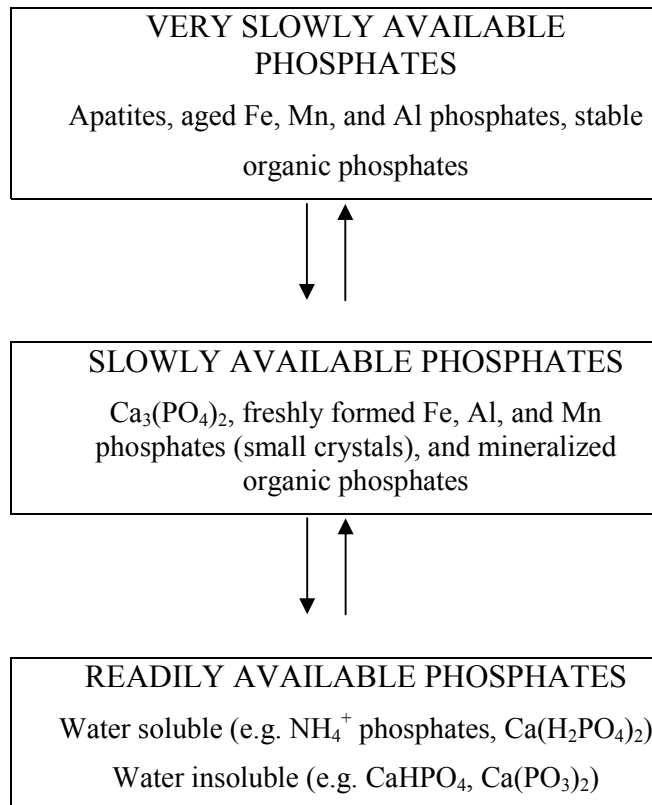


Figure 3.6. Classification of phosphate compounds in three groups (6).

3.2.2.3. Phosphorus Cycle

The phosphorus cycle (Figure 3.7) is simpler than the nitrogen cycle because exchanges with the atmosphere do not occur for phosphorus. The dissolved inorganic phosphorus ions (H₂PO₄⁻ and HPO₄²⁻) can be adsorbed either by positively charged clay

minerals or by organic matter. There is equilibrium between the dissolved phosphorus and the adsorbed and solid forms of phosphorus in soil (7).

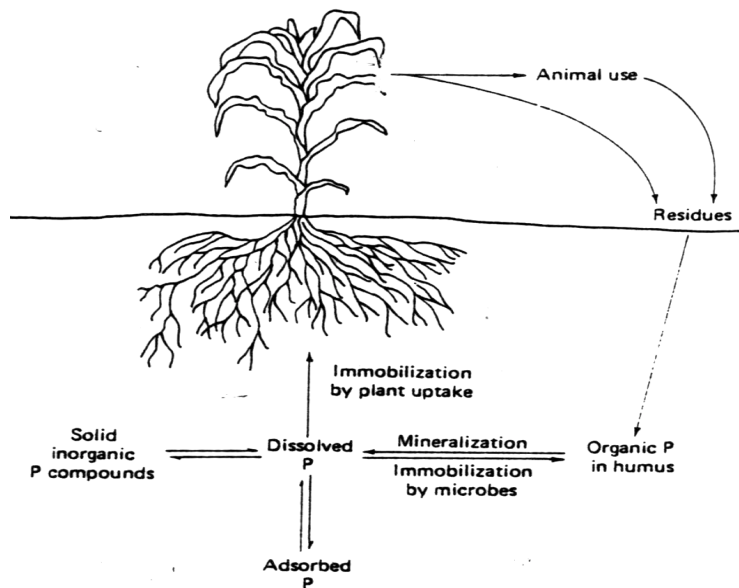


Figure 3.7. Phosphorus cycle (7).

3.2.2.4. Factors Affecting the Availability of Phosphorus

Inorganic phosphorus

The major problem of phosphorus in soils arises because of its insolubility. Although the amount of phosphorus taken up by crops is low, the application of phosphorus fertilizers to soil exceeds that of other nutrients except nitrogen. This is due to the rapid fixation or precipitation of available forms into insoluble compounds and to the unavailability of native solid phosphorus compounds in soil. In Figure 3.8, the thickness of arrows show that the major source of phosphorus is application of fertilizers and the major depletion is by fixation. The total available phosphorus in soil solution is always in very low amount.

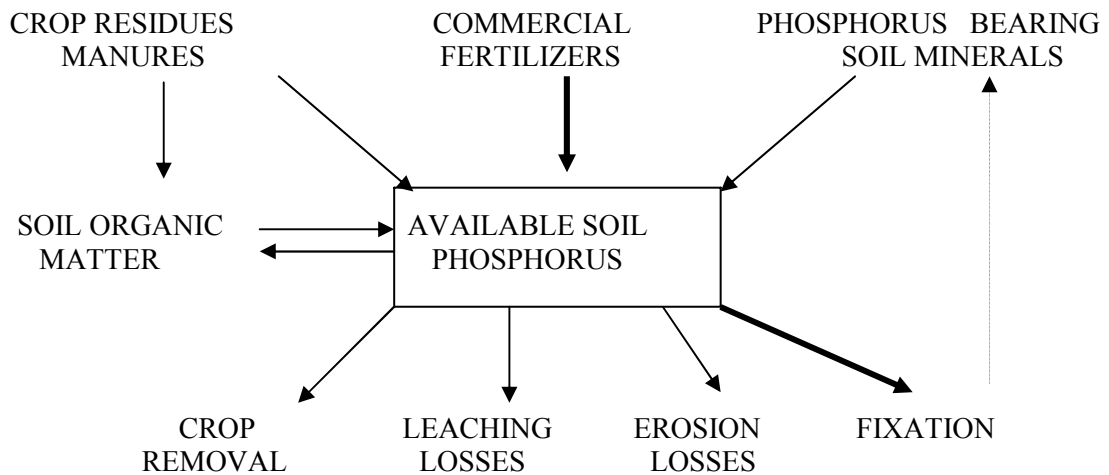


Figure 3.8. Gains and losses of available phosphorus in soil solution (6).

Consequently, rather than supplying sufficient amount of phosphorus to soil, increasing the availability of native soil phosphorus and prevention of fixation are of greater importance. The solubility of phosphorus strongly depends on soil pH, because pH affects both the types of phosphorus ions present in soil solution and the concentrations of precipitating ions, aluminum, iron and calcium. In addition to this, the clay mineral type, amount of organic matter and water present in soil solution and the decomposing microorganisms are some other factors effecting inorganic phosphorus availability. The presence of organic matter increases the availability of phosphorus by tying up the aluminum and iron ions to its structure. This results in the presence of lesser amounts of these ions in soil solution to precipitate into insoluble phosphorus compounds. The microorganisms decomposing organic matter can also temporarily tie up the dissolved phosphorus ions into their microbial tissue. The amount of water in soil is important since the dissolved phosphorus ions can be carried to the plant roots by the aid of water. Moreover, leaching and weathering are also significant in obtaining an amount of available phosphorus from native solid phosphorus compounds such as apatite in time.

The practical control of phosphorus availability can be managed by several applications; however these precautions are not able to prevent the insolubility problem totally. In acid soils, liming is an alternative to the application of large amounts of fertilizers. Addition of lime increases the pH up to 6 or 7, which ensures the optimum conditions for highest solubility as well as precipitates the hydroxides of iron and aluminum and the other low solubility compounds (7). The low concentrations of iron and aluminum in soil solution mean that the precipitation rate of phosphorus with these

ions will be lower. Consequently, more phosphorus that is available can be acquired. The application of fertilizers should be performed in a manner that the distance between the fertilizer and the plant root should be as minimum as possible. Generally, the phosphorus fertilizers are applied in localized bands around the plant root to minimize the contact with soil, thereby any possible fixation (6). Table 3.4 explains the phosphorus fertilizers applied to soil.

Table 3.4. Phosphorus Fertilizers (6).

Fertilizer	Chemical Form	Phosphorus%	Approximate % of available P ₂ O ₅
Superphosphates	Ca(H ₂ PO ₄) ₂ and CaHPO ₄	7-22	16-50
Ammonium Phosphate	NH ₄ H ₂ PO ₄	21	48
Diammonium Phosphate	(NH ₄) ₂ HPO ₄	20-23	46-53
Phosphoric acid	H ₃ PO ₄	24	54
Calcium metaphosphate	Ca ₃ (PO ₃) ₂	27-28	62-63

Organic phosphorus

The availability of organic phosphorus depends on the soil pH, climate, and cultivation. In most soils in temperate regions, the mineralization of organic phosphorus is not considered as an important phosphorus source unlike the soils in tropical regions. This means that the mineralization of organic phosphorus increases with increasing temperature, particularly at 30°C. Moreover, increasing soil pH has also an increasing affect on the mineralization rate. Heating, drying, and liming are some other factors increasing mineralization rate (10).

3.2.3. Soil Potassium

Potassium is the third nutrient element to limit plant growth, which is commonly used in fertilizers. Plants require large amounts of potassium and sometimes they use even more than the soil can supply. It is absorbed by plants in the form of K⁺. Unlike nitrogen and phosphorus, potassium nutrient is not involved in the internal part of the structure of any organic compound because its single electron is not involved in any

covalent bonding. Thus, potassium is always ionisable and is present in the solution of either soil or plant (7).

3.2.3.1. Effect on Plant Growth and Food

The major function of potassium in plant is to maintain swelling of cells by regulating osmotic concentration. It is essential in the formation and transportation of starch and protein as well as in the development of chlorophyll. Potassium ions tend to be located in the growing tissues. In case of deficiency, they are carried from the older tissues to the younger ones. Therefore, symptoms of deficiency can be observed first on the older parts of plant. For example, the color of leaves turn into yellow or brown color or small, brown, and dead spots can be observed on the leaves as in the case of cabbage. In addition, the leaves of cabbage become curly and they dry soon. The potassium deficiency effects on carrots are reduced sugar content thereby a change in the taste and reduced lasting during storage (9). Potassium also aids in the uptake of other nutrients and their movement within the plant. For instance, K^+ and NO_3^{2-} ions may move together. The damaging effects due to the utilization of excessive nitrogen in plant tissue can be cured by adequate supply of potassium to plant. Moreover, the toughness of tissue can be enhanced with this element thereby the resistance of crops to certain diseases can also be increased. Consequently, the deficiency of potassium affects fruit quality, plant health and growth (6, 12).

3.2.3.2. Forms of Potassium in Soil

The problem of potassium deficiency is due to its unavailability. In fact, the total amount of potassium in soil is high except the sandy soils, such that the amount exceeds that of any other major nutrient element. However, the available form to plant (K^+) is generally in very low amounts as in the case of nitrogen and phosphorus. Also, much of it can be readily leached from soil (6).

Structural potassium

The original source of potassium in soil is formed from weathering of potassium bearing minerals. Feldspars and micas are the two most important minerals containing potassium in their structure. Structural potassium is the unavailable form to plants and its release to soil solution throughout a growing season is not of considerable significance due to the resistance of feldspars and micas to weathering processes.

However, their contribution to the overall available potassium content of soils from year to year should not be neglected (6, 13).

Fixed potassium

As the structures of the primary minerals are physically and chemically altered (broken or opened) by weathering or by the action of solvents such as carbonated water, secondary layer silicate clays can be formed. These minerals such as vermiculite, illite bare potassium ions in the crystal structure or in interlayer positions such that the potassium ions perfectly fit into the holes of minerals and become fixed there as in the case of ammonium ions. These fixed potassium ions are also called as non-exchangeable potassium in soil. Such minerals may enhance the amount of dissolved potassium slowly in time due to the degree of weathering and to the amount of potassium they contain (6, 7, 13).

Exchangeable potassium

The negatively charged sites of clay minerals and organic matter attract the potassium ions in soil solution and due to the relatively low energy of attraction, these potassium ions are called as exchangeable. They can readily become available unless a plant root reaches them and an exchange of cations occurs. Soil organic matter also has negative charged parts such as acidic functional groups (carboxyls, phenols, enols) or organic polymers. However, the affinity of these exchange sites for potassium ion is relatively low (7, 13).

Dissolved potassium

Potassium ion in the soil solution is the available form of this nutrient to plants. Exchangeable and dissolved potassium together matches for the 1 to 2% of total potassium content in an average mineral soil. And about 90% of this readily available form is dissolved potassium (6). These ions can be rapidly converted to the less available forms. The relationship between the forms of potassium is shown in Figure 3.9.



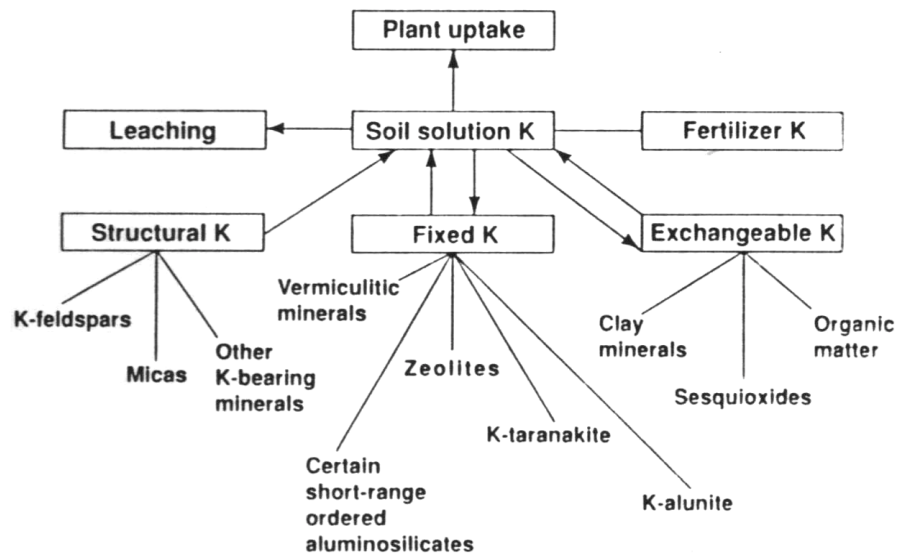


Figure 3.9. Forms of soil potassium (13).

3.2.3.3. Factors Affecting Availability of Potassium

The mineral type of soil strongly affects the rate of potassium fixation. For example, the 1:1 (Si:O) type clays such as kaolinite have the ability to fix little potassium. On the other hand, 2:1 type clays such as vermiculite and illite have a high fixing capacity of potassium. The same mechanism is valid for the fixation of ammonium. The potassium deficiency is more likely to occur in acid soils than in neutral soils due to the presence of many H^+ ions and less of all other cations on exchange sites and in solution. The application of lime to soil enhances the rate of potassium fixation. This factor is sometimes used in a beneficial way such that in well-limed soils, the loss of potassium by leaching can be prevented. Leaching and erosion causes a loss of potassium exceeding that of nitrogen and phosphorus. The other factors are environmental factors, which are wetting and drying, warming and cooling, and freezing and thawing. These physical effects break down the structure of minerals in which potassium can be more easily released. The potassium deficiency can be improved by the application of potassium containing commercial fertilizers. These fertilizers are called as potash fertilizers (Table 3.5) and are water-soluble thereby readily available to plants (6, 7).

Table 3.5. Potash Fertilizers (6).

Fertilizers	Chemical Form	K ₂ O%	K%
Potassium chloride	KCl	48-60	40-50
Potassium sulfate	K ₂ SO ₄	48-50	40-42
Potassium nitrate	KNO	44	37

Chapter 4

SPECTROSCOPIC TECHNIQUES COUPLED WITH MULTIVARIATE CALIBRATION METHODS

4.1. Near Infrared Spectroscopy

4.1.1. Theory of near infrared spectroscopy

Near infrared spectroscopy is a spectrophotometric method that deals with the interactions of near infrared radiation with the sample under investigation. It is based on the absorption of electromagnetic radiation at wavelengths in the range of 780-2500 nm.

The absorption of infrared radiation depends on the net change in dipole moment of the molecule as a consequence of its vibrational motion. The atoms in a molecule are not positioned fixed but instead fluctuate continuously due to the different types of vibrational motions about the bonds in the molecule (1). These vibrations fall into two basic categories, stretching and bending vibrations as shown in Figure 4.1.

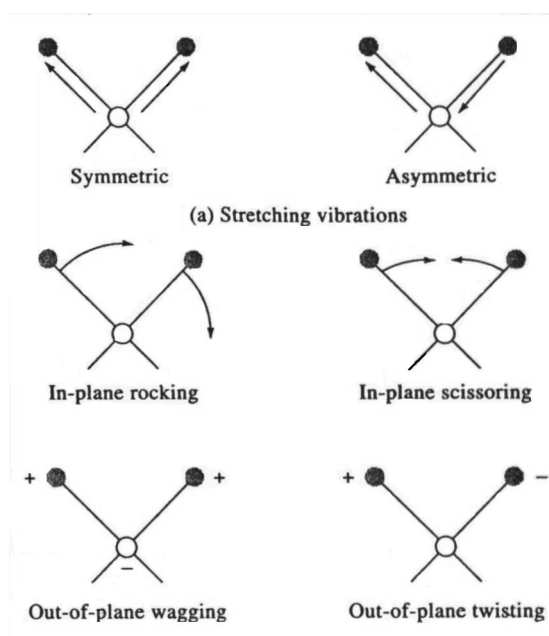


Figure 4.1. Types of molecular vibrations (1).

When the vibrations are accompanied by a change in dipole moment, and when the frequency of vibration matches the frequency of infrared radiation, a transfer of net

energy from the radiation to the molecule will be observed. This results in a change in the amplitude of the molecular vibration. That is, the vibration absorbs the infrared radiation and the molecule is excited to a higher energy level. This energy transmission can be measured as the plot of energy (reflectance, absorption or transmittance) versus wavelength, which is called as a spectrum.

All the molecules except the symmetric molecules (homonuclear diatomic molecules) such as H₂, O₂ or Cl₂, can absorb the infrared radiation as mentioned, hence are called as infrared active. However, the vibrations of symmetric molecules are not accompanied by a change in dipole moment and are considered as infrared inactive (5). The vibrational motion of two atoms can be illustrated by the movement of two spheres connected by a spring (Figure 4.2).

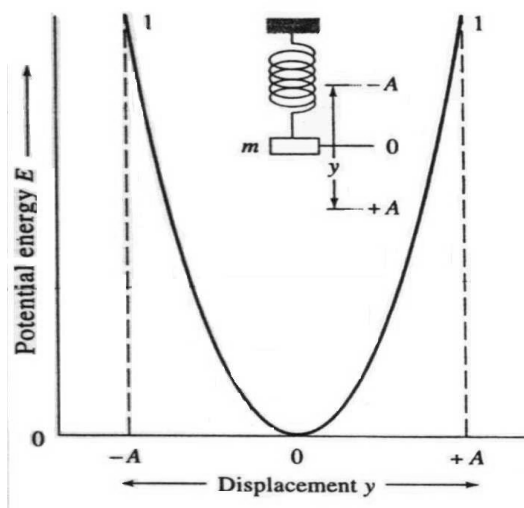


Figure 4.2. Potential diagram of harmonic oscillation (1).

The stiffness of the spring represents the bond strength and the masses of spheres represent the masses of the atoms. If one of these masses is disturbed along the axis of the spring, the vibrations obey the law of simple harmonic oscillation, in other words Hooke's Law.

The frequency of vibration can be calculated as:

$$\nu = \frac{1}{2\pi} \times \left(\frac{k}{\mu} \right)^{1/2} \quad 4.1$$

$$\mu = \frac{m_1 \times m_2}{m_1 + m_2} \quad 4.2$$

$$\nu = \frac{1}{2\pi} \times \sqrt{\frac{k \times (m_1 + m_2)}{m_1 \times m_2}} \quad 4.3$$

where ν is vibrational frequency (cm^{-1}), k is the classical force constant, μ is the reduced mass of the two atoms and m_1 and m_2 are the masses of atoms, 1 and 2 respectively.

And the potential energy of simple harmonic oscillation is:

$$E = \frac{1}{2} \times k \times x^2 \quad 4.4$$

where x is the displacement of the internuclear distance.

However, the harmonic oscillation equations do not adequately explain the behaviour of atoms. The energy is not transferred continuously, but in discrete packets, which are called quanta (14). The discrete energy levels are defined by whole numbers 0, 1, 2... and the potential energy can be written as:

$$E = \left(\nu + \frac{1}{2} \right) \times \frac{h}{2\pi} \times \sqrt{\frac{k}{\mu}} \quad 4.5$$

where h represents the Planck's constant and ν is the vibrational quantum number.

Thus, unlike harmonic oscillation equation in which the vibrations can have any potential energy, quantum mechanical equations can take only certain discrete energies. By substituting Equation 4.1 into 4.5, the energy equation will be:

$$E = \left(\nu + \frac{1}{2} \right) \times h \times \nu \quad 4.6$$

From this equation, the net energy transition between two energy levels can be calculated:

$$\nu = 0 \quad E = \frac{1}{2} \times h \times \nu \quad 4.7$$

$$\nu = 1 \quad E = \frac{3}{2} \times h \times \nu \quad 4.8$$

$$\Delta E = \frac{3}{2} \times h \times \nu - \frac{1}{2} \times h \times \nu = h \times \nu \quad 4.9$$

At room temperature, all the molecules remain at zero energy level. The possible transition from 0 to 1 in any one of the vibrational state ($\nu_1, \nu_2, \nu_3, \dots$) is called a fundamental transition ($\Delta\nu = \pm 1$) (1). This kind of transition is allowed in harmonic oscillation due to the selection rule of the quantum theory, which states that the only

transition can take place in a unit change in the vibrational quantum number ($\Delta v = \pm 1$). As the stretching vibration of a chemical bond is extended in a molecule, the chemical bond can break if the vibrational energy level reaches the dissociation energy that is the energy required to dissociate two atoms repelling each other. In this case, transitions from energy level 0 to 2, 0 to 3 etc. are observed and are considered as first, second, etc. overtones. The overtones have frequencies two, three etc. times that of the fundamental but have intensities much weaker than the fundamental bonds. The vibration of higher energy levels can be illustrated by the anharmonic oscillation (Figure 4.3).

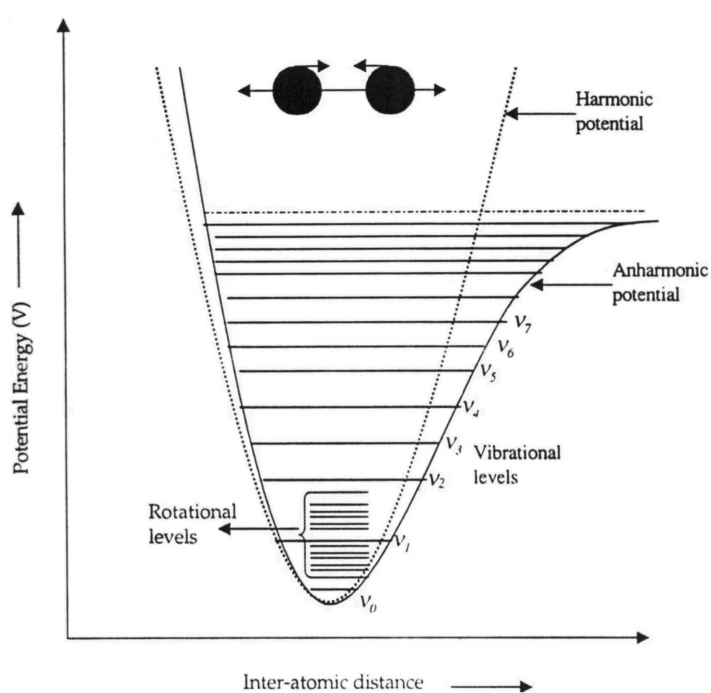


Figure 4.3. Potential energy of anharmonic oscillation (16).

As it can be seen from Figure 4.3, due to the dissociation at higher energy levels, the molecules do not return to their equilibrium states. In addition to the overtone lines, combination bands can also be observed as a result of simultaneous excitation of two vibrational modes by a photon. This event occurs when the energy is absorbed by two bonds rather than one, and the frequency of combination band can be the sum or difference of two fundamental frequencies. As a consequence, according to the selection rules of an ideal harmonic oscillation, only fundamental vibrations are allowed and transitions between more than one vibrational state (overtones and combination bands) are not allowed, but do appear as weak bands as a result of anharmonic oscillation

(1,15). Most of the absorption bands observed in the near infrared region are overtones and combinations of fundamental stretching vibrational bands in the mid infrared region. The bonds responsible for this kind of absorption bands, are strong bonds having the lightest atom (hydrogen) and a heavier atom such as carbon, oxygen or nitrogen (C-H, N-H, O-H) (Figure 4.4).

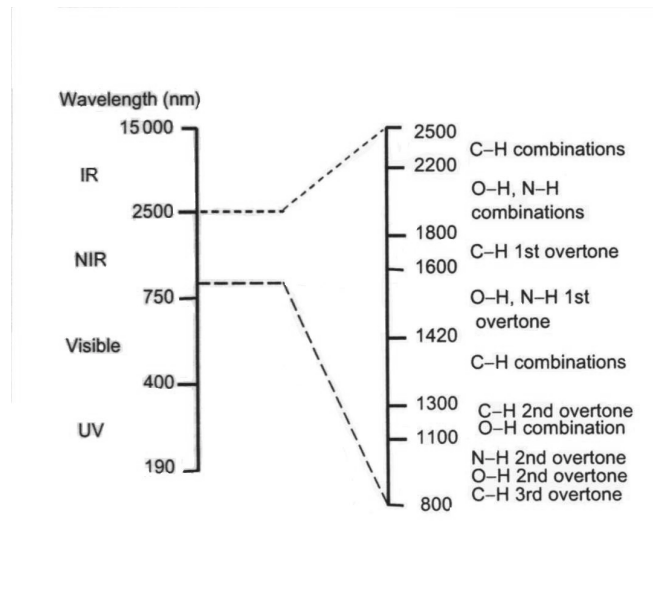


Figure 4.4. Near infrared absorption bands and their locations (14).

The near infrared spectroscopy has some advantages over the other infrared spectroscopy types. In contrast to mid-infrared spectroscopy, near infrared spectroscopy can be used for the quantitative determination of species such as water, proteins, fats and low molecular weight hydrocarbons in agricultural, food, petroleum and chemical industries (1). Several modes of operation such as diffuse reflectance, transmittance or absorbance measurements are possible which reduce the sample preparation steps. Thus, this technique is simple and rapid which can make multiple measurements within a few seconds. Furthermore, the technique is non-invasive and non-destructive since the energies in the near infrared region are low. Near infrared spectroscopy has high sensitivity relative to other infrared techniques and the instrumentation is cheaper (16).

The near infrared instrumentation is generally divided into two classes according to their properties. The first one is dispersive near infrared spectrophotometers and the other is Fourier transform infrared spectrophotometer. The instrumentation of dispersive near infrared spectroscopy resembles to that of UV-visible spectroscopy hence the UV-

visible instruments are generally designed to cover the near infrared region as well. Tungsten-halogen lamps are the most common sources with quartz windows, which are capable of working in the visible and near infrared region. Sample cells vary from 0.1 to 10 cm and are made up of quartz or fused silica. The optical configurations of dispersive instruments depend on the employed monochromator type, which is used for the selection of desired wavelengths. Some of these employ interference filters to provide radiation in a narrow range. And, some use grating monochromators, which are suitable for transmittance or reflectance measurements. In addition, infrared-emitting diodes can also be employed as both the wavelength selection system and the light source (400-1700 nm). The detectors used are generally silicon detectors covering the range 400-1100 nm, Indium gallium arsenide (800-1700 nm), lead sulfide (PbS) (1100-2500 nm), or lead selenide (PbSe) (1000-5000 nm). For online monitoring of samples, remote sensors or fiber-optic probes are used which are low cost, rapid and capable of making accurate and stable calibration (1,14).

In this study, the experiments were performed with a near infrared reflectance spectrophotometer, operating in the diffuse reflectance mode (Figure 4.5). Diffuse reflectance is the scattering of incident radiation from the sample (Figure 4.6).

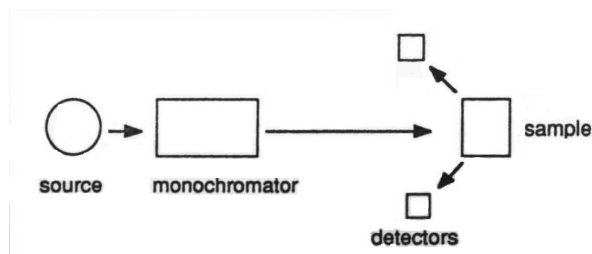


Figure 4.5. Near infrared reflectance spectrometer (15).

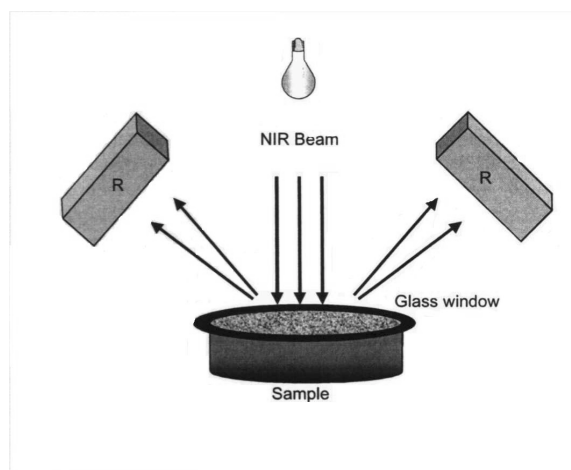


Figure 4.6. Diffuse reflectance analysis (14).

As it can be seen from Figure 4.6, the near infrared radiation penetrates the surface layer of powdered sample and excites molecular vibration and then it is scattered from the sample. In this case, the diffusely reflected radiation (R) is the ratio of the intensity of the radiation reflected from the sample to that of the standard reflector, such as a ceramic disk and it is converted to absorbance by the expression $\log 1/R$. It depends on the concentration (c) of the analyte in the sample based on the Beer's law.

$$-\log R = \log (1/ R) = k \times c \quad 4.10$$

k is the factor of both absorptivity and path length (14).

4.1.2. Applications of Near Infrared Spectroscopy

The applications of near infrared spectroscopy (NIRS) involve the analysis of agricultural products, food products, polymers, wool, textiles as well as pharmaceutical, biomedical and process analysis. In food industry, the applications are cereals and cereal products, milk and dairy products, meat, fish, fruit and vegetables confectionery and beverages (14,15).

In cereal industry, near infrared spectroscopy can be applied to the analysis of moisture, protein, fat, starch, sugars and fiber in products such as bread, biscuits, cake mixes, breakfast cereals, pasta and snack foods as shown in Table 4.1.

Table 4.1. Near infrared applications of cereal products (14).

Product	Moisture	Protein	Fat	Starch	Sugars	Fiber
Bread	✓	✓	✓	✓	✓	
Biscuits			✓		✓	
Cake mixes			✓		✓	
Breakfast cereals			✓			✓
Pasta	✓	✓	✓			
Snack foods				✓		✓

For instance, extrusion cooking is applied to cereal-based raw materials to produce extruded snack foods, breakfast cereals or pet foods. During this process, the structure of starch in cereals mainly affects the quality parameters, texture and density of the final product. For this aim, the possibility of applying near infrared spectroscopy was examined to monitor the changes in starch structure during extrusion. First the extruded products, which were prepared by several processing conditions, were freeze-dried and

ground before near infrared analysis. Since satisfactory calibrations were obtained related to starch structure, the second attempt was to monitor the changes during cooking by installing a fiber optic probe into the extruder. The spectral characteristics of starch in the extruder were close to that of powdered samples. Hence, with this research a way to monitoring online the extrusion process and controlling was opened (14).

Another study with the cereal products is, detecting the changes of wheat bread during storage. As bread staling is an important problem during storage, bread firmness becomes an important parameter in assessing the staling rate. The results obtained by physical compression with a texture analyser were compared with the near infrared reflectance (550-1700 nm) results of the same bread. The near infrared measurements were based on the detection of moisture loss and starch crystallinity. Starch crystallinity is extensively hydrogen bonded to water and this results in a decrease in the absorbance over time. The near infrared spectra had high relationship with the texture analyser firmness results ($R^2=0.8029$ with a partial least squares factor of 8) which indicates that near infrared spectroscopy has the ability to follow firmness during bread staling (17).

In dairy industry, near infrared reflectance spectroscopy has a role in the analysis of protein, fat, lactose, moisture and process control. Milk, dried whole milk, skim milk and whey powders, cream and traditional and processed cheese are the wide range of dairy products (14).

Sorensen et al. (1998) studied the prediction of consistency (springy, sticky, coherent, soluble, and hard) and flavour (cheesy, acid, sweet, unclear) properties of cheese during ripening by near infrared spectroscopy. Thirty-two samples of cheese were produced in a pilot plant with three control variables, pH, moisture and microbiological contamination. The transmittance (850-1050 nm) and reflectance (1110-2490 nm) measurements were taken during ripening at the same time as a panel of 10 performed the sensory analyses. Calibration equations for consistency and texture properties obtained by partial least squares regression and regression coefficients for consistency and flavour were 0.74-0.88 and 0.27-0.59, respectively. The results show that for certain sensory properties (consistency), near infrared spectroscopy may provide rapid and reproducible results (18).

In meat industry, near infrared spectroscopy has been used for sorting of carcasses due to their fat contents together with fiber optic probes as well as for the determination of protein, fat and moisture contents of ground meat and meat products (14). The following quality attributes sensory tenderness, texture, flavour acceptability and

Warner-Bratzler shear force of beef were predicted by near infrared reflectance spectroscopy (750-1098 nm) coupled with fiber optic probe. In this study, the measurement was neither transmission nor reflectance, but a combination of these two, which is called as interactance. The radiation is transmitted through the sample and then reflected from the surface of the sample. Furthermore, this illumination and detection are performed at laterally different points on the sample's surface with the aid of fiber-optic bundle. This kind of measurement is useful for the analysis of large samples as in the case of beef. The near-infrared reflectance measurements were taken after 1, 2, 7 and 14 days post mortem from freshly cut beefs. And predictive models were produced by principal component regression and partial least square between the near infrared and sensory analysis results. The beef quality attributes were studied and near infrared data were in good correlations especially for the Warner-Bratzler shearforce and tenderness values. However, more number of animals could be used in the study to increase the variability range for a better predictive ability of near infrared reflectance spectroscopy (14,19).

Either in fish samples, it is possible to analyze fat moisture and protein contents which was studied by Valdes et al (1997). 68 samples of 9 different fish species were analyzed for their moisture, fat and protein contents by freeze-drying, extraction with petroleum ether and macro-Kjeldahl method, respectively. Following chemical analyses, the freeze-dried samples were scanned with near-infrared spectrophotometer and calibrations were developed using partial least squares. The coefficients of regression, which were calculated by PLS method, were 0.93, 0.97 and 0.48 for protein, fat and moisture, respectively (20).

Furthermore, fruits such as peaches, mandarins, melons, mangoes, etc. can be sorted due to their ripeness by fiber-optic interactance probes coupled to near infrared spectrophotometers. The measurement is based on the determination of sugar content of fruit. In addition to this, alcoholic beverages such as beer, wine can be analyzed for their alcohol, water and sugar contents. However, in this case, the measurement is done by transreflectance, which is another type of combination of transmittance and reflectance. In transreflectance, the transmitted radiation through the sample is reflected from the sample holder. Other applications of non-alcoholic beverages involve the analysis of moisture, caffeine, and sugar in tea, coffee and fruit juices (14,15)

In agricultural industry, soil and plants have been also used in the analysis of several constituents with near infrared spectroscopy. For instance, the carbon, nitrogen and

phosphorus contents of several plant materials of which are green needles, falling needles and litter were predicted with near infrared reflectance spectroscopy. The aim was to analyze whether good calibrations could be performed within each stage of transformation of needles. Principal component analysis were carried out to discriminate the three sets of sample and partial least-squares regression was used to develop a calibration between near infrared reflectance data (400-2500 nm) and the standard wet chemical analyses. The results showed that there was an increase in the absorbance in the UV region as the samples were scanned in the order of, green needles, falling needles and litter (brown in color). The reverse pattern was valid in the near infrared region. On the other hand, the accuracy of calibration equations of nitrogen ($R^2=0.94-0.99$) and carbon ($R^2=0.97-0.99$) was better than that of phosphorus ($R^2=0.94-0.99$). This was due to the fact that phosphorus does not directly absorb the radiation and the calibrations for this kind of constituent depend on the secondary correlations. That is, the correlations between the constituent to be predicted and another component of the sample that can be measured by the near infrared spectroscopy (21).

The studies on determining the soil attributes with the near infrared spectrophotometer include sensing of soil organic matter, moisture, organic carbon, total nitrogen and cation exchange capacity. R. C. Dalal and R. J. Henry (1986) performed a study on the simultaneous determination of soil organic carbon, moisture and total nitrogen by near infrared spectrophotometer. Three soil types, sampled at five different points of field, were air dried and grinded for the organic carbon and total nitrogen analysis with the near infrared spectrophotometer. The equipment operated in a wavelength range of 1100 to 2500 nm and the calibration equations for moisture, organic carbon and total nitrogen were calculated according to the wavelengths which gave the lowest standard error of estimate in the multiple regression analysis. The soil samples were also analyzed for total nitrogen, organic carbon and moisture contents in the laboratory by Kjeldahl method, Walkley-Black method and gravimetric method respectively. The results showed that a reliable prediction of organic carbon and total nitrogen amount in soil was possible with near infrared spectrophotometer together with multivariate analysis. The regression coefficients were 0.96 for moisture and 0.93 for organic carbon and total nitrogen and the standard error of prediction for moisture was greater than organic carbon and total nitrogen. These values imply that the prediction of moisture could be more accurately performed than the organic carbon and total nitrogen predictions. It was also understood that the near infrared spectra were very sensitive to

moisture changes and to the particle size of the sample. The smaller the particle sizes the higher the reliability of measurements especially for moisture. The only disadvantage is that the prediction of organic carbon and total nitrogen could be more accurately performed within a narrow range of soil color (22).

Cropping system management is generally practiced with fertilizers, pesticides and seeds applied over the whole field to manage the variability of requirements of soil by obtaining a uniform structure. For the effective control of weed on farm, herbicide application is a very useful tool. However, the excessive application of this chemical causes an environmental problem in groundwater and in surface water. Thus, the control of herbicide application is necessary and important in the aspect of site-specific crop production (23). For this aim, Sudduth and Hummel (1993a) developed a portable near infrared spectrophotometer for the rapid analyses of soil organic matter as a control input for herbicide application. The instrument was composed of a broadband halogen lamp as the illumination source, and a circular variable filter monochromator for the selection of wavelength, which ensures a simpler operation and ruggedness. The fiber optic bundle before the sample was used for remote sensing, and a lead sulfide photodetector capturing the energy reflected from soil surface has the advantages of lower cost, higher responsivity and ability to operate without cooling. Finally, a software algorithm supplied a zero baseline in the AC-coupled instrument readings. As a result of performance tests in the laboratory, a sensing range of 1650 to 2650 nm, an optical bandwidth of 52 nm and a data acquisition rate of 5 Hz were found to be optimal. A good agreement between the reflectance curves of this instrument and the research grade spectrophotometer data was obtained as well (24).

The further studies of Sudduth and Hummel (1993b) were development and evaluation of laboratory calibrations of soil organic carbon, soil moisture and cation exchange capacity determined with the portable near infrared spectrophotometer and field test the instrument together with the evaluation of accuracy of soil organic carbon predictions. Thirty Illinois soils were used for the laboratory analysis. They were removed from foreign particles and were crushed to pass through a 2 mm sieve. After oven drying, the soil samples were moisturised into two moisture tension levels, 0.033 MPa (field capacity) and 1.5 Mpa (wilting point). Finally, they were stored in plastic bags at 10°C for 5 days to equilibrate the moisture with the soil. The best prediction of organic carbon by the laboratory tests was obtained for average of 100 scans of each soil sample over a wavelength range of 1640-2640 nm [R^2 : 0.89 with a standard error of

prediction (SEP) 0.23% organic carbon]. The prediction of moisture and cation exchange capacity (CEC) for thirty Illinois soils were successfully performed with a SEP of 1.59% moisture (R^2 : 0.97), and 3.59 mEq/100g for CEC (R^2 : 0.86). In addition to the calibration tests, it has been also found that normalisation of wavelength data reduced the effect of sample to sensor height variability on the calibration organic carbon. Furthermore, moving soil sample during data acquisition decreased the predictive capability of organic carbon. Hence, for the prediction of organic carbon in the field, some modifications on the instrument were made. A suitable sample presentation mechanism was added and the sensor was packaged to enable it to operate on a moving vehicle and withstand harsh field conditions. Although the mechanism of the instrument worked quite well in the field, the prediction of soil organic carbon was not accurate (25).

4.2. Laser Induced Fluorescence Spectroscopy

As mentioned in the previous section, near infrared reflectance spectroscopy has wide application in food and agriculture industries and possesses the possibility of making on-line analysis with the aid of fiber optic sensors. Laser induced fluorescence spectroscopy (LIFS) is the second instrumental technique that is investigated which is applicable to soil and food samples and has the potential to be integrated to on-line analyses.

Fluorescence is a spectrochemical method in which the analyte in the molecule absorbs radiation at a certain wavelength (usually UV and visible regions). The electrons of the analyte are excited to higher energy states from ground state, but soon relaxation occurs from higher vibrational states to the lower vibrational state of the excited electronic state. Following this relaxation, the electrons return back to their ground state by emitting a photon. This is called as fluorescence emission (Figure 4.7) (2,26). This process is relatively rapid and is non-resonance. Resonance means that the excitation and emission energies are equal. However, in fluorescence emission, due to energy losses between vibrational states, the energy of excitation energy is greater than the emission energy. This is referred to as Stokes shift (1).

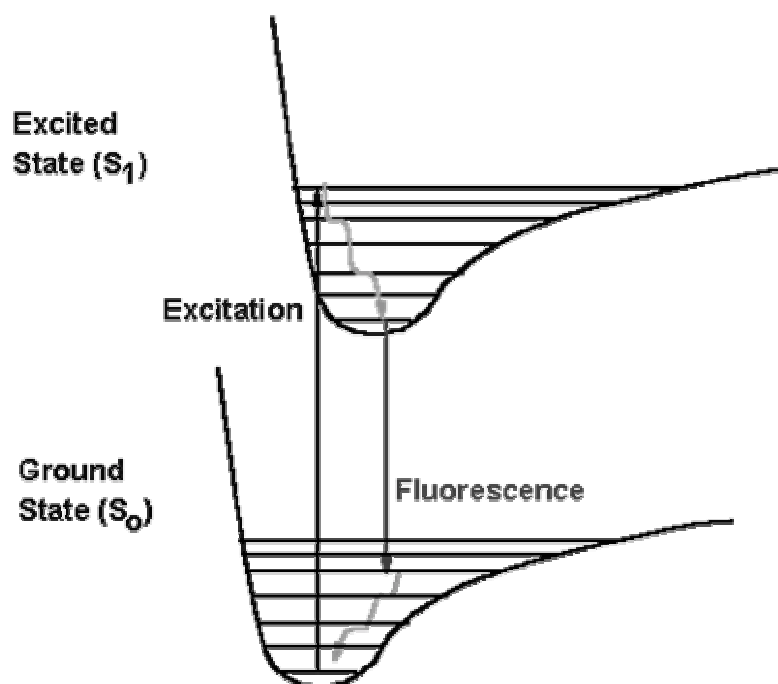


Figure 4.7. Transition between electronic energy levels (26).

Fluorescence spectroscopy offers several advantages for the analytical analyses. Its main advantage compared to absorption measurements like near infrared spectroscopy, is the greater sensitivity achieved because the fluorescence signal has a very low background (zero background). Thus, it enables working at very low concentrations. Furthermore, LIF is useful to study the electronic structure of molecules and to make quantitative measurements of analyte due to the high sensitivity of fluorescent compounds to their environment (26). For example, the tryptophan molecules that are on the hydrophobic part of a protein have different fluorescent properties than the ones on a hydrophilic part (14). It provides selective excitation of the analyte to avoid interferences and provides rapid real time data with high spatial resolution. Fluorescence detection technique is relatively rapid and easy to implement.

The most intense fluorescence is observed in the molecules containing aromatic functional groups, aliphatic carbonyl structures or highly conjugated double bonds. Some examples are tryptophan, tyrosine, phenylalanine in proteins, vitamin A and B₂, NADH derivatives of pyridoxal and chlorophyll, benzene, toluene, phenol, benzoic acid, etc. These compounds are naturally present in the sample structure, hence are called as intrinsic fluorophores. On the other hand, extrinsic fluorophores are added to

the sample to obtain a fluorescence emission or to change the emission of the sample (1,2).

The intensity of fluorescence is called as quantum yield, which is simply the ratio of the number of molecules that emit photon to the total number of excited molecules. If this value is close to a unit, then the molecule is a highly fluorescent molecule.

The components of a fluorescence instrument involves a laser source or lamps, sample cells, focusing and collecting optics, filters and monochromators, transducers and signal processor and readout devices as shown in Figure 4.8.

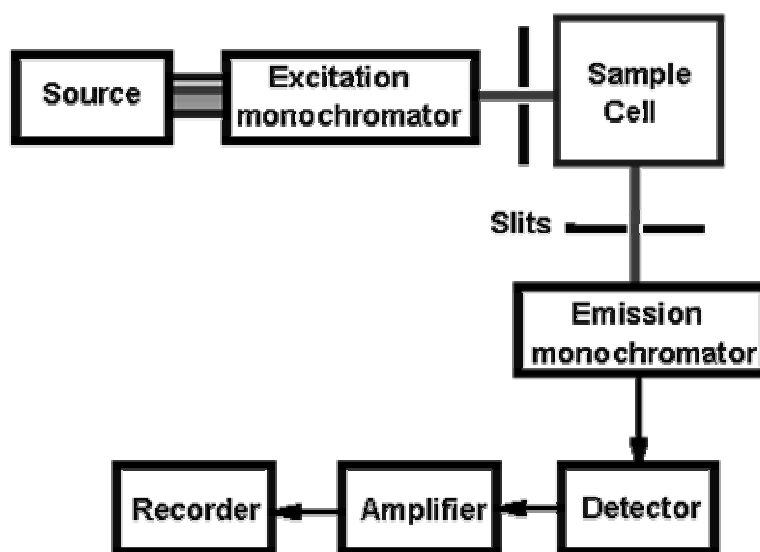


Figure 4.8. A schematic view of a typical fluorimeter (26).

As the generator of radiation with sufficient power, lamps or lasers can be used in instruments detecting fluorescence. For instance, a mercury vapour lamp can be used in fluorimeters or a xenon arc lamp in spectrofluorimeters where a source of continuum radiation is required. Although they are more expensive than lamps, lasers can also be used in spectrofluorimeters because of their advantages as remote or in-situ sensors. Today, laser technology such as microchip lasers can produce laser beams with a quality that is required in spectroscopic applications. These laser beams can be adjusted to a level of intensity and wavelength that will make fluorescent excitation possible. Some examples are Nd:YAG, Gas or Dye lasers. Beam splitters, mirrors, lenses, etc. are used to focus light onto the sample and fiber optics carry the radiation from the source to the sample or vice versa. To enhance the sensitivity of measurements, radiation

should be consisted of a limited or narrow group of wavelength. For this aim, filters and monochromators are used to select the desired wavelength. For instance, most spectrofluorometers contain at least one grating monochromators. However, using lasers as the illumination source eliminates the use of excitation monochromators to select the wavelength range because they have their characteristic wavelength due to the material in their structure and using combination of crystals in laser enables working at different wavelengths. The sample cells are generally composed of quartz, fused silica or glass. Transducers, in other words detectors convert the radiant energy into electrical signals. For instance, the most common transducer used in sensitive fluorescence instruments is the photomultiplier tube. Diode-array and charge transfer detectors are also used in spectrofluorometry (1).

Development in the field of integrated optic, laser and fiber optic technologies make it possible to design integrated spectroscopy devices with a reasonable size and cost. That is why laser induced fluorescence spectroscopy is thought to be a good method for food and soil analyses.

4.2.1. Applications of Laser Induced Fluorescence Spectroscopy

In food industry, laser induced fluorescence spectroscopy is commonly used for protein analysis and to understand the conformational changes within the molecule. For instance, β -lactoglobulin protein, which is a constituent of milk, contains two tryptophan residues. These two tryptophan residues are buried in the hydrophobic parts of the protein. As a denaturation of β -lactoglobulin by urea, organic solvents and temperature, there will be a change in the intensity and energy of emission (27).

In addition to β -lactoglobulin, five other proteins of milk α 1-, α 2-, α -lactalbumin, β - and κ -CN also contain at least one tryptophan residue. This gives the possibility of studying protein structure or protein-hydrophobic molecule interactions. Spectral changes can be detected due to the tertiary structure change, binding of ligands, protein-protein association or the exposure of tryptophan residues to the aqueous phase. It was recorded that the excitation and emission wavelengths of tryptophan were at 290 nm and 305-400 nm, respectively. On the other side, the use of extrinsic fluorophores such as fuchsin acid can also be used to label proteins when the intrinsic fluorophores are not present in the molecule or not enough for the experiment. However, it should be taken into consideration that the extrinsic fluorophore is only specific to the proteins in that molecule. Another intrinsic fluorophore is vitamin A, which is located in the core of the

fat globules. It has an excitation wavelength between 250-350 nm and an emission wavelength at 410 nm. This fluorophore enables the study of solid fat content in edible oils, which is considered as a quality control parameter. Furthermore, it was also shown that the excitation spectra of vitamin A in milk, fat in water emulsion showed a change as the temperature varied between 4-45°C. This means that the fluorescence of the molecule is dependent on the physical state of triglycerides in the fat molecules of an emulsion (2).

Another study performed by Mazerolles et al. (2001) involves both the fluorescence and mid infrared spectroscopies in the analysis of fat, protein and moisture contents of cheeses during ripening. The data collected at 1, 21, 51 and 81 days of ripening were processed with canonical correlation analysis which makes it possible to identify and quantify the relation between two sets of variables collected from the same sample. The results for the first two sets of variable were 0.87 and 0.58 canonical regression coefficients and the spectral data of fluorescence and infrared were similar. According to these results, the researchers have concluded that the changes during ripening stage of cheese could be non-invasively and rapidly observed by the two spectroscopic techniques (2).

Similarly, the reflectance and fluorescence techniques were used together to discriminate the crop residues in field after harvest by Daughtry et al. (1995). The crop residues are important in controlling soil erosion. As the amount of crops covering the surface increases, the rate of eroded soil with its nutrients and pesticides carried into rivers and streams decreases. The samples were 37 agricultural soils (wet and dry) and recently harvested residues of corn (*Zea mays* L.), soybean sorghum and wheat. The reflectance spectra, taken over the wavelength range of 400-1000 nm, were not capable of discriminating all the crop residues from soil. This was due to the overlapping of reflectance spectra of soils and residues. The residues may have brighter or darker colours than soils depending on their moisture level, residue age and microbial degradation. In addition to this, a wide range in reflectance of a whole corn was observed which was collected from a single field. This depends on the extent of microbial colonies on the surface or residues, which cause a difference in the colour of residues. It was concluded that the discrimination might be possible by using a combination of visible and near infrared reflectance data. On the other hand, the fluorescence measurements over the 250-280 nm range showed similar excitation and emission wavelengths for the whole and ground crop residues. And the fluorescence

intensity of soils was one or two orders of magnitude less than that of crop residues (28).

Another study involves the detection of changes in the fluorescence properties of leaves of corn (*Zea mays* L.) grown under different levels of nitrogen fertilization. The study aims to develop a non-destructive remote sensing technique to determine the optimum rate of nitrogen fertilization in corn crops. Corn was grown under eight different nitrogen treatments ranging from deficient to excessive amounts of nitrogen levels in laboratory (concentrations ranging from 0% to 150% of the recommended nitrogen rate, 162 kg N/ ha). And fluorescence images taken at 450 nm (blue), 525 nm (green), 680 nm (red) and 740 nm (far-red) were compared with the chlorophyll contents, N:C ratio, pigment concentrations and grain yields. At three different growth stages of leaves (vegetative, tasselling and grainfill) high correlations were acquired among the red/blue, red/green, far-red/green and far-red/blue bands to total chlorophyll ($r=0.96$), N:C ratio ($r=0.94$), pigment concentration ($r=0.82$) and grain yield ($r=0.92$) (r =correlation coefficient) (29).

Laser induced fluorescence spectroscopy has been widely used for monitoring, screening and characterizing the contamination and pollution in soil, water and the atmosphere. For instance, the investigation of Löhmannsröben and Schober (1999) included the quantitative analysis of petroleum products in soil with an appropriate calibration of laser induced fluorescence spectroscopy with a UV-near infrared diffuse reflectance spectroscopy operating in a range of 250-950 nm. The quartz sand and soil collected from different areas were contaminated with diesel fuel at different concentrations in laboratory, and they were excited by a Nd:YAG laser source at 266 nm. A linear correlation was attained between the laser induced fluorescence signal intensities and the diesel fuel contamination in soil. The accuracy of detection of laser induced fluorescence intensity for a definite contaminated soil was approximately $\pm 10\%$, which was accepted as a good experimental accuracy. The data acquired by diffuse reflectance spectroscopy approved the results of subsurface fluorescence measurements. However, further investigations were required for the calibration of different soils (32).

In- situ detection of BTEX (benzene, toluene, ethylene and xylene) compounds in subsurface soil by a novel microlaser based probe combined to a cone penetrometer, was performed by Bloch et al (1998). The novel microlaser is a combination of several optical crystals (Nd:YAG, Cr:YAG, KTP and BBO) which produced laser light at 266

nm. The excitation light was carried by fibre optics onto a sapphire window. And these components were mounted into a cone penetrometer, which was pushed into soil for subsurface characterization. The results of field experiments indicated that the highest contamination was present at 3.5 m depth under soil. The wavelength-time spectra analyses showed that the shorter wavelengths (<315 nm) belonged to BTEX compounds whereas the longer wavelengths (315-350 nm) indicated the presence of aromatic compounds such as naphthalene (33).

4.3. Multivariate Calibration Methods

Laser induced fluorescence spectroscopy, near infrared reflectance spectroscopy can give quantitative information about the sample of interest, and these analyses are usually based on the detection of differences in the concentration of the analyte in the sample. This is only possible by using calibration processes, which relates the measured analytical signal to the concentration of the analyte. In other words, the idea of a calibration method is to develop a mathematical model between the dependent (instrument response) and independent variables (analyte concentration) and then to use this model for the prediction of analyte concentrations in the coming instrumental analyses. Together with the development of advanced instrumental techniques, calibration of the analytical method has gained much interest. These calibration methods can be univariate or multivariate depending on the number of variables and presence of interferences (16).

4.3.1. Univariate calibration methods

In univariate calibration methods, to determine the analyte concentration, the measurement of the instrument is at a specific wavelength. That is, there is only one dependent variable and it is assumed that the instrument response is dependent on the analyte concentration without interferences. The interferences can be observed due to errors in matching the matrix of complex samples. In univariate calibration methods, calibration is a two step process, a calibration model is developed from the samples whose concentrations are known and then the model is used to predict the concentrations of samples from their instrument responses.

In univariate calibration model, the response of the instrument (r), is related to the analyte concentration (c) by the calibration function defined as:

$$r = f(c) + e_r \quad 4.11$$

where e_r is the error associated with the instrument response.

In spectroscopy, $f(c)$ is assumed to be linear according to the Beer's law, which states that the absorbance of an analyte at the maximum absorbing wavelength is proportional to the analyte concentration:

$$A = \varepsilon \times c \times l \quad 4.12$$

where A is absorbance, ε is the extinction coefficient, l is the thickness of the sample and c is the concentration of sample.

The two most common univariate calibration models are the classical and inverse univariate calibration models. The classical univariate calibration model, which assumes to be linear according to Beer's law, is:

$$a_i = b_0 + b_1 \times c_i + e_i \quad 4.13$$

where a_i is the absorbance or in other words instrument response, c_i is the analyte concentration, e_i is the measurement error for the i th sample of m calibration standards and b_0 and b_1 are the unknown parameters. In case of zero error, the b_0 and b_1 would be the intercept and slope of the linear curve, respectively. However, in real applications, there is always an amount of error related to the instrument measurements. Thus, the best straight line that fits the data is produced by estimating b_0 and b_1 values. This estimation is done by the method least squares, which is a procedure that the sums of squares of residuals take the least possible values. The sum of squares for m calibration standards is:

$$SS = \sum_{i=1}^m e_i^2 = \sum_{i=1}^m (a_i + b_0 - b_1 \times c_i)^2 \quad 4.14$$

To minimize SS , partial derivatives of SS need to be taken with respect to the two parameters that are to be estimated (b_0 and b_1) and the resulting equation is set to zero.

Thus:

$$\frac{\partial SS}{\partial b_0} = 2 \sum_{i=1}^m (a_i - b_0 - b_1 \times c_i)(-1) = 0 \quad 4.15a$$

$$\frac{\partial SS}{\partial b_1} = 2 \sum_{i=1}^m (a_i - b_0 - b_1 \times c_i)(-c_i) = 0 \quad 4.15b$$

After dropping 2 and -1 from Equations 4.15 a and b, the solutions of b_o and b_l can be obtained by solving normal equations:

$$\sum_{i=1}^m (a_i - b_o - b_l \times c_i) = 0 \quad 4.16a$$

$$\sum_{i=1}^m (a_i c_i - b_o c_i - b_l \times c_i^2) = 0 \quad 4.16b$$

When these equations are solved:

$$mb_o + b_l \sum_{i=1}^m c_i = \sum_{i=1}^m a_i \quad 4.17a$$

$$b_o \sum_{i=1}^m c_i + b_l \sum_{i=1}^m c_i^2 = \sum_{i=1}^m c_i a_i \quad 4.17b$$

Finally the least square estimates of b_o and b_l can be calculated as:

$$\hat{b}_l = \frac{\sum_{i=1}^m c_i a_i - \left(\sum_{i=1}^m c_i \right) \left(\sum_{i=1}^m a_i \right) / m}{\sum_{i=1}^m c_i^2 - \left(\sum_{i=1}^m c_i \right)^2 / m} \quad 4.18a$$

$$\hat{b}_o = \bar{a} - \hat{b}_l \times \bar{c} \quad 4.18b$$

where \bar{a} and \bar{c} are the mean values of instrument response and analyte concentrations for m calibration samples, respectively.

The estimated calibration equation can be written as:

$$\hat{a} = \hat{b}_o + \hat{b}_l \times \bar{c} \quad 4.19$$

The concentration of unknown sample can be found from the equation below:

$$c_u = \frac{a_u - \hat{b}_o}{\hat{b}_l} \quad 4.20$$

where c_u is the unknown analyte concentration and a_u is its instrument response. As the calibration equation is predicted, the calibration curve between the absorbance and concentration values is drawn together with its regression coefficient (R^2). This is a numerical value which represents the strength of the linear model for a and c . The value of R^2 can be neither smaller than 0 nor greater than 1. The ideal linear equation should have an R^2 value that is close to 1 (1,16).

$$R^2 = \frac{\sum_{i=1}^m (\hat{a}_i - \bar{a})^2}{\sum_{i=1}^m (a_i - \bar{a})^2} \quad 4.21$$

The classical univariate calibration methods can also be described with the matrix notations. This time the model can be written as:

$$\mathbf{a} = \mathbf{C} \times \boldsymbol{\beta} + \mathbf{e}_a \quad 4.22$$

where \mathbf{a} is $m \times 1$ vector of instrument responses, \mathbf{C} is the matrix of analyte concentrations, $\boldsymbol{\beta}$ is the 2×1 vector of regression parameters (b_o and b_l) and \mathbf{e}_a is the $m \times 1$ vector of errors associated with \mathbf{a} or residuals that are not fit by the model. Note that the first column of the \mathbf{C} matrix is a vector of ones, which is necessary to estimate b_o when the multiplication is done. The matrix form of b_o and b_l estimates can be written as:

$$(\mathbf{C}' \times \mathbf{C}) \times \boldsymbol{\beta} = \mathbf{C}' \times \mathbf{a} \quad 4.23$$

Then the least square solution to Equation 4.23 during calibration is:

$$\hat{\boldsymbol{\beta}} = (\mathbf{C}' \times \mathbf{C})^{-1} \times \mathbf{C}' \times \mathbf{a} \quad 4.24$$

where $\hat{\boldsymbol{\beta}}$ is the 2×1 vector of least square estimate parameters b_o and b_l with the sum of squared residuals not fit by the model being minimized. Once the unknown parameters are estimated, the concentration of an unknown sample can be calculated from Equation 4.20.

The inverse univariate calibration model assumes the inverse of Beer's law and can be expressed as:

$$c_i = p_o + p_l \times a_i + e_i \quad 4.25$$

where e_i is the error associated with the analyte concentration, c_i and a_i is the instrument response. This time the analyte concentration is a function of instrument response (absorbance). The estimates of p_o and p_l can be calculated from the least squares method as explained in classical univariate calibration.

$$\hat{p}_1 = \frac{\sum_{i=1}^m a_i c_i - \left(\sum_{i=1}^m a_i \right) \left(\sum_{i=1}^m c_i \right) / m}{\sum_{i=1}^m a_i^2 - \left(\sum_{i=1}^m a_i \right)^2 / m} \quad 4.26a$$

$$\hat{p}_o = \bar{c} - \hat{p}_1 \times \bar{a} \quad 4.26b$$

where \bar{a} and \bar{c} are the mean values of instrument response and concentrations for m calibration samples.

The estimated calibration equation can be written as:

$$\hat{c} = \hat{p}_o + \hat{p}_1 \times a \quad 4.27$$

And the unknown analyte concentration can be calculated by:

$$c_u = \hat{p}_o + \hat{p}_1 \times a_u \quad 4.28$$

where c_u is the unknown analyte concentration and a_u is the instrument response of unknown sample.

The univariate calibration methods have some limitations due to their assumption of no interference and single measurement based analysis. However, modern instruments provide hundreds of spectra of the sample and the sample composition is generally very complex that interferences are very frequently observed. Because of these limitations, they are not very suitable for instrumental analysis (16).

4.3.2. Multivariate Calibration Methods

Multivariate calibration methods deal with the data collected at multiple wavelengths of measurement of the sample containing more than one component. Thus, they are useful in analysing instrumental data. The multivariate calibration techniques can eliminate some problems, which occur in univariate calibration methods. As they handle multiple pieces of data to predict the analyte concentrations, they can also predict the presence of interfering species in samples by giving outliers, which can not be detected in univariate calibration methods. The interfering species can be the components other than the analyte, which are present in the sample or they may occur as a result of some chemical reactions in the sample. In addition to the chemical structure of samples, the physical behaviour of the sample also affects the instrument response. Moreover, human mistakes and measurement errors are the other sources that can be recognized by the multivariate calibration methods (16).

In this thesis study, genetic inverse least squares and partial least squares methods were used for the prediction of the three soil constituents.

Genetic Inverse Least Squares (GILS)

Inverse least squares (ILS) method is based on the inverse Beer's law where the concentrations of the analyte are proportional to the absorbance measurements. In

classical least squares method where absorbance at each wavelength is proportional to the analyte concentrations, all the interfering species and their concentrations must be known and used in the model. However, in inverse least squares, this requirement is eliminated and it is assumed that the errors arise from the reference values of calibration sample, not from their spectral measurements.

The ILS model for m calibration samples containing l analytes with n wavelengths at each spectrum can be written as:

$$\mathbf{C} = \mathbf{A} \times \mathbf{P} + \mathbf{E}_c \quad 4.29$$

\mathbf{C} is the $m \times l$ matrix of constituent concentrations, \mathbf{A} is the $m \times n$ matrix of spectral absorbances, \mathbf{P} is the $n \times l$ matrix of unknown calibration coefficients relating l component concentrations to the spectral intensities, and \mathbf{E}_c is the $m \times l$ matrix of random concentration error or residuals that are not fit by the model.

The major advantage of ILS is that the model can be reduced for the prediction of concentration of a single component in a sample.

$$\mathbf{c} = \mathbf{A} \times \mathbf{p} + \mathbf{e}_c \quad 4.30$$

where \mathbf{c} is the $m \times 1$ vector of concentrations of constituents, \mathbf{p} is the $n \times 1$ vector of calibration coefficients, \mathbf{A} is the $m \times n$ matrix of absorbance spectra of calibration set and \mathbf{e}_c is the $m \times 1$ vector of errors associated with analyte concentrations not fit by the model. The least squares estimate of \mathbf{p} is:

$$\hat{\mathbf{p}} = (\mathbf{A}' \times \mathbf{A})^{-1} \times \mathbf{A}' \times \mathbf{c} \quad 4.31$$

where $\hat{\mathbf{p}}$ is the estimated calibration coefficients.

Following the $\hat{\mathbf{p}}$ calculation, the predicted analyte concentrations can be calculated:

$$\hat{\mathbf{c}} = \mathbf{a}' \times \hat{\mathbf{p}} \quad 4.32$$

where \mathbf{a} is the absorbance spectra of the analyte and $\hat{\mathbf{c}}$ is the estimated concentration of the analyte. In this way, ILS enables prediction of concentrations of several components in a sample at a time. Although the ILS technique has the advantages of requiring only the knowledge of constituents of interest and being a relatively rapid method, it has some disadvantages. The first thing is that the number of wavelengths selected for the model development can not exceed the number of calibration set though the number of wavelengths in a spectrum is generally more than the number of calibration samples. The second thing is that the selected wavelengths should not be collinear, namely dependent to each other. This is often a problem when too many wavelengths are used in the model, which is known as over fitting.

Genetic inverse least squares method is a modified version of ILS in which a small set of wavelength is chosen from the whole spectral data matrix and used in the genetic algorithm. “Genetic algorithms are global search and optimisation methods based upon the principles of natural evolution and selection” (16). Here, the term gene refers to the solution to a given problem. In other words, it is the collection of wavelength pairs combined with simple mathematical operators (+, -, ×, /).

The score of each gene relates the instrument response to the analyte concentration. The implementation of genetic algorithm is of five basic steps:

- 1-Initialization of gene population
- 2-Evaluation and ranking of the population
- 3-Selection of parent genes for breeding and mating
- 4-Crossover and mutation
- 5-Replacing the parents with their offsprings

The names of these steps come from the biological foundation of the algorithm. The term gene population is referred to the collection of individual genes in a generation. To understand the success of each gene in predicting the analyte concentration, a fitness function is used which is the inverse of standard error of calibration (SEC) and standard error of prediction (SEP).

In GILS, the term gene is a vector of randomly selected wavelengths from the whole spectral data matrix A and must have a size smaller than that of the calibration set because the number of wavelengths is restricted in response matrix A . In the first step, which is the initialization of the gene population, an even number of genes are created from the whole spectral data matrix and each is used to develop an ILS model. The second step is the evaluation of genes using fitness function, which is the inverse of standard error of calibration ($1/SEC$) and then ranking the genes according to their fitness function from the highest to the lowest value. The SEC is a derivative of the standard error (SE), which is:

$$SE = \sqrt{\frac{\sum_{i=1}^m (\hat{c}_i - c_i^2)^2}{df}} \quad 4.33$$

where c_i and \hat{c}_i are the known and predicted analyte concentrations for m samples and df is the degrees of freedom, which is given by:

$$df = m - k \quad 4.34$$

k is the number of parameters extracted from the sample set.

For the calibration data set, linear model is assumed and there are two parameters to be extracted from the data set, which are the slope of line and the intercept. Thus, the degrees of freedom equals to $m-2$ in the Equation 4.34. The equation for standard error of calibration can be written as:

$$SEC = \sqrt{\frac{\sum_{i=1}^m (\hat{c}_i - c_i)^2}{m-2}} \quad 4.35$$

The third step, selection of parent gene population for breeding is done according to the roulette wheel method. In roulette wheel selection method, each slot in the roulette represents a gene. The gene having the highest fitness function has the biggest slot, which means that the genes having high fitness functions have a higher chance of being selected for the breeding. However, there will be some genes that are selected multiple times whereas some are not selected at all; thereby they are thrown out from the gene pool. Fourth step is the mating and single point crossover operations. After selection of parent genes, they mate with each other from top to down whereby the first gene mates with second and the third with the fourth one etc. The single point crossover operation is only done in the middle of each gene vector. Thus, the first part of the first gene combines with the second part of second gene and likewise, the second part of the first gene combines with the first part of the second gene to give two new offspring genes. In this way, new generations, which have smaller number of wavelengths than the number of calibration samples, will be created. Finally, the parent genes are replaced by their offsprings and these offsprings are ranked by their fitness values and evaluated. The selection for breeding step repeats again until the predefined number of iterations is reached. At the end, the gene with the lowest SEC is chosen for the model development. This model is used to predict the concentrations in the validation set (test set) (16). The success of the model used in the prediction of validation set is evaluated by using the standard error of prediction (SEP) which is calculated as:

$$SEP = \sqrt{\frac{\sum_{i=1}^m (\hat{c}_i - c_i)^2}{m}} \quad 4.36$$

where m is the number of validation set.

Partial Least Squares (PLS)

PLS is considered as a soft modelling technique, in which the whole spectral data is divided into new variables that are uncorrelated linear combinations of the measured data. These new variables are called as factors or principal components. The formation of these new variables can be shown with a two dimensional system. Suppose, there are m samples with n components in each sample. The instrument responses at two wavelengths are plotted against each other. The axis passing through the points account for maximum variability of the data, which is called as the first principal component or first eigenvector. If all the points fall on the axis, then the variables can be described with one eigenvector. If not, a second eigenvector will be drawn representing the maximum amount of residuals, not fit by the first eigenvector. This continues until all the variables fall on the axis. If the wavelength number exceeds two, the graph will be multidimensional and several eigenvectors can be found. The calibration model for PLS with m samples, n components and h loading vectors is:

$$\mathbf{A} = \mathbf{T} \times \mathbf{B} + \mathbf{E}_A \quad 4.37$$

where \mathbf{A} is the $m \times n$ matrix of absorbance spectra, \mathbf{B} is the $h \times n$ matrix of loading spectra or basis vector, \mathbf{T} is $m \times h$ matrix of intensities or scores in the coordinate system defined by h loading vectors and \mathbf{E}_A is the $m \times n$ matrix of spectral residuals not fit by the factor model. The number of basis vectors, h , to represent original calibration spectra is determined by an algorithm during the calibration step. \mathbf{B} is the uncorrelated linear combinations of the original calibration spectra.

The model can either be written with an ILS model relating the analyte concentrations to the spectral intensities.

$$\mathbf{c} = \mathbf{T} \times \mathbf{v} + \mathbf{e}_c \quad 4.38$$

where \mathbf{c} is the $m \times 1$ vector of analyte concentration, \mathbf{v} is the $h \times 1$ vector of coefficients which relate spectral intensities to the analyte concentration, \mathbf{e}_c is the $m \times 1$ vector of errors in the reference values and \mathbf{T} is the $m \times h$ matrix of intensities or scores in the new coordinate system defined by h loading factors.

The least square estimate of \mathbf{v} is given as:

$$\hat{\mathbf{v}}_h = (\mathbf{T}' \times \mathbf{T})^{-1} \times \mathbf{T}' \times \mathbf{c} \quad 4.39$$

In PLS, the decomposition of whole spectral matrix is dependent on the analyte concentrations. The model uses a modified version of NIPALS (nonlinear iterative partial least squares) in which the concentration information is used to extract the

loading vectors. It is developed in two different methods, PLS 1 and PLS 2 methods. PLS 1 method performs the analysis of complex chemical mixtures by considering only concentration of one component at a time and the rest are not included in the model. This method is the most commonly used one and the more useful one than PLS 2.

Prior to the analysis with these methods, the data should be pretreated with mean centering and scaling. Mean centering is subtracting the average spectrum and concentration of the analyte of interest from each of all spectra and concentrations. Then the PLS 1 algorithm calculates the estimates of regression coefficients ($\hat{\mathbf{v}}_h$) and the PLS loading vector ($\hat{\mathbf{b}}_h$). First h is set to 1, and the estimate of first weighted loading vector is calculated:

$$\hat{\mathbf{w}}_h = \mathbf{A}' \times \mathbf{c} \times (\mathbf{c}' \times \mathbf{c})^{-1} \quad 4.40$$

$\hat{\mathbf{w}}_h$ is $n \times 1$ vector of first order approximation of the analyte spectra.

Then, the score vector is calculated by regressing \mathbf{A} to $\hat{\mathbf{w}}_h$:

$$\hat{\mathbf{t}}_h = \mathbf{A} \times \hat{\mathbf{w}}_h \quad 4.41$$

The estimates of $\hat{\mathbf{v}}_h$ and $\hat{\mathbf{b}}_h$ are then calculated:

$$\hat{\mathbf{v}}_h = \hat{\mathbf{t}}_h' \times \mathbf{c} \times (\hat{\mathbf{t}}_h' \times \hat{\mathbf{t}}_h)^{-1} \quad 4.42$$

$$\hat{\mathbf{b}}_h = \hat{\mathbf{t}}_h' \times \mathbf{A} \times (\hat{\mathbf{t}}_h' \times \hat{\mathbf{t}}_h)^{-1} \quad 4.43$$

These estimates are used in the calculation of concentration residuals (\mathbf{e}_c) and the spectral residues (\mathbf{E}_A)

$$\mathbf{e}_c = \mathbf{c} - \hat{\mathbf{v}}_h \times \hat{\mathbf{t}}_h \quad 4.44$$

$$\mathbf{E}_A = \mathbf{A} - \hat{\mathbf{t}}_h \times \hat{\mathbf{b}}_h' \quad 4.45$$

In this way, one iteration is completed in the calibration step. The following step after calibration is prediction. The final calibration coefficient (\mathbf{b}_f) is calculated which is used in the calculation of concentration of a new sample.

$$\mathbf{b}_f = \hat{\mathbf{W}} \times (\hat{\mathbf{B}} \times \hat{\mathbf{W}}')^{-1} \times \hat{\mathbf{v}} \quad 4.46$$

where $\hat{\mathbf{W}}$ and $\hat{\mathbf{B}}$ contain the individual $\hat{\mathbf{w}}_h$ and $\hat{\mathbf{b}}_h$ vectors and $\hat{\mathbf{v}}$ is formed from the individual regression coefficient ($\hat{\mathbf{v}}_h$).

$$\hat{c} = \mathbf{a}' \times \mathbf{b}_f + c_o \quad 4.47$$

where \hat{c} is the predicted unknown sample concentration, \mathbf{a} is the spectrum of that sample and c_o is the average concentration of calibration samples.

Once the concentrations of unknown samples are predicted, the prediction error sum of the squares (PRESS) can be calculated for each added factor, which defines the performance of a model to fit the calibration data.

$$PRESS = \sum_{i=1}^m (\hat{c}_i - c_i)^2 \quad 4.48$$

\hat{c}_i is the reference concentration of i th sample and c_i predicted concentration of i th sample for m calibration standard.

The evaluation of PRESS values of two factors is done by the F test and it is not the smallest PRESS value, giving the optimum factor number which may cause overfitting. The models need to be compared for h and $h+1$ factors (16).

Chapter 5

MATERIALS AND METHODS

5.1. Materials

The soil samples used in this study were collected from Menemen Application and Research Farms. Two fields were used for the sample collection, which were approximately 50 da in size. The first one, called as the clover field, contained clean soil in which no cultivation, fertilizer or pesticide application was performed. In the second field, melon was grown where NPK fertilizer was applied in the beginning of year 2003.

The commercial fertilizers used in this study are listed below.

Table 5.1. Fertilizers and their properties.

Fertilizer	Chemical Form	Fertilizer %	Producer
Ammonium nitrate	NH_4NO_3	26% N	Ege Gübre Inc.
Ammonium sulfate	$(\text{NH}_4)_2\text{SO}_4$	21% N	Ege Gübre Inc.
Calcium nitrate	$\text{Ca}(\text{NO}_3)_2$	15.5% N - 26.5% CaO	Ege Gübre Inc.
Potassium nitrate	KNO_3	13% N - 46% K_2O	Ege Gübre Inc.
Triple super phosphate (TSP)	$\text{Ca}_3(\text{PO}_4)_2$	43% P_2O_5	Ege Gübre Inc.
N-P-K		15% N- P_2O_5 - K_2O	Ege Gübre Inc.

5.2. Methods

In this thesis study, two methods have been developed which involved the use of various fertilizers to simulate soils having varying concentrations of nitrogen, phosphorus and potassium. An additional study was performed with laboratory analyzed soil samples collected from different agricultural fields.

5.2.1. First Method

Soil sample collection and preparation:

The soil samples were collected from several points of the clover field down to a depth of 25 cm because the major nutrients are mostly accumulated on the surface of

soil. Approximately 15 kg of total soil was collected. They were stored in plastic bags in the refrigerator to prevent moisture loss and composition changes as the biological activity slows at low temperature. Prior to near-infrared analyses, they were oven dried, hand cleaned to remove foreign particles and ground to pass through a 2 mm sieve (25). The sample preparation steps according to the first method are explained in Figure 5.1.

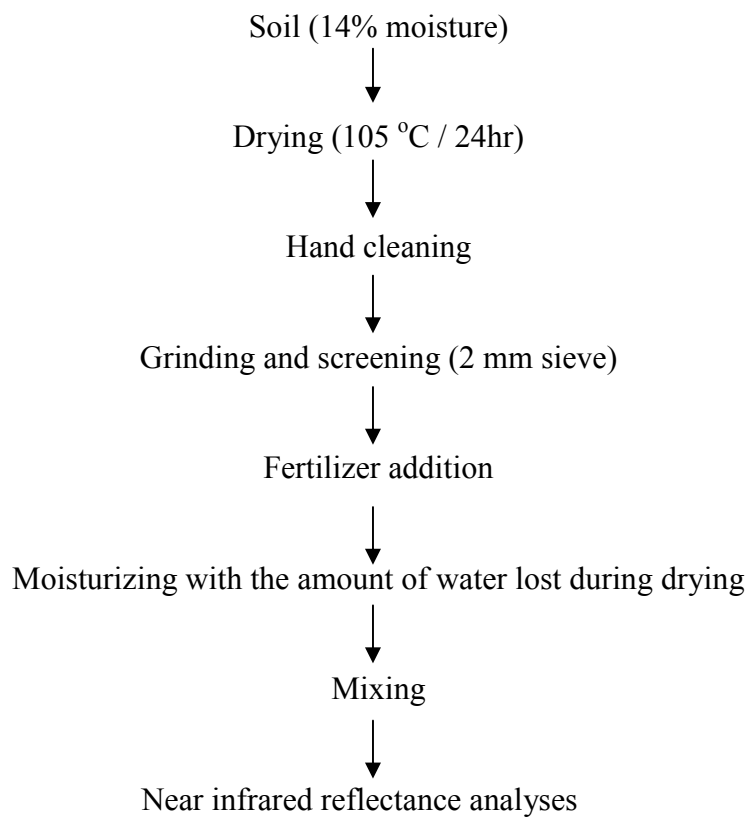


Figure 5.1. Sample preparation steps for the near infrared reflectance analyses according to the first method.

Using this method, two experiments were performed in which the fertilizer types and their concentrations were different. In the first experiment, following the common soil preparation steps, soils were mixed with NPK fertilizer at definite concentrations, which are listed in Table 5.2. The application of fertilizer is usually performed together with the addition of water into soil to dissolve the fertilizer in soil solution. Thereby, the next step after fertilizer addition was to add the amount of water lost during drying. Finally, the mixture is mixed thoroughly to obtain homogenous dispersion. Before the near infrared analyses, the mixture was stored for three days to let the added water equilibrate in the soil. The concentrations of nutrient elements in the samples were calculated from their percentage in that fertilizer and by using conversion factors. These

calculations are shown in Appendix A. In this experiment, seven samples (100 g) were prepared for the near infrared reflectance analyses.

Table 5.2. Nutrient and fertilizer concentrations (g/100 g) in the samples containing NPK fertilizer in the first experiment.

Fertilizer	Nitrogen (N)	Phosphorus (P)	Potassium (K)
1	0.15	0.066	0.125
2.5	0.375	0.164	0.311
5	0.75	0.328	0.623
7.5	1.125	0.492	0.934
10	1.5	0.655	1.245
12.5	1.875	0.819	1.557
15	2.25	0.983	1.868

Using the same method, which was shown in Figure 5.1, a second experiment was performed with different fertilizer types and at different concentrations. NH_4NO_3 and TSP fertilizers were used in the preparation of ten sample (100 g) at various concentrations which are listed in Table 5.3.

Table 5.3. Nutrient and fertilizer concentrations (g/100 g) in the samples containing NH_4NO_3 and TSP fertilizers in the second experiment.

Fertilizer	Nitrogen (N)	Phosphorus (P)
0.075	0.0195	0.0141
0.1	0.026	0.0188
0.125	0.0325	0.0235
0.15	0.039	0.0282
0.175	0.0455	0.0329
0.2	0.052	0.0376
0.225	0.0585	0.0423
0.25	0.065	0.047
0.275	0.0715	0.0517
0.3	0.078	0.0564

Near infrared reflectance analyses

The diffuse reflectance spectra of the samples were recorded with a FTS-3000 near infrared spectrometer (Bio-Rad, Excalibur, Cambridge, MA), set in the near infrared region (1000-2500 nm). The resolution of the instrument was 32 cm^{-1} and 64 scans were recorded. The light source was a Tungsten-Halogen lamp with a Calcium Fluoride (CaF_2) beam splitter and a lead selenide (PbSe) detector was used. The sample cup has a 10 mm diameter and a 2.3 mm depth, as shown in Figure 5.2. The spectrum for each sample was produced from 391 data points and the spectral data were recorded as $\log 1/R$ (R: Reflectance) with a background taken by the pure soil sample. Three replicate scans were recorded for each sample containing NPK fertilizer prepared in the first experiment in which the first two were collected without changing the position of sample cup and the third one collected by rotating the sample cup about 90° around itself. For the second experiment, two replicate scans were recorded for the samples containing NH_4NO_3 and TSP fertilizers.

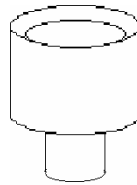


Figure 5.2. Sample cup of near infrared reflectance spectrometer.

Data analyses

The near infrared reflectance data was processed with genetic inverse least squares method to predict the nutrient amounts in the samples. Genetic inverse least squares method was written by Durmuş Özdemir in Matlab programming language using Matlab 5.3 (MathWorks Inc., Natick, MA). A calibration set that would be used in the development of calibration model and a validation set to verify the prediction ability of the developed model were prepared in the form of text files. The choice of samples for the calibration and validation sets was randomly performed. The important point to be considered at this step is that the calibration set should contain the samples having the minimum and maximum fertilizer concentration values. In Table 5.4 and Table 5.5, the calibration and validation sets of nutrient concentrations for the first and second experiment are listed, respectively and it can be seen that the calibration sets for each nutrient contain the minimum and maximum concentrations.

Table 5.4. Calibration and validation sets of nutrients in the samples containing NPK fertilizer (g/100 g) in the first experiment.

Calibration	Nitrogen	Phosphorus	Potassium	Validation	Nitrogen	Phosphorus	Potassium
1	0.15	0.066	0.12447	1	0.375	0.164	0.311175
2	0.15	0.066	0.12447	2	0.375	0.164	0.311175
3	0.15	0.066	0.12447	3	0.375	0.164	0.311175
4	0.75	0.328	0.62235	4	1.125	0.491	0.933525
5	0.75	0.328	0.62235	5	1.125	0.491	0.933525
6	0.75	0.328	0.62235	6	1.125	0.491	0.933525
7	1.5	0.655	1.2447	7	1.5	0.655	1.2447
8	1.5	0.655	1.2447	8	1.875	0.819	1.555875
9	1.875	0.819	1.555875				
10	1.875	0.819	1.555875				
11	2.25	0.983	1.86705				
12	2.25	0.983	1.86705				
13	2.25	0.983	1.86705				

Table 5.5. Calibration and validation sets of nutrients in the samples containing NH_4NO_3 and TSP fertilizer (g/100g) in the second experiment.

Calibration	Nitrogen	Phosphorus	Validation	Nitrogen	Phosphorus
1	0.0195	0.0141	1	0.026	0.0188
2	0.0195	0.0141	2	0.026	0.0188
3	0.0325	0.0235	3	0.039	0.0282
4	0.0325	0.0235	4	0.039	0.0282
5	0.0455	0.0329	5	0.065	0.047
6	0.0455	0.0329	6	0.065	0.047
7	0.052	0.0376			
8	0.052	0.0376			
9	0.0584	0.0423			
10	0.0584	0.0423			
11	0.0715	0.0517			
12	0.0715	0.0517			
13	0.078	0.0564			
14	0.078	0.0564			

The calibration set of samples in the first experiment contained 13 data of 5 samples and the validation set contained 8 data of 4 samples. For the NH_4NO_3 and TSP containing samples in the second experiment, a calibration set of 14 data from 7 samples and a validation set of 6 data from 3 samples have been prepared.

5.2.2. Second Method

Soil sample collection and preparation:

The second method differed from the first method by the elimination of drying and moisturizing steps during sample preparation. The soil samples used in this method were from the 15 kg of total soil collected from the clover field as explained in soil sample collection and preparation part of Section 5.2.1. Five fertilizer types [KNO_3 , CaNO_3 , TSP, $(\text{NH}_4)_2\text{SO}_4$, NPK] were used during sample preparation which is explained in Figure 5.3. 100 grams of mixtures were prepared at 25 different concentrations in the range of 0.02%-0.5% (wt/wt). The concentrations of nutrients in the samples according to the fertilizer type are listed in Table B.1 and Table B.2 in Appendix B.

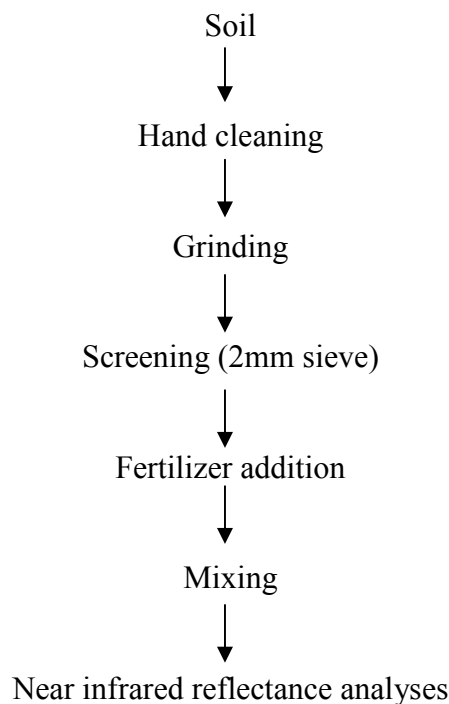


Figure 5.3. Sample preparation steps for the near infrared reflectance analyses according to the second method.

Near infrared reflectance analyses

The diffuse reflectance spectra of the samples were recorded with the same instrument operating under same conditions as explained in near infrared reflectance analyses part of Section 5.2.1. Three replicate scans were recorded for each sample in which the first two were collected without changing the position of sample cup and the

third one collected by rotating the sample cup about 90° around itself. The spectral data were recorded as $\log(1/R)$ (R: Reflectance) with a background taken by golden disk.

Data analyses

The near infrared reflectance data was processed with two multivariate calibration methods, genetic inverse least squares and partial least squares methods. As three replicate scans were recorded for 25 samples, the calibration set contained 51 data of 17 samples which were randomly selected and the validation set contained 24 data of 8 samples. The calibration and validation sets of nutrient concentrations are listed Tables C.1, C.2, C.3, C.4 and C.5 in Appendix C according to the fertilizer type used in the sample. The partial least squares method was commercially taken from Grams/32 Galactic Inc. The same calibration and validation sets prepared for genetic inverse least squares were used in this method.

5.2.3. Near infrared analyses of soil samples collected from clover and melon fields

In this part of the study, the prediction of nutrient concentrations was performed by relating the measured instrumental data to the nitrogen, phosphorus and potassium concentrations determined in laboratory by conventional methods. Hence, the samples were not soil-fertilizer mixtures, but pure soil collected randomly from several points of two different fields. Ten samples were obtained from the clover field and fifteen samples from the melon field, which was located next to the clover field. The samples were divided into two portions and were prepared for the analyses as explained in Figure 5.4.

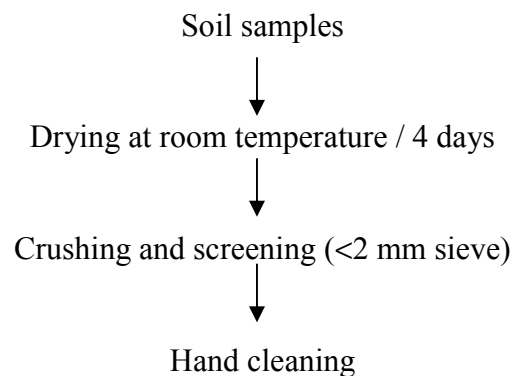


Figure 5.4. Sample preparation steps for laboratory analyses and near infrared reflectance analyses.

Following sample preparation, the first portion of samples was sent to the soil laboratory of Agricultural Engineering Department of Ege University. Total nitrogen, extractable phosphorus and exchangeable potassium analyses were performed with Kjeldahl, Bingham and ammonium acetate methods, respectively. These methods are explained in Figures D.1, D.2 and D.3 in Appendix D. The remaining portion was analyzed with near infrared spectrometer operating at the same working conditions as explained in near infrared reflectance analyses part of Section 5.2.1. Three replicate scans were recorded and genetic inverse least squares and partial least squares methods were used to relate the near infrared reflectance data to the laboratory results. The calibration set was composed of 51 data of 17 samples and the validation set contained 24 data of eight samples, which were randomly selected (Tables 5.6, 5.7 and 5.8).

Table 5.6. Calibration and validation sets of total nitrogen (N) (g/100 g).

Calibration	N	Calibration	N	Validation	N
1	0.0308	27	0.1008	1	0.084
2	0.0308	28	0.1064	2	0.084
3	0.0308	29	0.1064	3	0.084
4	0.0896	30	0.1064	4	0.0924
5	0.0896	31	0.1064	5	0.0924
6	0.0896	32	0.1064	6	0.0924
7	0.0896	33	0.1064	7	0.1064
8	0.0896	34	0.1148	8	0.1064
9	0.0896	35	0.1148	9	0.1064
10	0.0924	36	0.1148	10	0.1064
11	0.0924	37	0.1288	11	0.1064
12	0.0924	38	0.1288	12	0.1064
13	0.0952	39	0.1288	13	0.112
14	0.0952	40	0.1428	14	0.112
15	0.0952	41	0.1428	15	0.112
16	0.098	42	0.1428	16	0.1148
17	0.098	43	0.1512	17	0.1148
18	0.098	44	0.1512	18	0.1148
19	0.1036	45	0.1512	19	0.1316
20	0.1036	46	0.154	20	0.1316
21	0.1036	47	0.154	21	0.1316
22	0.1064	48	0.154	22	0.154
23	0.1064	49	0.1764	23	0.154
24	0.1064	50	0.1764	24	0.154
25	0.1008	51	0.1764		
26	0.1008				

Table 5.7. Calibration and validation sets of extractable phosphorus (P) (ppm).

Calibration	P	Calibration	P	Validation	P
1	0.72	27	3.67	1	1.51
2	0.72	28	3.89	2	1.51
3	0.72	29	3.89	3	1.51
4	1.94	30	3.89	4	2.16
5	1.94	31	4.03	5	2.16
6	1.94	32	4.03	6	2.16
7	2.16	33	4.03	7	3.38
8	2.16	34	5.83	8	3.38
9	2.16	35	5.83	9	3.38
10	2.16	36	5.83	10	3.89
11	2.16	37	7.2	11	3.89
12	2.16	38	7.2	12	3.89
13	3.17	39	7.2	13	4.32
14	3.17	40	9.58	14	4.32
15	3.17	41	9.58	15	4.32
16	3.31	42	9.58	16	6.26
17	3.31	43	12.02	17	6.26
18	3.31	44	12.02	18	6.26
19	3.38	45	12.02	19	7.63
20	3.38	46	14.18	20	7.63
21	3.38	47	14.18	21	7.63
22	3.53	48	14.18	22	13.68
23	3.53	49	14.33	23	13.68
24	3.53	50	14.33	24	13.68
25	3.67	51	14.33		
26	3.67				

Table 5.8. Calibration and validation sets of exchangeable potassium (K) (ppm).

Calibration	K	Calibration	K	Validation	K
1	14.5614	27	17.4908	1	14.5614
2	14.5614	28	17.4908	2	14.5614
3	14.5614	29	17.4908	3	14.5614
4	14.5614	30	17.4908	4	14.5614
5	14.5614	31	18.4672	5	14.5614
6	14.5614	32	18.4672	6	14.5614
7	15.5378	33	18.4672	7	15.5378
8	15.5378	34	18.4672	8	15.5378
9	15.5378	35	18.4672	9	15.5378
10	15.5378	36	18.4672	10	16.5143
11	15.5378	37	19.4437	11	16.5143
12	15.5378	38	19.4437	12	16.5143
13	15.5378	39	19.4437	13	16.5143
14	15.5378	40	20.4202	14	16.5143
15	15.5378	41	20.4202	15	16.5143
16	15.5378	42	20.4202	16	17.4908
17	15.5378	43	22.3731	17	17.4908
18	15.5378	44	22.3731	18	17.4908
19	16.5143	45	22.3731	19	19.4437
20	16.5143	46	23.3496	20	19.4437
21	16.5143	47	23.3496	21	19.4437
22	16.5143	48	23.3496	22	22.3731
23	16.5143	49	27.2554	23	22.3731
24	16.5143	50	27.2554	24	22.3731
25	17.4908	51	27.2554		
26	17.4908				

Chapter 6

RESULTS AND DISCUSSION

6.1. Results of near infrared reflectance analyses of soil-fertilizer mixtures prepared according to the first method.

According to the first method, two experiments were performed in which the fertilizer types and their concentrations were different. In Table 6.1, the differences in the two experiments are presented.

Table 6.1. Concentration profiles of nutrients (g/100 g) for the first and second experiments.

	Fertilizer Type	Fertilizer Concentration	Nitrogen	Phosphorus	Potassium
First experiment	NPK	1-15%	0.15-2.25	0.065-0.983	0.125-1.868
Second experiment	NH ₄ NO ₃ TSP	0.075-0.3%	0.0195-0.078	0.0141-0.0564	

In the first experiment, NPK fertilizer was used in the preparation of seven samples. The concentrations of nutrients in the samples simulate soils containing normal to rich amounts of nitrogen, phosphorus and potassium. According to the literature, soils containing total nitrogen amounts (N%) between 0.1-0.15% are considered as soils containing normal amounts of nitrogen. The values greater than 0.15% indicate rich amounts of nitrogen in soils. Furthermore, for soils containing normal amounts of phosphorus (P₂O₅%), the values range from 0.1% to 0.15%. For potassium nutrient (K₂O%), the concentrations greater than 0.3% indicate soils rich in potassium content (34). In the first experiment, the actual amounts of nitrogen, phosphorus and potassium can not be as high as the maximum concentrations in the samples. However, working at high concentrations would give an idea about the ability of near infrared reflectance spectroscopy in the determination of major nutrients of soil. The diffuse reflectance spectra of samples containing the minimum (1%) and maximum (15%) concentrations of NPK fertilizer and pure fertilizer are shown in Figure 6.1. As mentioned before, the term R denotes reflectance and it is converted to absorbance in terms of log (1/R).

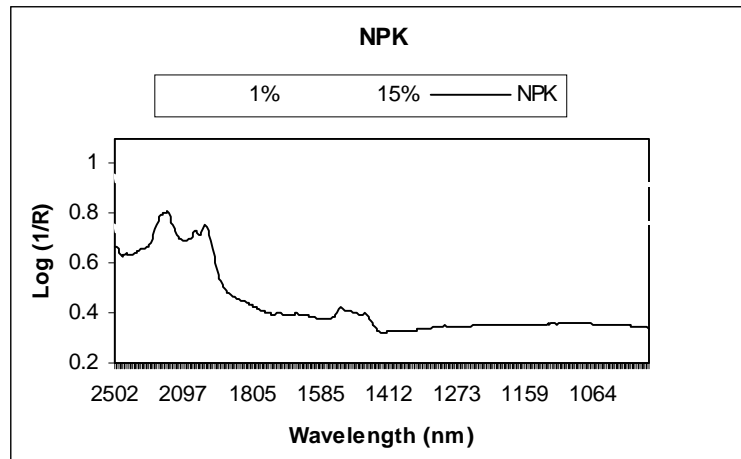


Figure 6.1. Diffuse reflectance spectra of NPK fertilizer and samples containing the minimum (1%) and maximum (15%) concentrations of NPK fertilizer.

The difference in the spectral features of NPK fertilizer and samples is obvious however it is difficult to interpret accurately the fertilizer concentrations from the sample spectra as they have similar spectral characteristics though the samples contain diverse amounts of nutrients. A baseline shift can be observed between the two samples due to the presence of moisture (14% moisture) and the large absorption peak around 1900 nm is an indication of moisture. The other observed small peak around 2190 nm indicates the combination vibrations of N-H bonds. As the absorbance bands in the near infrared region are very complex and broad, accurate and consistent quantification of components of interest can be possible through the use of multivariate statistics (37). Genetic inverse least squares method was used to predict the concentrations of nitrogen, phosphorus and potassium in the samples. The standard error of calibration (SEC) and standard error of prediction (SEP) values have been calculated for a calibration set of 13 data and a validation set of 8 data (Table 6.2 and Figure 6.2).

Table 6.2. SEC, SEP and R^2 (calibration) values of the nutrients in the samples containing NPK fertilizer.

Soil constituent	SEC (g/100 g)	SEP (g/100 g)	R^2
Nitrogen	0.0206	0.0917	0.9994
Phosphorus	0.029	0.035	0.9943
Potassium	0.0325	0.0588	0.9980

For the validation set, regression coefficients of 0.9820, 0.9779 and 0.9906 were found for the prediction to nitrogen, phosphorus and potassium concentrations in the samples, respectively.

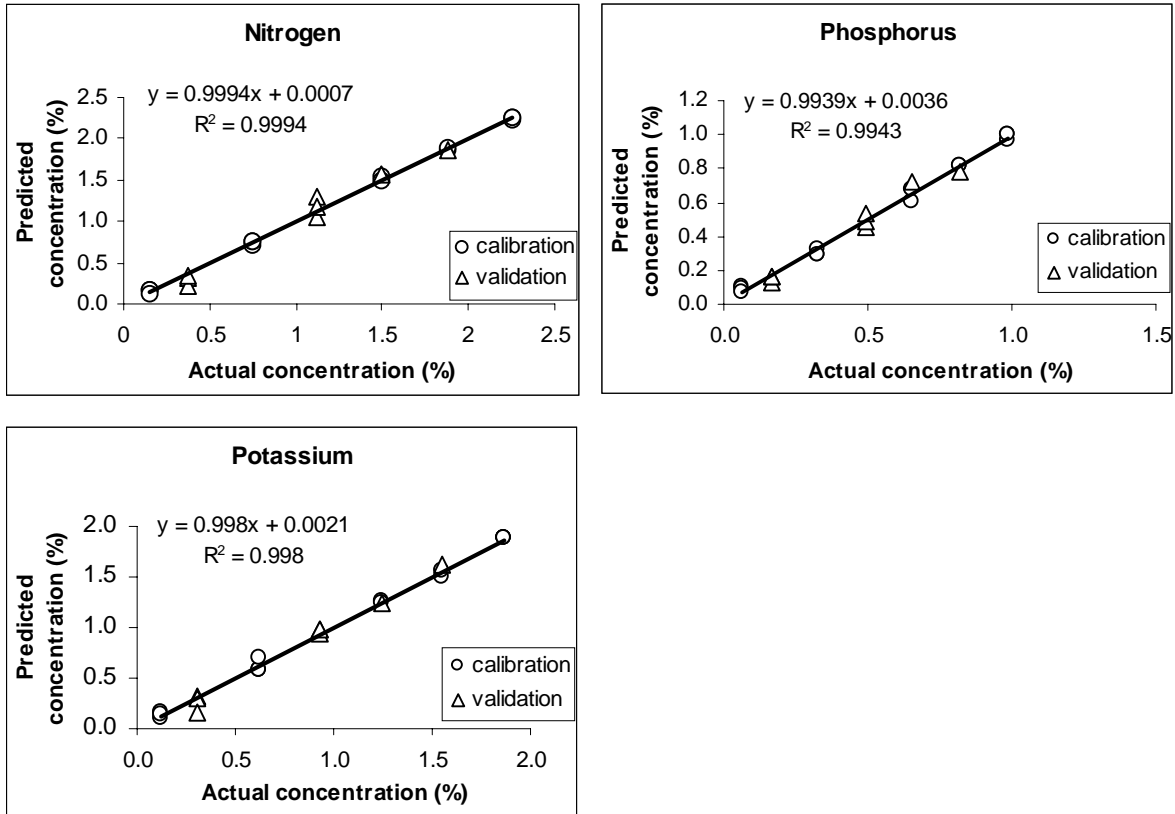


Figure 6.2. Calibration curves of nitrogen, phosphorus and potassium nutrients in the samples containing NPK fertilizer.

The near infrared reflectance spectroscopy is very sensitive to moisture content of samples due to the high intensity and high extinction coefficient of moisture O-H bands in the near infrared region (15). Dalal and Henry (1986) have also indicated that the visual changes in the absorbance in near infrared spectra were mainly because of changes in moisture contents of samples studied (22). Although the strong influence of moisture on the near infrared spectra, near infrared spectrometer was able to predict the nitrogen, phosphorus and potassium levels at high concentrations of NPK fertilizer, accurately.

In the second experiment, the same procedure was followed but for lower concentrations of nutrients, which simulate soils containing nutrients ranging from poor to approximately normal amounts. The concentrations of nutrients in the samples are in

the range of 0.075% to 0.3% (wt/wt). NH_4NO_3 (containing 26% nitrogen) and TSP [$\text{Ca}_3(\text{PO}_4)_2$ containing 43% P_2O_5] fertilizer types were used in the preparation of ten samples. The diffuse reflectance spectra of samples containing the maximum (0.3%) and minimum (0.075%) concentrations of NH_4NO_3 and TSP fertilizers together with the pure fertilizers are shown in Figure 6.2 and Figure 6.3.

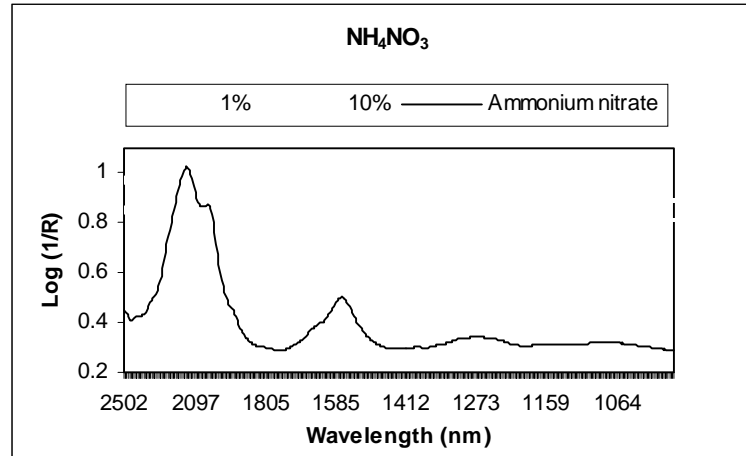


Figure 6.3. Diffuse reflectance spectra of NH_4NO_3 fertilizer and samples containing the minimum (0.075%) and maximum (0.3%) concentrations of NH_4NO_3 fertilizer.

As it can be seen from Figure 6.2, the pure fertilizer spectra gives a large absorption peak around 2130 nm due to the high content of nitrogen (26%). Additionally, in the soil-fertilizer mixtures, the water absorption peaks are observed at around 1900 and 1400 nm.

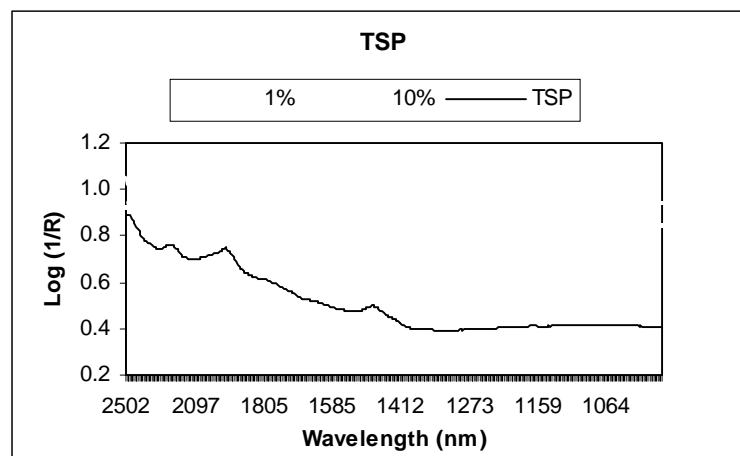


Figure 6.4. Diffuse reflectance spectra of TSP fertilizer and samples containing the minimum (0.075%) and maximum (0.3%) concentrations of TSP fertilizer.

Genetic inverse least squares method was used to predict the nutrient concentrations in the samples and the results of this method are shown in Table 6.3 and Figure 6.4.

Table 6.3. SEC, SEP and R^2 (calibration) values of the nutrients in the samples containing NH_4NO_3 and TSP fertilizers.

Soil constituent	SEC (g/100 g)	SEP (g/100 g)	R^2
Nitrogen	0.0034	0.0081	0.9728
Phosphorus	0.0028	0.0076	0.9608

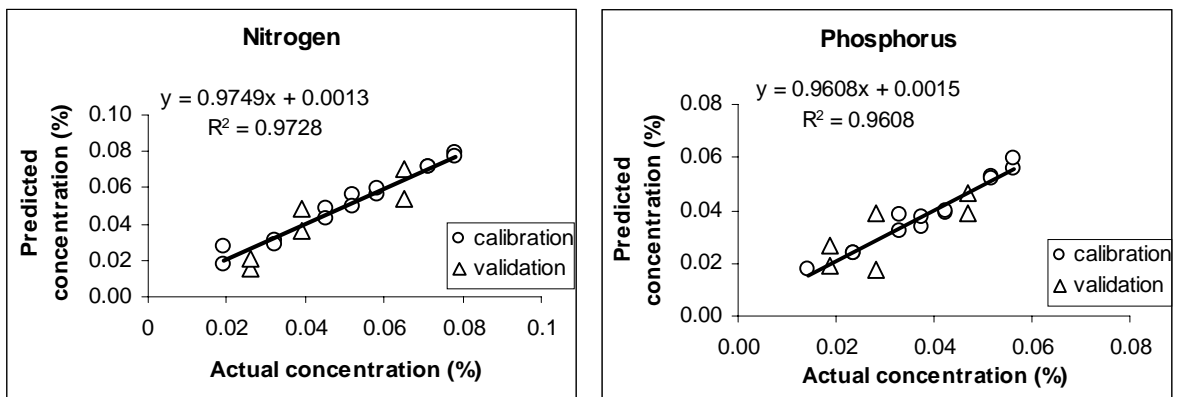


Figure 6.5. Calibration curves of nitrogen and phosphorus nutrients in the samples containing NH_4NO_3 and TSP fertilizers.

Relative to the previous results, lower coefficient of correlation values were obtained for the calibration model due to the lower nutrient concentrations. Although the nutrient levels were low, the calibration model worked well in the prediction of nitrogen and phosphorus concentrations that the regression coefficients of validation sets for nitrogen and phosphorus were 0.8409 and 0.60, respectively. In literature, generally predictions with regression coefficients greater than 0.50 were considered as reliable predictions and the ones with regression coefficients greater than 0.80 were considered as accurate predictions (39,40,41).

Besides these two experiments, the diffuse reflectance spectra of pure fertilizers were also investigated. For this aim, the ground fertilizers (< 2 mm size) were analyzed with near infrared reflectance spectroscopy. The diffuse reflectance spectra of pure fertilizers are shown in Figure 6.6.

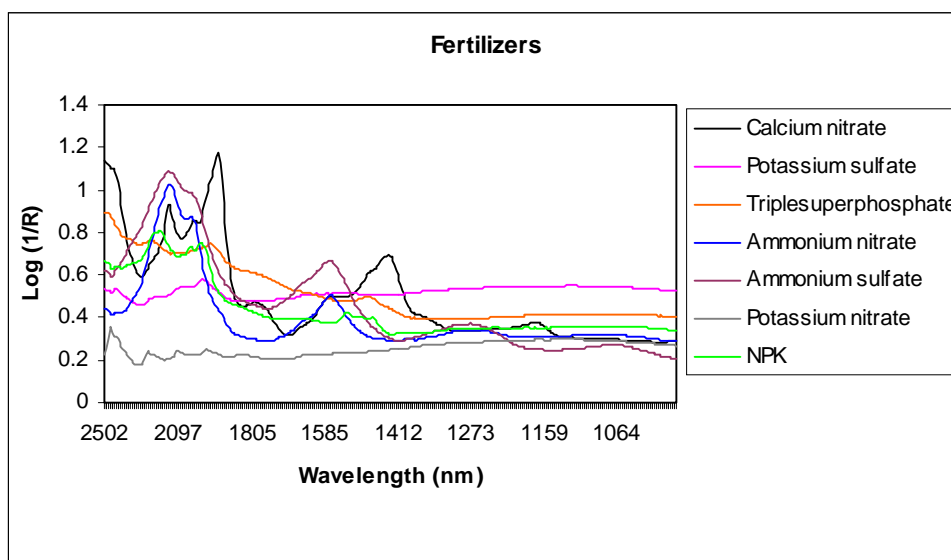


Figure 6.6. Diffuse reflectance spectra of pure fertilizers.

The diffuse reflectance spectra of nitrogen containing fertilizers show broad peaks around 2000-2200 nm. According to the literature, these are the combination vibrations of N-H bonds, which are observed between 1800-2200 nm region. In addition to this, the smaller peaks located between 1430-1560 nm indicate the first overtones of N-H bonds, which are observed between 1420-1600 nm (14). For phosphorus and potassium containing fertilizers, a specific absorption peak is not observed. It was mentioned that the possible absorption bands in the near infrared region arise from O-H, N-H and C-H bands. Thus, for mineral species there are no absorption bands in the near infrared region as it can be understood from the reflectance spectra of pure fertilizers containing phosphorus and potassium (15). However, according to the literature, the ability of near infrared reflectance spectrometer to determine phosphorus and potassium contents is based on the correlation between the primary and secondary properties of soil (21,39). The primary properties of soil respond to near infrared radiation by absorbing the energy. Some examples to those soil attributes which can be directly measured in the near infrared region are organic matter, moisture content or particle size distribution, total carbon or total nitrogen contents (39). On the other hand, the secondary properties can not be measured directly in the near infrared region due to the inability of the molecules to absorb the near infrared radiation. Some of these secondary properties of soil are cation exchange capacity, calcium, magnesium, phosphorus and potassium contents etc. Due to the correlation of secondary properties with one or more of the

primary ones, the prediction may be possible. For instance, Chang et al. (2001) indicated that cation exchange capacity could be predicted depending on the correlation with organic matter or clay content (38). They have also indicated that the size, shape and arrangement of particles in a sample affect the path of light transmission and reflectance spectra. Based on the primary response of soil texture and structure, sand and silt contents of soil could be predicted using near infrared technique with principal component regression method ($R^2 > 0.82$). They have also predicted the potassium amounts in the samples determined by ammonium acetate and Mechlich 3 methods. An information about the correlation of potassium with the primary properties was not given. The phosphorus amounts determined by Mechlich 3 method could not be predicted by near infrared reflectance and principal component regression method (38). On the other hand, it is also quite possible that the near infrared region can directly measure the organic phosphorus which is organically bound to organic matter (15).

6.2. Results of near infrared reflectance analyses of soil-fertilizer mixtures prepared according to the second method.

In the second method, different from the first one, the drying and moisturizing steps were eliminated. The aim was to prevent the formation of baseline shift due to moisture differences in the samples. All the samples had the same moisture content (approximately 14%). The number of samples was increased up to 25 in the concentration range of 0.02-0.5% (wt/wt) fertilizer. Five fertilizer types [(NH₄)₂SO₄, TSP, NPK, KNO₃, Ca(NO₃)₂] were used in the preparation of samples and two multivariate calibration techniques (genetic inverse least squares and partial least squares methods) were used to process the near infrared reflectance data. The results of genetic inverse least squares method are summarized in Table 6.4.

Table 6.4. SEC, SEP and R² (calibration) values of the nutrients in the samples prepared according to the second method.

Constituent	R ²	SEC (g/100 g)	SEP (g/100 g)
NPK-N	0.9034	0.007	0.0116
NPK-P	0.9265	0.0027	0.0051
NPK-K	0.9204	0.0053	0.0083
(NH ₄) ₂ SO ₄ -N	0.9769	0.00478	0.01083
(NH ₄) ₂ SO ₄ -S	0.9813	0.0049	0.013
Ca(NO ₃) ₂ -N	0.9676	0.00418	0.0216
Ca(NO ₃) ₂ -Ca	0.8095	0.0096	0.0203
KNO ₃ -N	0.9217	0.00545	0.01826
KNO ₃ -K	0.8116	0.00845	0.0149
TSP-P	0.81	0.01314	0.0203

As it can be seen from Table 6.4, the regression coefficients for the calibration model were greater than 0.80 for each sample containing different fertilizer types. However, the model was not satisfactory in predicting the nutrient amounts except for the samples containing NPK and (NH₄)₂SO₄ fertilizers. The regression coefficients for the prediction of nutrient concentrations in the samples containing TSP, KNO₃, Ca(NO₃)₂ fertilizers were all smaller than 0.50. For nitrogen and sulfur in (NH₄)₂SO₄ containing samples, the regression coefficients were 0.8620 and 0.8555, respectively. These values indicate accurate predictions of the nutrient amounts, which may be due to the absorption of near infrared radiation by the N-H and O-H bonds as well as the strong absorption of the overtones of SO₄²⁻ groups (39). The regression coefficients for the prediction of nitrogen, phosphorus and potassium amounts in samples containing NPK fertilizer were 0.6737, 0.7633 and 0.8724, respectively. The calibration curves for (NH₄)₂SO₄ and NPK fertilizer nutrients in the mixtures are shown in Figure 6.7.

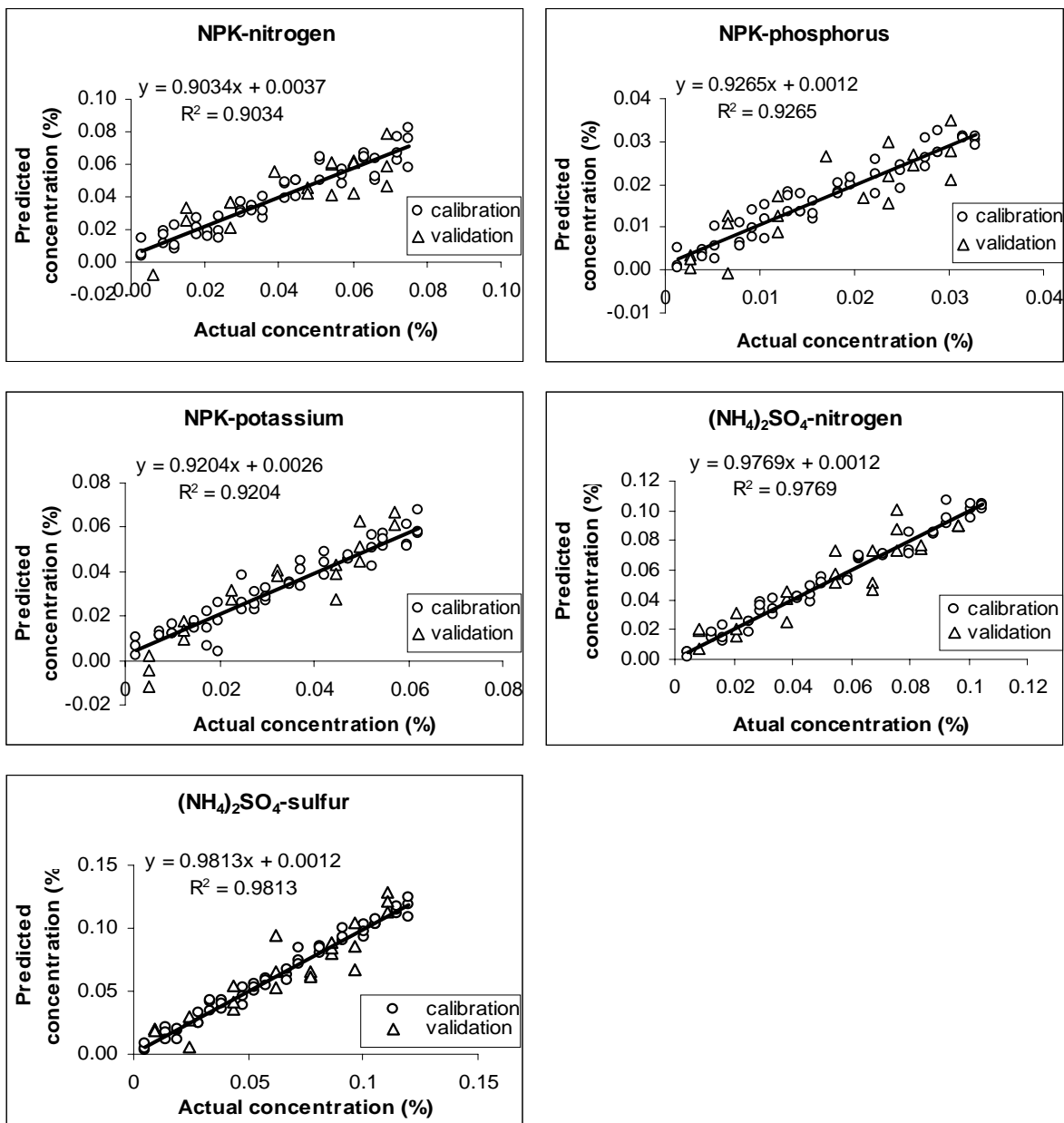


Figure 6.7. Calibration curves of nitrogen and phosphorus, potassium and sulfur nutrients in the samples containing $(\text{NH}_4)_2\text{SO}_4$ and NPK fertilizers.

In the first experiment, which was explained in Section 6.1, accurate predictions of nitrogen, phosphorus and potassium levels in soil-NPK mixtures were obtained at high concentrations of fertilizer. With these results, it can be said that the prediction of major nutrients can either be accurately done at very low concentrations in the NPK containing samples. The reason that high prediction was obtained only for $(\text{NH}_4)_2\text{SO}_4$ and NPK fertilizer containing samples may be due to the measurement of N-H bonds in the structure of fertilizers. The NPK fertilizer has its nitrogen coming from $(\text{NH}_4)_2\text{SO}_4$ or NH_4NO_3 . The concentrations of nutrients in this experiment were at the lowest

detection limits of near infrared instrument (0.001-1%), which is a reason of poor prediction of nitrogen, phosphorus and potassium coming from the other fertilizers. Additionally, elimination of moisturizing step could be another reason of poor prediction. Addition of water and mixing provided solubilization and homogenous dispersion of fertilizer in soil. To prevent the moisture changes in the samples, a drying operation to the samples could be applied as a final step.

The reflectance data of the same samples in the second method were processed with partial least squares method as well. Successful predictions could be obtained only for the samples containing $(\text{NH}_4)_2\text{SO}_4$ fertilizer. The regression coefficients of calibration set for nitrogen and sulfur in $(\text{NH}_4)_2\text{SO}_4$ containing samples were 0.9049 with a SEC value of 0.0092 for nitrogen and with a SEC of 0.01 for sulfur (factor number=6). During the development of calibration model, nine data were excluded from the whole data as outliers, which were the first, seventh and twenty-first samples. The regression coefficients for the validation set of nitrogen and sulfur were 0.9301 with a SEP value of 0.0091 for nitrogen and 0.01 for sulfur. During the prediction of nitrogen and sulfur, the outliers come from the first, third, fourth, seventeenth, twenty-fourth and twenty fifth samples. The prediction of nitrogen, phosphorus and potassium amounts in the other samples containing NPK, KNO_3 and $\text{Ca}(\text{NO}_3)_2$ fertilizers by partial least squares was poor ($R^2 < 0.20$). The calibration and validation curves of nitrogen and sulfur are presented in Figure 6.8 and Figure 6.9. The results of partial least squares analyses for the samples containing the other fertilizers [NPK, KNO_3 , $\text{Ca}(\text{NO}_3)_2$] are summarized in Table 6.5.

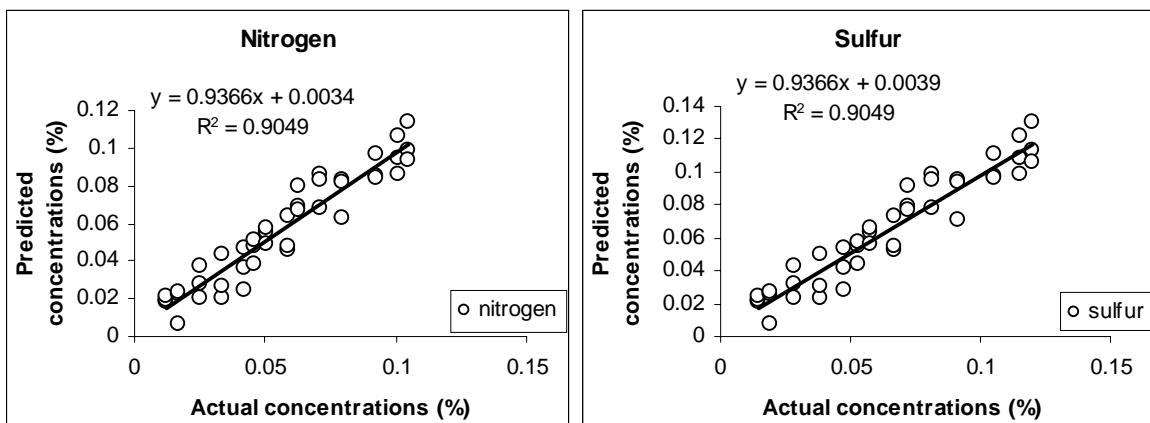


Figure 6.8. Calibration curves of nitrogen and sulfur nutrients in the samples containing $(\text{NH}_4)_2\text{SO}_4$ fertilizers.

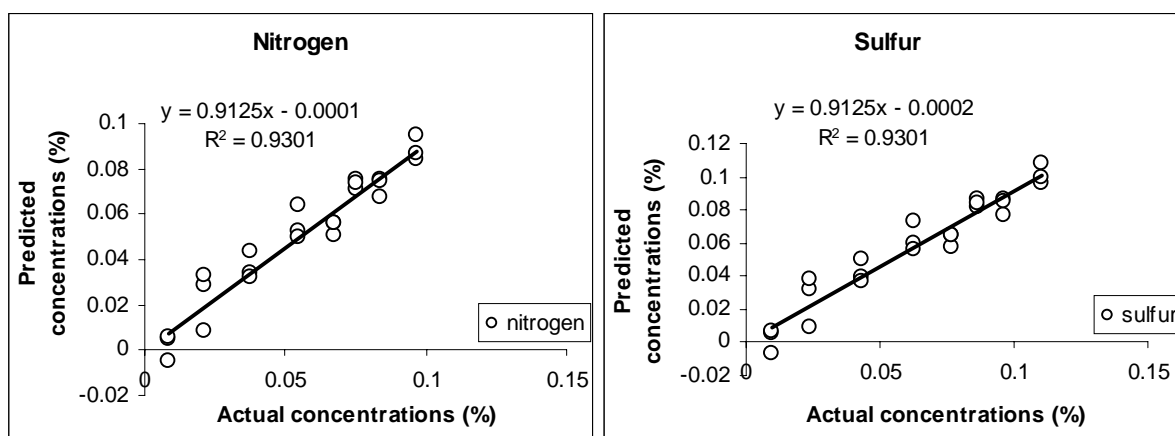


Figure 6.9. Validation curves of nitrogen and sulfur nutrients in the samples containing $(\text{NH}_4)_2\text{SO}_4$ fertilizers.

Table 6.5. Partial least squares analyses of samples containing fertilizers NPK, KNO_3 and $\text{Ca}(\text{NO}_3)_2$.

Constituent	SEC (g/100 g)	SEP (g/100 g)	R ²	Factor Number	Number of samples excluded
NPK-N	0.0069	0.031	0.7841	6	9
NPK-P	0.003	0.0136	0.7841	6	9
NPK-K	0.0057	0.0258	0.7841	6	9
$\text{Ca}(\text{NO}_3)_2$ -N	0.006	0.026	0.9247	5	20
$\text{Ca}(\text{NO}_3)_2$ -Ca	0.0057	0.024	0.9447	5	20
KNO_3 -N	0.0061	0.022	0.8889	5	22
KNO_3 -K	0.018	0.064	0.8889	5	22

6.3. Results of near infrared reflectance analyses of soil samples collected from different fields

In this part of the study, 25 soil samples collected from two agricultural fields were analyzed with near infrared reflectance spectroscopy. Genetic inverse least squares and partial least squares were used to relate the near infrared reflectance data to the known concentrations of nutrients, which were determined by the laboratory analyses. The laboratory analyses were carried out by the soil laboratory of Agricultural Engineering Department of Ege University. Kjeldahl, Bingham and ammonium acetate methods were used for the determination of nitrogen, phosphorus and potassium concentrations. The genetic inverse least square results of the samples are listed in Table 6.6 and the results of laboratory tests are shown in Table 6.7. The first fifteen results are from the melon field and the last ten results belong to the clover field. No replicates were done in the laboratory analyses. The calibration coefficients obtained by genetic inverse least

square method were greater than 0.80 for the three constituents, however their prediction were poor ($R^2 < 0.20$). The partial least square method did not calculate any factor numbers for nitrogen, phosphorus and potassium. Better prediction of nutrients could be possible by increasing the soil sample numbers having a wider range of nutrient contents. Additionally, the conventional methods applied in the laboratory for the determination of nutrient amounts in soil also affect the prediction ability of near infrared technique. Ludwig et al. (2002) indicated that the near infrared reflectance technique was able to predict the phosphorus content in soil as the phosphorus amounts were determined using Olsen method. However, the phosphorus concentrations determined by Bray-2 method could not be predicted (41). Thus, the laboratory methods also affect the prediction ability of near infrared technique. Considering results of several laboratory methods with replicate analyses may improve the prediction ability of this technique.

Table 6.6. SEC, SEP, R^2 (calibration) values of nitrogen, phosphorus and potassium in soil samples.

Constituent	SEC (g/100 g)	SEP (g/100 g)	R^2
Nitrogen	0.013	0.027	0.8195
Phosphorus	1.844	5.154	0.8147
Potassium	1.501	6.6711	0.8102

Table 6.7. Results of laboratory analyses done by the soil laboratory of Agricultural Engineering Department of Ege University.

Number	Total nitrogen (%)	Extractable Phosphorus (ppm)	Exchangeable Potassium (ppm)
1	0.0308	2.16	14.56
2	0.0896	2.16	16.51
3	0.154	3.67	16.51
4	0.1064	4.03	15.54
5	0.1008	3.89	17.49
6	0.112	3.31	15.54
7	0.1064	7.20	19.44
8	0.098	7.63	18.47
9	0.0896	3.38	14.56
10	0.0924	3.53	15.54
11	0.1064	13.68	15.54
12	0.0924	14.33	16.51
13	0.1148	4.32	22.37
14	0.1064	3.38	23.35
15	0.0952	5.83	14.56
16	0.084	0.72	16.51
17	0.1148	2.16	14.56
18	0.1064	1.94	15.54
19	0.1036	1.51	17.49
20	0.1428	6.26	18.47
21	0.1316	9.58	17.49
22	0.154	12.02	19.44
23	0.1288	14.18	20.42
24	0.1512	3.89	27.26
25	0.1764	3.17	22.37

Chapter 7

CONCLUSIONS AND RECOMMENDATIONS

7.1. Conclusions

Determination of major soil nutrient concentrations (nitrogen, phosphorus and potassium) using near infrared reflectance technique with two multivariate calibration methods of which are genetic inverse least squares and partial least squares was investigated. Within this dissertation, two new methods have been developed which involved the use of fertilizers in the preparation of samples containing nutrients at various concentrations. In addition to this, a new statistical method, genetic inverse least squares has been introduced to the calibration strategies which are used in the determination of soil nutrients using near infrared reflectance spectroscopy. The main advantage of this method was that only the nutrient concentrations were required for the development of calibration model. In this way, the necessity of knowing the concentrations of other interfering constituents in soil such as moisture or carbon content was eliminated. The results of the experiments indicate that the sample preparation steps influenced the prediction ability of near infrared reflectance technique. Moisturizing and mixing of soil samples following fertilizer addition provided solubilization and homogenous dispersion of fertilizer in soil which enhanced the prediction of nutrient concentrations in soil-fertilizer mixtures. Furthermore, fertilizer concentrations and fertilizer types were the other contributing factors that affected the prediction of nutrient concentrations in the samples. Nitrogen, phosphorus and potassium concentrations were at the lowest detection limits of near infrared reflectance spectroscopy (0.001-1%). Mostly for the ammonium containing fertilizers [NPK, $(\text{NH}_4)_2\text{SO}_4$, NH_4NO_3], reliable predictions of nitrogen, phosphorus and potassium concentrations could be achieved due to the N-H bonds in the structure of fertilizers. The prediction of phosphorus and potassium was possible by the correlation of these nutrients with the primary properties of soil such as total carbon, total nitrogen, moisture, particle size and organic matter content. Consequently, nitrogen, phosphorus and potassium levels could be predicted reliable according to the first method (R^2 values all greater than 0.60 using genetic inverse least squares method). On the other hand, with the second method, satisfactory predictions of these nutrient levels could be

obtained only for the samples containing NPK and $(\text{NH}_4)_2\text{SO}_4$ fertilizers (R^2 values greater than 0.60 according to genetic inverse least squares method). Using near infrared technique with partial least squares for the second method, only prediction of nitrogen and sulfur in samples containing $(\text{NH}_4)_2\text{SO}_4$ could be achieved with a regression coefficient value of 0.93.

According to the literature, near infrared reflectance spectroscopy is considered as a rapid, non-destructive and simple analytical method that can be used for the determination of several soil properties such as organic carbon, total nitrogen, organic matter, moisture, clay content, cation exchange capacity, and several nutrients depending on the laboratory analyses (e.g.: calcium, magnesium, phosphorus, mangan, potassium, iron, etc.) (22,24,36,37,38,41). In food industry, this technique can be used for the determination of fat, moisture, protein, sugar etc. contents of various food products, and commercially available portable instruments based on the working principle of near infrared spectroscopy have been developed. It can be concluded that, adapting the near infrared technique to field use for on-line analysis of soil nutrients would be very useful for the farmers in terms of precision agriculture.

7.2. Recommendations

The future study of this work could concentrate on the evaluation of moisture effect on the prediction ability of near infrared reflectance spectroscopy with genetic inverse least squares and partial least squares methods. The samples containing 14% moisture could be dried as a final step during sample preparation for near infrared analyses.

A complementary study to near infrared reflectance technique could also be done with a laser spectroscopy. The experimental set-up shown in Figure 7.1 is present in the optics laboratory of Electronic Engineering Faculty, İzmir Institute of Technology. It is worth to investigate the interactions between electromagnetic radiation at 1062 nm produced by the Nd:LSB laser source and the samples containing fertilizers as well as the pure fertilizers. According to a study by Cremers et al. (2001), the total soil carbon content was measured with laser induced breakdown spectroscopy (LIBS). The working principle of LIBS is based on the atomic emission spectroscopy. By focusing the output of a Nd:YAG laser source at 1064 nm (50mJ pulses of 10 ns), a microplasma was formed on the sample due to the excitation of carbon atoms. The emitted light, which is characteristic to carbon atom (247.8 nm) is collected, spectrally resolved and detected using a photodiode array detector. The LIBS data is related to the total carbon

concentrations determined by conventional laboratory analyses (dry combustion analyses) with a regression coefficient of 0.96 (42).

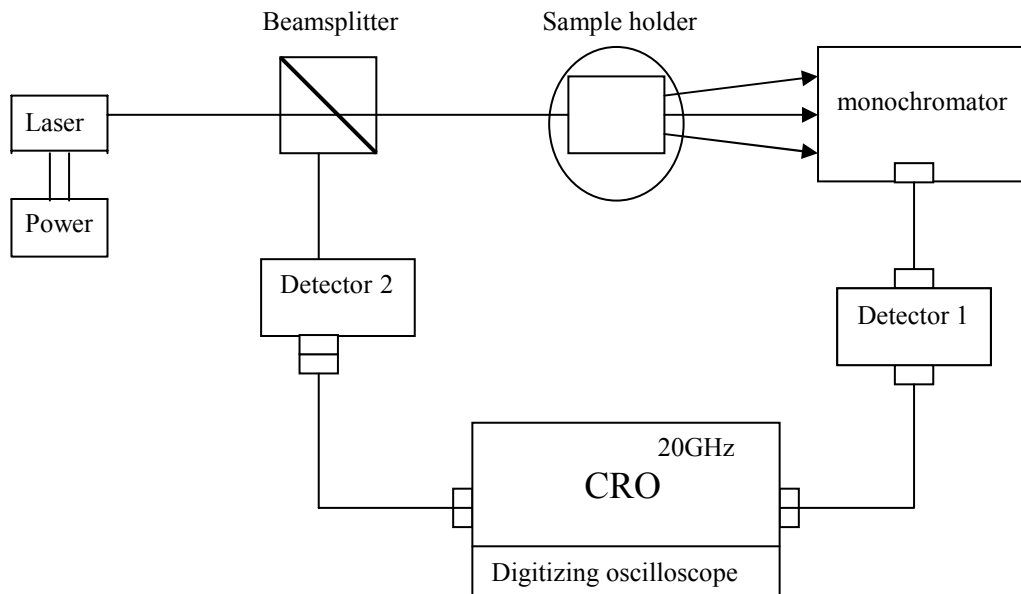


Figure 7.1 Experimental set up of laser spectroscopy established in the optics laboratory of Electronic Engineering Department, İzmir Institute of Technology.

1-Laser source: Diode pump Nd:LSB microchip solid state laser

Wavelength range: 1062 nm	Pulse energy	: >3mJ
Pulse duration : <0.7 ns	Polarization ratio	: >100:1

2-Beamsplitter

3-Quartz sample holder

4-Monochromator

5-Detector 1 (818 BB 21)

Spectral range : 300-1100 nm	Rise time	: <300 ps
Material : silicon	Responsivity	: 0.4 A/W

Cut-off frequency : > 1.2 GHz

6-Scope 54750 digitizing oscilloscope

Bandwidth : 20 GHz

7-Detector 2 (818 BB 31)

Spectral range : 1000-1600 nm
Material : InGaAs
Rise time : < 200ps.
Cut-off frequency : > 15 GHz

REFERENCES

1. Skoog, D.A., Holler, F.J., Nieman, T.A., *Principles of Instrumental Analysis*, (Harcourt Brace College Publishers, Chicago, 1998), p.1-191, 404-426.
2. Karoui, R., Mazerolles, G., Dufour, E., “Spectroscopic techniques coupled with chemometric tools for structure and texture determinations in dairy products”, *International Dairy Journal*, 13 (8), (2003), 607-620.
3. Schulz, H., Engelhardt, U.H., Wegent, A., Drews, H.-H., Lapczynski, S., “Application of near-infrared reflectance spectroscopy to the simultaneous prediction of alkaloids and phenolic substances in green tea leaves”, *Journal of Agric. Food Chemistry*, 47, (1999), 5064-5067.
4. Sudduth, K.A., Hummel, J.W., Birrell, S.J., “Sensors for Site-specific Management”, *ASA-CSSA-Soil Science Society of America*, (1997), p.183-192.
5. Tan, K.H., *Soil sampling, preparation, and analysis*, (Marcel Dekker Inc., New York, 1996), p.135-175, 278-286.
6. Buckmann, H.O., Brady, N.C., *The nature and properties of soil*, (the Macmillan Company, London, 1969), p.1-39, 137-163, 422-483, 503-515.
7. Troeh, F.R., Thompson, L.M., *Soils and Soil Fertility*, (Oxford University Press Inc., New York, 1993), p.3-15, 193-253.
8. Barber, A.S., Nitrogen, in *Soil Nutrient Bioavailability*, (John Wiley and Sons, Inc., New York, 1995), p.181-199.
9. Günay, A., *Sebzecilik*, (Ankara Üniversitesi Ziraat Fakültesi Bahçe Bitkileri Bölümü, Ankara, 1984), p. 45, 72, 204.

10. Jacks, G.V., Nitrogen, sulphur and phosphorus, their interactions and availability, in *Soil Chemistry and Fertility Meeting Commissions 2 and 4 of the International Society of Soil Science*, edited by Williams, C.H., (International Society of soil Science, 1967), p.93-111.
11. Aydeniz, A., Brohi, A., *Gübreler ve Gübreleme*, (Cumhuriyet Üniversitesi Ziraat Fakültesi Yayınları, Tokat, 1991).
12. Jacob, A., Uexküll, H., Bitki Besinleri, in *Gübreleme (Toprak Mahsüllerinin Beslenme ve Gübrenmeleri)*, (Ege Üniversitesi Ziraat Fakültesi Yayınları, İzmir, 1961), p.1-9.
13. Westerman, R.L., Testing soils for potassium, calcium, and magnesium, in *Soil Testing and Plant Analysis*, edited by Haby, V.A., Ruselle, M.P., Skogley, E.O., (Soil Science Society of America, Madison, 1990), p. 184-189.
14. Osborne, B.G., Near-infrared Spectroscopy in Food analysis, in *Encyclopedia of analytical Chemistry*, edited by Meyers, R.A., (John Wiley and Sons Ltd., New York, 1986), p.1-13.
15. Burns, D.A., Ciurczak, E.W., *Handbook of Near-Infrared analysis*, (Marcel Dekker Inc., New York, 2001), p.7-59, 419-543.
16. Özdemir, D., “Multi-Instrument Calibration Using Genetic Regression in UV-Visible and Near-Infrared Spectroscopy”, Ph.D. Thesis, Clemson University, 1999.
17. Xie, F., Dowell, F.E., Sun, X.S., “Comparison of Near-Infrared Reflectance Spectroscopy and Texture Analyzer for Measuring Wheat Bread Changes in Storage”, *Cereal Chemistry*, 80(1), (2003), 25-29.
18. Sorensen, L.K., Jepsen, R., “Assessment of Sensory properties of Cheese by Near-Infrared Spectroscopy”, *International Dairy Journal*, 8, (1998), 863-871.

19. Byrne, C.E., Downey, G., Troy, D.J., Buckley, D.J., “Non-destructive Prediction of Selected Quality Attributes of Beef by Near-infrared Reflectance Spectroscopy Between 750 and 1098 nm”, *Meat Science*, 49(4), (1998), 399-409.
20. Valdes, E.V., Dierenfeld, E.S., Fitzpatrick, M.P., “Application of a Near Infrared Reflectance Spectroscopy (NIR) to Measure protein, Fat and Moisture in Fish Samples”, *Proceedings of the Second Conference of the Nutrition Advisory Group of the American Zoo and Aquarium Association on Zoo and Wildlife Nutrition*, (1997), 8: 159-161.
21. Gillon, D., Houssard, C., Joffre, R., “Using near-infrared reflectance spectroscopy to predict carbon, nitrogen and phosphorus content in heterogeneous plant material”, *Oecologia*, 118, (1999), 173-182.
22. Dalal, R.C., Henry, R.J., “Simultaneous determination of moisture, organic carbon, and total nitrogen by near infrared reflectance spectrophotometry”, *Soil Science Society of American Journal*, 50(1), (1986), 120-123
23. Sudduth, K.A., Hummel, J.W., “Geographic operating range evaluation of a NIR soil sensor”, *Transactions of American Society of Agricultural Engineers*, 39(5), (1996), 1599-1604.
24. Sudduth, K.A., Hummel, J.W., “Portable, near-infrared spectrophotometer for rapid soil analysis”, *Transactions of American Society of Agricultural Engineers*, 36(1), (1993), 185-193.
25. Sudduth, K.A., Hummel, J.W., “Soil organic matter, CEC, and moisture sensing with a portable NIR spectrophotometer”, *Transactions of American Society of Agricultural Engineers*, 36(6), (1993), 1571-1582.
26. <http://elchem.kaist.ac.kr/vt/chem-ed/spec/laser/lif.htm>.

27. Strasburg, G.M., Ludescher, R.D., "Theory and applications of fluorescence spectroscopy in food research", *Trends in Food Science and Technology*, 6, (1995), 69-75.
28. Daughtry, C.S.T., McMurtrey, J.E., Chapelle, E.W., Dulaney, W.P., Irons, J.R., Satterwhite, M.B., "Potential for Discriminating Crop Residues from Soil by Reflectance and Fluorescence", *Agronomy Journal*, 87(2), (1995), 165-171.
29. Corp, L.A., Chapelle, E.W., McMurtrey, J.E., Mulchi, C.L., Daughtry, C.S.T., Kim, M.S., "Advances in Fluorescence Sensing Systems for the Remote Assessment of Nitrogen Supply in Field Corn", *Proceedings of the International Geoscience and Remote Sensing Symposium*, (2000), 1:351-353.
30. Kotzick, R., Niessner, R., "Application of time-resolved, laser-induced and fiber-optically guided fluorescence for monitoring of a PAH-contaminated remediation site", *Fresenius Journal of Analytical Chemistry*, 354, (1996), 72-76.
31. Moulin, C., Vitart, X., "Pulsed microchip laser induced fluorescence for in situ tracer experiments", *Fresenius Journal of Analytical Chemistry*, 361, (1998), 81-85
32. Löhmannsröben, H.G., Schober, L., "Combination of laser-induced fluorescence and diffuse-reflectance spectroscopy for the *in-situ* analysis of diesel-fuel-contaminated soils", *Applied Optics*, 38(9), 1999, 1404-1410
33. Bloch, J., Johnson, B., Newbury, N., Germaine, J., Hemond, H., Sinfield, J., "Field test of a novel microlaser-based probe for *in-situ* fluorescence sensing of soil contamination", *Applied Spectroscopy*, 52(10), 1299-1304.
34. Ceylan, A., *Tarla Tarımı*, (Ege Üniversitesi Basımevi Müdürlüğü, İzmir, 1994), p.335-358.
35. Kaçar, B., Gübrelerle toprağa verilecek bitki besin maddeleri miktarının hesaplanması, in *Gübre Analizleri*, (Ankara Üniversitesi Basımevi, Ankara, 1990), p.3.

36. Thomasson, J.A., Sui, R., Cox, M.S., Al-Rajehy, A., “Soil Reflectance Sensing for Determining Soil Properties in Precision Agriculture”, *ASAE Annual International Meeting*, (2000), Paper no: 001044.
37. Chang, C.-W., Laird, D.A., “Near-Infrared Reflectance Spectroscopic Analysis of Soil C and N”, *Soil Science*, 167(2), (2002), 110-116.
38. Chang, C.W., Laird, D.A., Mausbach, M.J., Hurburgh, C.R., “Near-Infrared Reflectance Spectroscopy-Principal Components Regression Analyses of Soil Properties”, *Soil Science Society of America Journal*, 65(2), (2001), 480-490.
39. Shepherd, K.D., Walsh, M.G., “Development of Reflectance Spectral Libraries for Characterization of Soil Properties”, *Soil Science Society of America Journal*, 66(3), (2002), 988-998.
40. Alrajehy, A., “Relationships between soil reflectance and soil physical and chemical properties”, M.S. Thesis, Mississippi State University, 2002.
41. Ludwig, B., Khanna, P.K., Bauhus, J., Hopmans, P., “Near infrared spectroscopy of forest soils to determine chemical and biological properties related to soil sustainability”, *Forest Ecology and Management*, 171, (2002), 121-132.
42. Cremers, D.A., Ebinger, M.H., Breshears, D.D., Unkefer, P.J., Kammerdiener, S.A., Ferris, M.J., Catlett, K.M., Brown, J.R., “Measuring Total Soil Carbon with Laser-Induced Breakdown Spectroscopy”, *Journal of Environmental Quality*, 30, (2001), 2202-2206.

APPENDICES

APPENDIX A

Calculation of nutrient concentrations

As it can be seen in Table 5.1, the phosphorus and potassium contents of commercial fertilizers are stated in the form of P_2O_5 and K_2O rather than the elemental forms. Hence, when calculating the elemental phosphorus and potassium amounts in samples, conversion factors are used. These factors convert the amounts given in terms of P_2O_5 or K_2O into elemental forms, P and K, respectively (35).

$$P = P_2O_5 \times 0.4369$$

$$K = K_2O \times 0.8302$$

For instance, in 100 g of a mixture prepared with 1% (wt/wt) of NPK fertilizer (containing 15% N, P_2O_5 and K_2O), the amount of nutrients in the sample can be calculated by:

$$N\% = 0.15 \times 1 = 0.15 \text{ g/100 g sample}$$

$$P_2O_5\% = 0.15 \times 1 = 0.15 \text{ g/100 g sample}$$

$$K_2O\% = 0.15 \times 1 = 0.15 \text{ g/100 g sample}$$

The elemental form of potassium (K) and phosphorus (P) in the sample can be calculated by:

$$P\% = 0.15 \times 0.4369 = 0.065 \text{ g/100 g sample}$$

$$K\% = 0.15 \times 0.8302 = 0.124 \text{ g/100 g sample}$$

The same procedure is applied for the calculation of elemental phosphorus and potassium in the other samples containing different concentrations and types of fertilizer.

APPENDIX B

Nutrient Concentrations

Table B.1. Nutrient and fertilizer concentrations (g/100 g) in the samples prepared with KNO_3 , $\text{Ca}(\text{NO}_3)_2$ and $(\text{NH}_4)_2\text{SO}_4$ fertilizers according to the second method.

Fertilizer types:

KNO_3

Fertilizer	Nitrogen	Potassium
0.02	0.0026	0.00763416
0.04	0.0052	0.01526832
0.06	0.0078	0.02290248
0.08	0.0104	0.03053664
0.1	0.013	0.0381708
0.12	0.0156	0.04580496
0.14	0.0182	0.05343912
0.16	0.0208	0.06107328
0.18	0.0234	0.06870744
0.2	0.026	0.0763416
0.22	0.0286	0.08397576
0.24	0.0312	0.09160992
0.26	0.0338	0.09924408
0.28	0.0364	0.10687824
0.3	0.039	0.1145124
0.32	0.0416	0.12214656
0.34	0.0442	0.12978072
0.36	0.0468	0.13741488
0.38	0.0494	0.14504904
0.4	0.052	0.1526832
0.42	0.0546	0.16031736
0.44	0.0572	0.16795152
0.46	0.0598	0.17558568
0.48	0.0624	0.18321984
0.5	0.065	0.190854

$\text{Ca}(\text{NO}_3)_2$

Nitrogen	Calcium
0.0031	0.002944
0.0062	0.005888
0.0093	0.008832
0.0124	0.011776
0.0155	0.01472
0.0186	0.017664
0.0217	0.020608
0.0248	0.023552
0.0279	0.026496
0.031	0.02944
0.0341	0.032384
0.0372	0.035328
0.0403	0.038272
0.0434	0.041216
0.0465	0.04416
0.0496	0.047104
0.0527	0.050048
0.0558	0.052992
0.0589	0.055936
0.062	0.05888
0.0651	0.061824
0.0682	0.064768
0.0713	0.067712
0.0744	0.070656
0.0775	0.0736

$(\text{NH}_4)_2\text{SO}_4$

Nitrogen	Sulfur
0.0042	0.0048
0.0084	0.0096
0.0126	0.0144
0.0168	0.0192
0.021	0.024
0.0252	0.0288
0.0294	0.0336
0.0336	0.0384
0.0378	0.0432
0.042	0.048
0.0462	0.0528
0.0504	0.0576
0.0546	0.0624
0.0588	0.0672
0.063	0.072
0.0672	0.0768
0.0714	0.0816
0.0756	0.0864
0.0798	0.0912
0.084	0.096
0.0882	0.1008
0.0924	0.1056
0.0966	0.1104
0.1008	0.1152
0.105	0.12

Table B.2. Nutrient and fertilizer concentrations (g/100 g) in the samples prepared with NPK and TSP fertilizers according to the second method.

Fertilizer types:

NPK

Fertilizer	Nitrogen	Phosphorus	Potassium
0.02	0.003	0.0013104	0.0024894
0.04	0.006	0.0026208	0.0049788
0.06	0.009	0.0039312	0.0074682
0.08	0.012	0.0052416	0.0099576
0.1	0.015	0.006552	0.012447
0.12	0.018	0.0078624	0.0149364
0.14	0.021	0.0091728	0.0174258
0.16	0.024	0.0104832	0.0199152
0.18	0.027	0.0117936	0.0224046
0.2	0.03	0.013104	0.024894
0.22	0.033	0.0144144	0.0273834
0.24	0.036	0.0157248	0.0298728
0.26	0.039	0.0170352	0.0323622
0.28	0.042	0.0183456	0.0348516
0.3	0.045	0.019656	0.037341
0.32	0.048	0.0209664	0.0398304
0.34	0.051	0.0222768	0.0423198
0.36	0.054	0.0235872	0.0448092
0.38	0.057	0.0248976	0.0472986
0.4	0.06	0.026208	0.049788
0.42	0.063	0.0275184	0.0522774
0.44	0.066	0.0288288	0.0547668
0.46	0.069	0.0301392	0.0572562
0.48	0.072	0.0314496	0.0597456
0.5	0.075	0.03276	0.062235

TSP

Fertilizer	Phosphorus
0.02	0.00375648
0.04	0.00751296
0.06	0.01126944
0.08	0.01502592
0.1	0.0187824
0.12	0.02253888
0.14	0.02629536
0.16	0.03005184
0.18	0.03380832
0.2	0.0375648
0.22	0.04132128
0.24	0.04507776
0.26	0.04883424
0.28	0.05259072
0.3	0.0563472
0.32	0.06010368
0.34	0.06386016
0.36	0.06761664
0.38	0.07137312
0.4	0.0751296
0.42	0.07888608
0.44	0.08264256
0.46	0.08639904
0.48	0.09015552
0.5	0.093912

APPENDIX C

Calibration and validation sets

Table C.1. Calibration and validation sets of nutrients in the samples prepared with KNO₃ fertilizer according to the second method (g/100 g).

Fertilizer type: KNO₃

Calib	Nitrogen	Potassium	Calib	Nitrogen	Potassium	Valid	Nitrogen	Potassium
1	0.0026	0.00763416	27	0.0312	0.09160992	1	0.0052	0.01526832
2	0.0026	0.00763416	28	0.0364	0.10687824	2	0.0052	0.01526832
3	0.0026	0.00763416	29	0.0364	0.10687824	3	0.0052	0.01526832
4	0.0078	0.02290248	30	0.0364	0.10687824	4	0.013	0.0381708
5	0.0078	0.02290248	31	0.039	0.1145124	5	0.013	0.0381708
6	0.0078	0.02290248	32	0.039	0.1145124	6	0.013	0.0381708
7	0.0104	0.03053664	33	0.039	0.1145124	7	0.0234	0.06870744
8	0.0104	0.03053664	34	0.0442	0.12978072	8	0.0234	0.06870744
9	0.0104	0.03053664	35	0.0442	0.12978072	9	0.0234	0.06870744
10	0.0156	0.04580496	36	0.0442	0.12978072	10	0.0338	0.09924408
11	0.0156	0.04580496	37	0.0494	0.14504904	11	0.0338	0.09924408
12	0.0156	0.04580496	38	0.0494	0.14504904	12	0.0338	0.09924408
13	0.0182	0.05343912	39	0.0494	0.14504904	13	0.0416	0.12214656
14	0.0182	0.05343912	40	0.0546	0.16031736	14	0.0416	0.12214656
15	0.0182	0.05343912	41	0.0546	0.16031736	15	0.0416	0.12214656
16	0.0208	0.06107328	42	0.0546	0.16031736	16	0.0468	0.13741488
17	0.0208	0.06107328	43	0.0572	0.16795152	17	0.0468	0.13741488
18	0.0208	0.06107328	44	0.0572	0.16795152	18	0.0468	0.13741488
19	0.026	0.0763416	45	0.0572	0.16795152	19	0.052	0.1526832
20	0.026	0.0763416	46	0.0624	0.18321984	20	0.052	0.1526832
21	0.026	0.0763416	47	0.0624	0.18321984	21	0.052	0.1526832
22	0.0286	0.08397576	48	0.0624	0.18321984	22	0.0598	0.17558568
23	0.0286	0.08397576	49	0.065	0.190854	23	0.0598	0.17558568
24	0.0286	0.08397576	50	0.065	0.190854	24	0.0598	0.17558568
25	0.0312	0.09160992	51	0.065	0.190854			
26	0.0312	0.09160992						

Table C.2. Calibration and validation sets of nutrients in the samples prepared with $\text{Ca}(\text{NO}_3)_2$ fertilizer according to the second method (g/100 g).

Fertilizer type: $\text{Ca}(\text{NO}_3)_2$

Calib	Nitrogen	Calcium	Calib	Nitrogen	Calcium	Valid	Nitrogen	Calcium
1	0.0031	0.002944	27	0.0372	0.035328	1	0.0062	0.005888
2	0.0031	0.002944	28	0.0434	0.041216	2	0.0062	0.005888
3	0.0031	0.002944	29	0.0434	0.041216	3	0.0062	0.005888
4	0.0093	0.008832	30	0.0434	0.041216	4	0.0155	0.01472
5	0.0093	0.008832	31	0.0465	0.04416	5	0.0155	0.01472
6	0.0093	0.008832	32	0.0465	0.04416	6	0.0155	0.01472
7	0.0124	0.011776	33	0.0465	0.04416	7	0.0279	0.026496
8	0.0124	0.011776	34	0.0527	0.050048	8	0.0279	0.026496
9	0.0124	0.011776	35	0.0527	0.050048	9	0.0279	0.026496
10	0.0186	0.017664	36	0.0527	0.050048	10	0.0403	0.038272
11	0.0186	0.017664	37	0.0589	0.055936	11	0.0403	0.038272
12	0.0186	0.017664	38	0.0589	0.055936	12	0.0403	0.038272
13	0.0217	0.020608	39	0.0589	0.055936	13	0.0496	0.047104
14	0.0217	0.020608	40	0.0651	0.061824	14	0.0496	0.047104
15	0.0217	0.020608	41	0.0651	0.061824	15	0.0496	0.047104
16	0.0248	0.023552	42	0.0651	0.061824	16	0.0558	0.052992
17	0.0248	0.023552	43	0.0682	0.064768	17	0.0558	0.052992
18	0.0248	0.023552	44	0.0682	0.064768	18	0.0558	0.052992
19	0.031	0.02944	45	0.0682	0.064768	19	0.062	0.05888
20	0.031	0.02944	46	0.0744	0.070656	20	0.062	0.05888
21	0.031	0.02944	47	0.0744	0.070656	21	0.062	0.05888
22	0.0341	0.032384	48	0.0744	0.070656	22	0.0713	0.067712
23	0.0341	0.032384	49	0.0775	0.0736	23	0.0713	0.067712
24	0.0341	0.032384	50	0.0775	0.0736	24	0.0713	0.067712
25	0.0372	0.035328	51	0.0775	0.0736			
26	0.0372	0.035328						

Table C.4. Calibration and validation sets of nutrients in the samples prepared with $(\text{NH}_4)_2\text{SO}_4$ fertilizer according to the second method (g/100 g).

Fertilizer type: $(\text{NH}_4)_2\text{SO}_4$

Calib	Nitrogen	Sulfur	Calib	Nitrogen	Sulfur	Valid	Nitrogen	Sulfur
1	0.0042	0.0048	27	0.0504	0.0576	1	0.0084	0.0096
2	0.0042	0.0048	28	0.0588	0.0672	2	0.0084	0.0096
3	0.0042	0.0048	29	0.0588	0.0672	3	0.0084	0.0096
4	0.0126	0.0144	30	0.0588	0.0672	4	0.021	0.024
5	0.0126	0.0144	31	0.063	0.072	5	0.021	0.024
6	0.0126	0.0144	32	0.063	0.072	6	0.021	0.024
7	0.0168	0.0192	33	0.063	0.072	7	0.0378	0.0432
8	0.0168	0.0192	34	0.0714	0.0816	8	0.0378	0.0432
9	0.0168	0.0192	35	0.0714	0.0816	9	0.0378	0.0432
10	0.0252	0.0288	36	0.0714	0.0816	10	0.0546	0.0624
11	0.0252	0.0288	37	0.0798	0.0912	11	0.0546	0.0624
12	0.0252	0.0288	38	0.0798	0.0912	12	0.0546	0.0624
13	0.0294	0.0336	39	0.0798	0.0912	13	0.0672	0.0768
14	0.0294	0.0336	40	0.0882	0.1008	14	0.0672	0.0768
15	0.0294	0.0336	41	0.0882	0.1008	15	0.0672	0.0768
16	0.0336	0.0384	42	0.0882	0.1008	16	0.0756	0.0864
17	0.0336	0.0384	43	0.0924	0.1056	17	0.0756	0.0864
18	0.0336	0.0384	44	0.0924	0.1056	18	0.0756	0.0864
19	0.042	0.048	45	0.0924	0.1056	19	0.084	0.096
20	0.042	0.048	46	0.1008	0.1152	20	0.084	0.096
21	0.042	0.048	47	0.1008	0.1152	21	0.084	0.096
22	0.0462	0.0528	48	0.1008	0.1152	22	0.0966	0.1104
23	0.0462	0.0528	49	0.105	0.12	23	0.0966	0.1104
24	0.0462	0.0528	50	0.105	0.12	24	0.0966	0.1104
25	0.0504	0.0576	51	0.105	0.12			
26	0.0504	0.0576						

Table C.5. Calibration and validation sets of nutrients in the samples prepared with TSP fertilizer according to the second method (g/100 g).

Fertilizer type: TSP

Calib	Phosphorus
1	0.00375648
2	0.00375648
3	0.00375648
4	0.01126944
5	0.01126944
6	0.01126944
7	0.01502592
8	0.01502592
9	0.01502592
10	0.02253888
11	0.02253888
12	0.02253888
13	0.02629536
14	0.02629536
15	0.02629536
16	0.03005184
17	0.03005184
18	0.03005184
19	0.0375648
20	0.0375648
21	0.0375648
22	0.04132128
23	0.04132128
24	0.04132128
25	0.04507776
26	0.04507776

Calib	Phosphorus
27	0.04507776
28	0.05259072
29	0.05259072
30	0.05259072
31	0.0563472
32	0.0563472
33	0.0563472
34	0.06386016
35	0.06386016
36	0.06386016
37	0.07137312
38	0.07137312
39	0.07137312
40	0.07888608
41	0.07888608
42	0.07888608
43	0.08264256
44	0.08264256
45	0.08264256
46	0.09015552
47	0.09015552
48	0.09015552
49	0.093912
50	0.093912
51	0.093912

Valid	Phosphorus
1	0.00751296
2	0.00751296
3	0.00751296
4	0.0187824
5	0.0187824
6	0.0187824
7	0.03380832
8	0.03380832
9	0.03380832
10	0.04883424
11	0.04883424
12	0.04883424
13	0.06010368
14	0.06010368
15	0.06010368
16	0.06761664
17	0.06761664
18	0.06761664
19	0.0751296
20	0.0751296
21	0.0751296
22	0.08639904
23	0.08639904
24	0.08639904

APPENDIX D

Appendix D.1. Kjeldahl Method

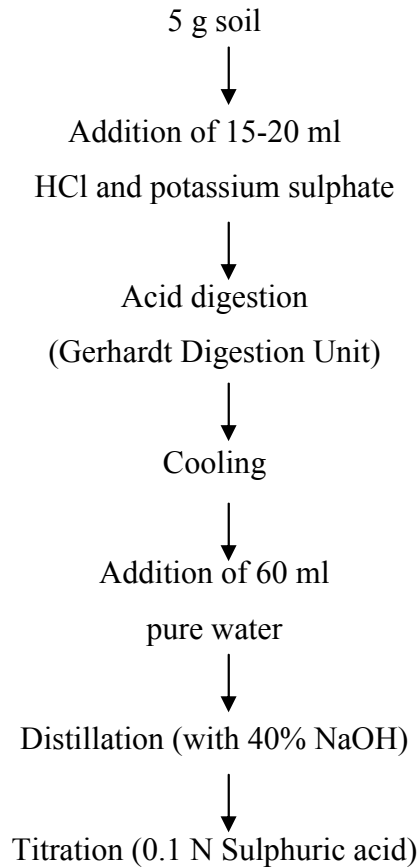


Figure D.1. Kjeldahl method, which is applied by soil laboratory of Agricultural Engineering Department of Ege University.

The results are reported as total nitrogen percentage in the soil and calculated according to the formula;

$$N\% = \frac{(T - V) \times n \times 1.4}{S}$$

T: Expense of sulphuric acid during titration (ml)

V: (Blank) 0.3 ml

n: Normality of acid

S: (Sample amount) 5 g

Appendix D.2. Bingham Method

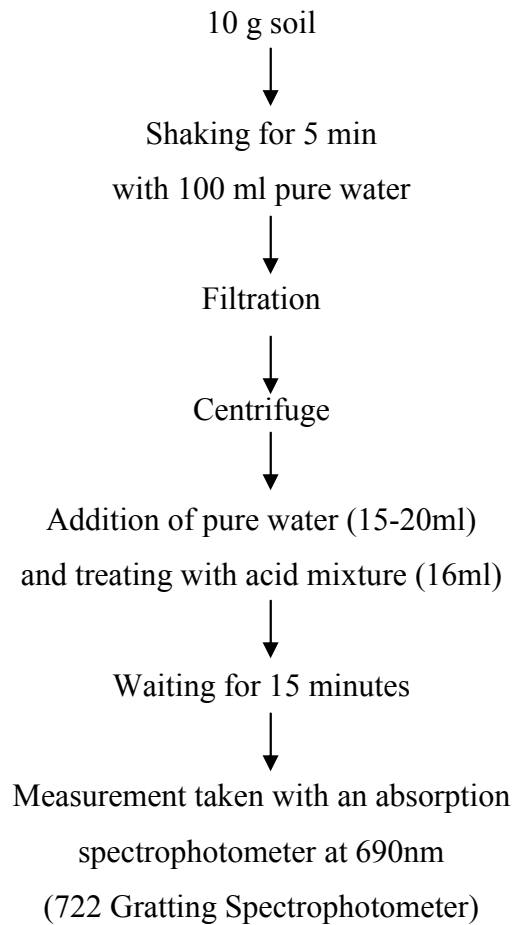


Figure D.2. Bingham method, which is applied by soil laboratory of Agricultural Engineering Department of Ege University.

The measurements are read from the calibration curve and recorded as parts per million of phosphorus in the soil.

Acid mixture is prepared from the following solvents

- 5 N 125 ml sulphuric acid
- 37.5 ml ammonium-molybdate
- 75 ml ascorbic acid
- 12.5 ml potassium antimontartrate

The calibration curve is prepared by using the standard solution (KH_2PO_4) and prepared according to the procedure described after centrifuging at 0, 0.1, 0.2, 0.4, 0.6, 0.8 and 1 ppm concentrations and measurement with the spectrophotometer at 690 nm.

Appendix D.3. Ammonium Acetate Method

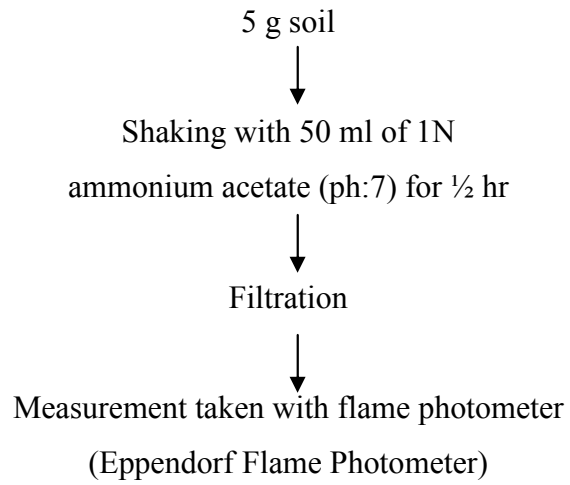


Figure D.3. Ammonium acetate method, which is applied by soil laboratory of Agricultural Engineering Department of Ege University.

The results are reported as parts per million (ppm) of potassium in the soil.